Reactive and Functional Polymers 183 (2023) 105509

Contents lists available at ScienceDirect

Reactive and Functional Polymers

journal homepage: www.elsevier.com/locate/react

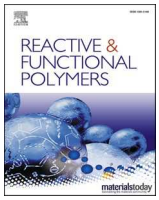

Cu(0)-RDRP of 2-hydroxyethyl methacrylate in a non-polar solvent enables rapid synthesis of high-molecular weight homopolymers and direct access to amphiphilic copolymers

Sachin Gupta, Vladimír Raus *

Institute of Macromolecular Chemistry, Czech Academy of Sciences, Heyrovského nám. 2, 162 06 Prague 6, Czech Republic

ARTICLE INFO

Keywords:
2-hydroxyethyl methacrylate
Cu-RDRP
Polymerization
High molecular weight
Amphiphilic

ABSTRACT

2-Hydroxyethyl methacrylate (HEMA) is an important functional monomer affording (co)polymers with numerous applications in different fields. Nevertheless, we still lack a reliable polymerization method for the synthesis of well-defined, high-molecular weight (MW) HEMA homopolymers, as well as for controlled copolymerization of unprotected HEMA with lipophilic comonomers. Herein, we report that rapid and well-controlled (co)polymerization of HEMA can be achieved via metallic copper-mediated reversible-deactivation radical polymerization (Cu(0)-RDRP) in a non-polar solvent (1,4-dioxane) using a chlorine-based initiation/catalytic system. With purified HEMA monomer, this protocol affords very well-defined ($Đ \leq 1.26$) HEMA homopolymers in an unprecedently wide range of molecular weights from 10,000 to 500,000. Conversely, the structurally analogous bromine-based initiation/catalytic system leads to an uncontrolled polymerization. The use of a non-polar solvent enables, for the first time, a direct access to low-dispersity HEMA-rich copolymers with non-polar comonomers, including highly lipophilic ones. This is demonstrated on the successful copolymerization of HEMA with an equimolar amount of 2-ethylhexyl methacrylate and of lauryl methacrylate, yielding well-defined amphiphilic copolymers at quantitative conversion. This work significantly expands the application scope of the HEMA monomer and demonstrates for the first time that Cu(0)-RDRP in a non-polar solvent is applicable also to comparatively polar monomers.

1. Introduction

Poly(2-hydroxyethyl methacrylate) (poly(HEMA)) is an important functional polymer with favorable properties such as biocompatibility and non-toxicity. Since Lím's and Wichterle's early work on poly(HEMA) hydrogels [1], poly(HEMA)-based materials have found numerous applications particularly in the biomedical field [2], including soft contact lenses [3,4], surgical implants [5], tissue engineering scaffolds [6], wound dressings [7], or drug delivery vehicles [8].

The development of reversible-deactivation radical polymerization (RDRP) techniques has allowed the synthesis of well-defined poly(HEMA)-based materials of diverse architectures [9]. Among these techniques, HEMA polymerization in polar solvents through various copper-mediated RDRP protocols (Cu-RDRP) was particularly thoroughly studied. Already in 1999, Matyjaszewski group reported the first successful atom transfer radical polymerization (ATRP) of HEMA in a methyl ethyl ketone (MEK)/1-propanol mixed solvent [10]. However, when high molecular weights (MWs) were targeted, the polymerization was plagued by limited conversion and increased dispersity (Đ), which was rectified only by protecting the monomer's hydroxyl function by a trimethylsilyl group. Later, Armes and coworkers prepared well-defined poly(HEMA) via ATRP in methanol or methanol/water mixtures [11–13], and in isopropanol/water mixtures [14]. Further, ATRP of HEMA was performed in ethylene glycol [15] and a MEK/methanol mixture [16]. The latter medium was employed also in activators generated by electron transfer (AGET) ATRP of HEMA [17] while methanol served as a solvent in activators regenerated by electron transfer (ARGET) ATRP of HEMA [18]. Nevertheless, the use of alcoholic solvents in ATRP of HEMA was later found to be problematic as monomer transesterification has been observed under standard ATRP conditions [19]. Finally, a polar aprotic solvent, dimethyl sulfoxide (DMSO), was utilized by Percec and coworkers in the synthesis of ultrahigh-MW poly(HEMA) via metallic copper-mediated RDRP (Cu(0)-RDRP) [20]. Nevertheless, it needs to be stressed that in these previous

* Corresponding author.
E-mail address: raus@imc.cas.cz (V. Raus).

https://doi.org/10.1016/j.reactfunctpolym.2023.105509
Received 31 October 2022; Received in revised form 3 January 2023; Accepted 6 January 2023
Available online 7 January 2023

studies employing polar media only limited conversions were attained [10,15–17,20] and/or the polymerization control deteriorated (Đ > 1.3) [10,15,16,18,20] when targeting poly(HEMA) of MW higher than several tens of thousands. Therefore, the field currently lacks a reliable method for well-controlled polymerization of HEMA in a broad range of MWs.

Due to the solubility reasons, non-polar solvents were not generally considered for HEMA homopolymerization; these media found use only when copolymerizing HEMA with an excess of a non-polar comonomer that ensured the solubility of the produced copolymer [21]. If this was not feasible, protected HEMA had to be used [22,23], which required an additional deprotection step. A development of an efficient and well-controlled method for direct HEMA homopolymerization and its copolymerization with nonpolar (lipophilic) comonomers via Cu-RDRP would therefore substantially increase the application potential of the monomer.

Cu(0)-RDRP, denoted also as single electron transfer living radical polymerization (SET-LRP) [24,25] or supplemental activators and reducing agents (SARA) ATRP [26] with reference to the proposed polymerization mechanism, is typically conducted in polar solvents, such as DMSO or alcohols [24,27,28], or in aqueous media [29–32]. Nevertheless, in early works by the groups of Percec and Haddleton, Cu(0)-RDRP of methyl acrylate in non-polar solvents (neat or with additives) was also considered [33–35], and this approach was later successfully applied to other non-polar monomers, using toluene as a solvent [36–39]. Additionally, our laboratory has also demonstrated the suitability of the method for the polymerization of a bulky, hydrophobic POSS-methacrylate monomer in benzene [40]. In relevance to the present study, Yuan et al. briefly reported on the preparation of the poly(HEMA) block in an amphiphilic triblock copolymer via Cu(0)-RDRP in toluene [21]. However, to the best of our knowledge, Cu(0)-RDRP and other Cu-RDRP methods have not been previously applied to the direct homopolymerization of unprotected HEMA in a non-polar solvent.

In this study, we investigated the applicability of copper wire-mediated Cu(0)-RDRP, conducted in 1,4-dioxane as a comparatively non-polar solvent, to HEMA (co)polymerization. We show that when chlorine-based initiation/catalytic system is used, unprecedently well-defined polymers can be rapidly obtained up to high MWs. In addition, we demonstrate the utility of the non-polar polymerization medium in the well-controlled copolymerization of HEMA with non-polar monomers, 2-ethylhexyl methacrylate (EHMA) and lauryl methacrylate (LMA), at the equimolar comonomer content.

2. Experimental

2.1. Materials

α-Chlorophenylacetate (ECPA; Sigma-Aldrich, 97%), α-bromophenylacetate (EBPA; Acros, 97%), methyl α-bromophenylacetate (MBPA; Sigma-Aldrich, 97%), $CuCl_2$ (Sigma-Aldrich, 99%), $CuBr_2$ (Sigma-Aldrich, 98%) were used as received. Cu-wire (Sigma-Aldrich, diameter = 0.64 mm) was activated before each polymerization by conc. HCl using the procedure provided below. N,N,N′,N″,N″-Pentamethyldiethylenetriamine (PMDETA; Sigma-Aldrich, 99%) was vacuum distilled and stored under argon at 4 °C. Tris[2-(dimethylamino)ethyl] amine (Me_6TREN) was synthesized using a literature protocol [41] and stored under argon at 4 °C. 1,4-Dioxane (Lachner, 99.9%) and DMSO (Acros Organics, 99.7 + %) were dried over 4 Å molecular sieves and purged with argon for 1 h. 2-Ethylhexyl methacrylate (EHMA; Sigma-Aldrich, 98%) and lauryl methacrylate (LMA; Sigma-Aldrich, 96%) were purified by passing through a short column of neutral alumina and purged with argon for 1 h. *N,N*-Dimethylacetamide (DMAc; VWR; HPLC Grade, 99.5%) and lithium bromide (Sigma-Aldrich, 99%) were used for the preparation of the SEC-LS mobile phase. 2-Hydroxyethyl methacrylate (HEMA; Sigma-Aldrich, 97%) was either vacuum distilled only to remove the stabilizer or purified using the protocol provided below in order to remove also the ethylene glycol dimethacrylate (EGDMA) crosslinker.

2.2. Procedures

2.2.1. Activation of Cu wire

The wire was placed into ca. 5 mL of conc. HCl for 5 min, removed and washed with water, and returned to conc. HCl for another 10 min. Afterwards, the activated wire was successively washed with water and acetone, dried in a stream of argon, and kept under argon until use.

2.2.2. Purification of HEMA monomer

The method was adopted from Wichterle and Chromeček [42] with slight modifications. HEMA (50 mL) was mixed with 200 mL of Milli-Q water, and the obtained mixture was extracted with hexane (4 × 200 mL) to remove EGDMA. NaCl was added to the aqueous layer to salt out any methacrylic acid present, and the final mixture was extracted with diethyl ether (3 × 200 mL). The etheric layer containing the HEMA monomer was dried with $MgSO_4$ and concentrated using a rotary evaporator. The obtained colorless liquid was then subjected to high vacuum distillation in order to obtain purified HEMA that was stored under argon at −20 °C afterwards.

2.2.3. Cu(0)-RDRP of HEMA

The protocol for a typical experiment conducted at M/I = 100:1 (Table 1; Entry 4) is provided as an example: Activated Cu wire (5 cm) and $CuCl_2$ (5.5 mg, 0.0412 mmol) were placed into a reaction flask equipped with a magnetic stirring bar and a three-way stopcock connected to an argon/vacuum inlet. After thorough deoxygenation by several vacuum-argon cycles, 1,4-dioxane (2.5 mL) was added, followed by the addition of HEMA (2.5 mL, 20.61 mmol) and ECPA (35.4 μl, 0.2062 mmol). The polymerization was started by adding PMDETA (43 μl, 0.2062 mmol), and the flask was placed into an oil bath preheated to 85 °C. After 60 min, the magnetic stirring of the mixture became impossible, and so the experiment was ended. The flask was cooled down, opened to air, the Cu-wire was removed, and samples of the reaction mixture were collected for NMR and SEC analyses. Since phenothiazine, that was used as an inhibitor, did not go readily into highly viscous mixtures, such samples were immediately diluted with the respective solvents before stabilization. Failing to do so might result into the polymerization of unreacted HEMA. In this context, it is noted that the residual HEMA monomer in insufficiently stabilized polymerization mixtures is able to polymerize even during the storage at −20 °C, which is possibly facilitated by the phase separation of the HEMA-rich layer from the frozen dioxane. Obviously, this may have a negative impact on the subsequently determined conversion and MW values and MWDs. The risk appears to be the highest for the experiments with high but incomplete conversions (around 70%) that afford mixtures that contain a considerable amount of unreacted monomer while their high viscosity prevents effective dissolution of the stabilizer. Furthermore, note that stock solutions of ECPA and PMDETA in dioxane were used in the experiments with high M/I ratios in order to ensure accurate sampling of these components. Finally, we also confirmed that adding ECPA as the last component (instead of PMDETA) leads to a practically identical product.

2.2.4. Copolymerization of HEMA with non-polar comonomers via Cu(0)-RDRP in dioxane

Copolymerization with LMA is given as an example; the copolymerization with EHMA was conducted in the same way. Activated Cu wire (5 cm) and $CuCl_2$ (5.5 mg, 0.0412 mmol) were placed into a reaction flask equipped with a magnetic stirring bar and a three-way stopcock connected to an argon/vacuum inlet. After thorough deoxygenation by several vacuum-argon cycles, 1,4-dioxane (4.25 mL) was added, followed by the addition of HEMA (1.25 mL, 10.31 mmol), LMA (3 mL, 10.31 mmol), and ECPA (35.4 μl, 0.2062 mmol). The

Table 1
Optimization of polymerization conditions for Cu(0)-RDRP of HEMA[a].

Entry	Initiator	Deactivator	Temp. (°C)	Time (min)	Conv. (%)[b]	M_n (theor.)[c]	M_n (SEC)[d]	Đ[d]
1	EBPA	–	85	120	75	9800	15,100	2.36
2	ECPA	–	85	60	94	12,200	17,700	1.84
3	EBPA	$CuBr_2$ (0.2 eq.)	85	120	81	10,500	16,000	2.26
4	ECPA	$CuCl_2$ (0.2 eq.)	85	60	95	12,400	19,000	1.23
5	EBPA	$CuCl_2$ (0.2 eq.)	85	120	94	12,200	22,000	1.76
6	ECPA	$CuCl_2$ (0.2 eq.)	r.t.	60	90	11,700	20,500	1.25

[a] Standard polymerization conditions: HEMA/initiator/PMDETA = 100:1:1, 5 cm of activated copper wire, dioxane/HEMA = 1:1 (*v*/v).
[b] Monomer conversion as determined by a ^{1}H NMR analysis.
[c] Theoretical M_n calculated from the M/I ratio and conversion.
[d] Determined by SEC with LS detection.

polymerization was started by adding PMDETA (43 μl, 0.2062 mmol), and the flask was placed into an oil bath preheated to 85 °C. After 3 h, the experiment was ended, the flask was cooled, and samples of the highly viscous but homogeneous mixture were collected and processed in the same way as HEMA homopolymers.

2.2.5. Copolymerization of HEMA and LMA via Cu(0)-RDRP in DMSO

The method reported by Nguyen et al. [20] was adapted. Activated Cu-wire (5 cm) and $CuBr_2$ (2.3 mg, 0.0103 mmol) were placed into a reaction flask equipped with a magnetic stirring bar and a three-way stopcock connected to an argon/vacuum inlet. After thorough de-oxygenation by several vacuum-argon cycles, DMSO (4.25 mL), HEMA (1.25 mL, 10.31 mmol), LMA (3 mL, 10.31 mmol), and MBPA (32.5 Ll, 0.2062 mmol) were added. The polymerization was started by adding Me_6TREN (5.5 μL, 0.0206 mmol), and the heterogeneous mixture was stirred at r.t. After 7 h, the experiment was ended, and samples were collected and processed as indicated above.

2.3. Characterization

The number-average molecular weights (M_n), weight-average molecular weights (M_w), and dispersity ($Đ$) of the (co)polymers were determined by SEC. Most of the analyses were performed using the Malvern Panalytical OMNISEC SEC system consisting of OMNISEC Resolve and OMNISEC Reveal units. Two PSS GRAM analytical linear columns with the dimensions of 8 × 300 mm and particle size of 10 μm were used. Triple detection with the following detectors was performed: differential refractive index (RI) detector, right-angle light scattering (RALS) + low-angle light scattering (LALS) measuring at an angle of 7° to the incident beam (laser wavelength of 640 nm), and a 4-capillary Wheatstone bridge viscometer. The columns and detectors were held at 55 °C. Dimethylacetamide with 5 g/L LiBr was used as an eluent at a flow rate of 1 mL/min. OMNISEC software from Malvern Panalytical was used for online monitoring and processing of the data. The dn/dc value 0.078 mL/g for poly(HEMA) was obtained by an on-line determination assuming 100% sample recovery. See the Supporting information for an additional discussion regarding the dn/dc determination.

An additional SEC analysis (for the poly(HEMA-*co*-LMA) copolymer prepared in DMSO) was performed using an SEC system equipped with a DeltaChrom P102 pump (Watrex, Czech Republic), two PLgel MIXED-C columns (300 × 7.5 mm, SDV gel with particle size 5 μm; Polymer Laboratories, USA) and a refractive index detector (RI-101; Shodex, Japan). Tetrahydrofuran was used as a mobile phase at 25 °C with a flow rate of 1 mL/min. The MW values were calculated using the Clarity software (Dataapex, Czech Republic). Calibration with poly(methyl methacrylate) standards (PSS, Germany) in the MW range of 2200 to 1,220,000 was used.

^{1}H NMR spectra were recorded on a Bruker Avance NEO 400 spectrometer operating at 400.13 MHz at 300 K. Poly(HEMA) samples were dissolved in DMSO-d_6 whereas poly(HEMA-*co*-LMA) samples were dissolved in $CDCl_3$ for the determination of monomer conversions in the crude polymerization mixtures.

The gas chromatography (GC) analysis was performed using the GC Autosystem (Perkin Elmer), equipped with the Rtx-5 (60 m × 0,53 mm × 3 μm; Restek) column and an FID detector (250 °C). Quantification of EGDMA was performed by the internal standard method (diethyl adipate was employed as an internal standard).

3. Results and discussion

3.1. Optimization of conditions for HEMA homopolymerization

In our investigation, copper wire (5 cm) was conveniently employed as a catalyst source, activated by conc. HCl before each polymerization. Dioxane, used in this study as a reaction medium, is classified as a rather non-polar solvent, yet it is readily miscible with a range of both polar and non-polar compounds [43,44]. Importantly, we confirmed that, despite only limited solubility of poly(HEMA) in dioxane, the polymer prepared under the conditions of this study (monomer/solvent = 1:1 (*v*/v)) does not precipitate from the polymerization mixture at high conversions even when targeting high-MW polymers or when conducting the experiment at r.t. N,N,N′,N″,N″-Pentamethyldiethylenetriamine (PMDETA) was selected as a ligand as it has been previously successfully employed in Cu(0)-RDRP in non-polar solvents [36,37]. We explored the use of alkyl α-halophenylacetates as highly active initiators [45] that proved to be rather universal options utilized in conjunction with different ligands in diverse Cu-RDRP protocols [27,31,32,46,47], including the Cu(0)-RDRP of HEMA in DMSO [20]. Specifically, we compared the performance of ethyl α-bromophenylacetate (EBPA) and its chlorinated analogue, ethyl α-chlorophenylacetate (ECPA). The polymerizations were conducted at an elevated temperature (85 °C) to facilitate the stirring of the highly viscous polymer solutions. Samples of crude reaction mixtures were collected to determine monomer conversions by ^{1}H NMR (see **Fig. S1** for a typical ^{1}H NMR spectrum) and MWs and dispersity via SEC with light scattering (LS) detection performed in DMAc/LiBr. It is noted that employing an accurate method for MW determination is highly desirable as the early works on HEMA polymerization via Cu-RDRP reported extensively on the mismatch between the actual MWs and the values obtained through SEC with relative calibration [10–12,17]. For an additional discussion on determining the accurate MWs, see the Supporting Information.

In trial experiments, we compared EBPA- and ECPA-initiated polymerizations at the HEMA/initiator/PMDETA ratio of 100:1:1 (entries 1 and 2, Table 1; **Fig. S2**). In both cases, an uncontrolled process was observed; however, the conversion was substantially higher with ECPA (94% vs. 75% for EBPA) despite the shorter polymerization time. In some of the previous reports on Cu(0)-RDRP conducted in non-polar solvents, the addition of a Cu^{2+} deactivator had a substantially positive effect on the polymerization control, presumably helping to offset the insufficient deactivator concentration at the initial polymerization stages [36–38]. Strikingly, in our case, this strategy had only a negligible impact on the bromine-based system (EBPA +0.2 eq. $CuBr_2$; entry 3, Table 1; **Fig. S2**) while the chlorine-based combination (ECPA +0.2 eq. $CuCl_2$) showed a dramatic improvement in the polymerization control as

illustrated by the decreased dispersity value of 1.23 and the unimodal and symmetrical SEC trace (entry 4, Table 1; Fig. 1). In addition, high conversion (95%) was again attained within 1 h when the experiment was ended because the high viscosity of the mixture precluded magnetic stirring. For a comparison, we performed also the experiment combining EBPA and 0.2 eq. of $CuCl_2$; however, a high-dispersity product was obtained also in this EBPA-based system (entry 5, Table 1; **Fig. S2**). These results clearly show that the chlorine-based initiation/catalytic system, often preferred in aqueous media [29,31,32], should be considered also when optimizing polymerizations in non-polar organic solvents. The choice of initiator halogen is expected to be particularly important in Cu(0)-RDRP protocols where, unlike in the conventional ATRP, the initiator is the major (or even the sole) source of the halogen atoms participating at the key steps of the polymerization mechanism and constituting polymer end groups. Furthermore, we demonstrated that practically identical results can be obtained with ECPA/$CuCl_2$ also at r. t. (entry 6, Table 1; Fig. 1), which illustrates well the high polymerization rate in this system. Nevertheless, slightly lower conversion was achieved before the polymerization mixture turned solid. Conducting the polymerization at a higher temperature is therefore preferable, particularly when targeting higher MWs where the viscosity effects are even more pronounced.

3.2. Synthesis of poly(HEMA) of different molecular weights

Next, in order to demonstrate the universality of the optimized conditions, we tested them at different monomer/initiator (M/I) ratios. When aiming for a lower-MW polymer (M/I = 50), the polymerization was very well controlled (Đ = 1.15) and achieved high conversion (92%) in only 30 min (entry 1, Table 2; Fig. 2). However, when we targeted high-MW polymers by adjusting the M/I ratio to 400:1 and 1000:1, a high-MW shoulder became prominent in the SEC elugrams of the products, increasing the product dispersity, especially in the latter case (entries 1 and 2, **Table S1**; **Fig. S3** and **S4**). Initially, we presumed that termination reactions might have contributed to the appearance of the high-MW fraction. However, increasing the initial concentration of the $CuCl_2$ deactivator in the polymerization with M/I = 400:1 to 0.5 eq. did not yield any improvement (entry 3, **Table S1**; **Fig. S3**). It is well known that commercial HEMA samples can contain EGDMA as an impurity that works as an efficient crosslinking agent in HEMA polymerizations. In literature, some authors used specific purification protocols to remove

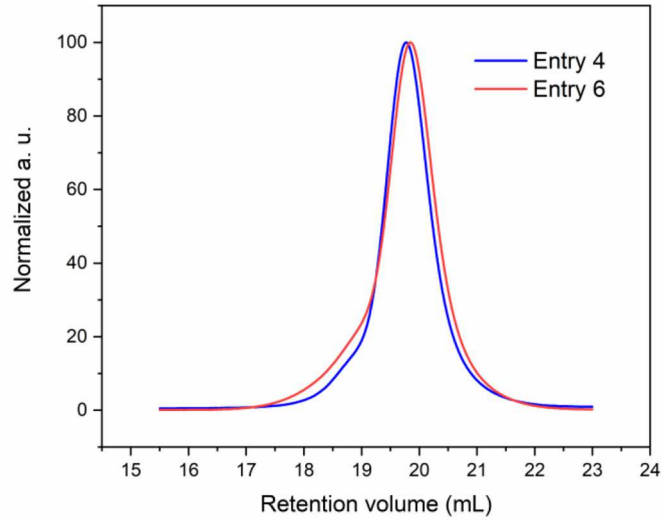

Fig. 1. SEC elugrams (RI traces) from the SEC-LS analyses of poly(HEMA) obtained via Cu(0)-RDRP in dioxane under optimized conditions. Numbering of the traces corresponds to Table 1.

Table 2
Cu(0)-RDRP of HEMA at different M/I ratios[a].

Entry	M/I	$CuCl_2$ (eq.)	Time (min)	Conv. (%)[b]	M_n (theor.)[c]	M_n (SEC)[d]	Đ[d]
1	50:1	0.2	30	92	6000	10,600	1.15
2[e]	400:1	0.2	60	88	45,800	59,700	1.14
3[e]	1000:1	0.5	60	77	100,200	138,200	1.22
4[e]	2000:1	0.5	80	62	161,400	205,800	1.26
5[e]	5000:1	1.25	150	58	377,400	469,000	1.25

[a] Standard polymerization conditions: ECPA/PMDETA = 1:1, 5 cm of activated copper wire, dioxane/HEMA = 1:1 (*v*/v).
[b] Monomer conversion as determined by a ^{1}H NMR analysis.
[c] Theoretical M_n calculated from the M/I ratio and conversion.
[d] Determined by SEC with LS detection.
[e] Purified HEMA with minimized EGDMA crosslinker content was used.

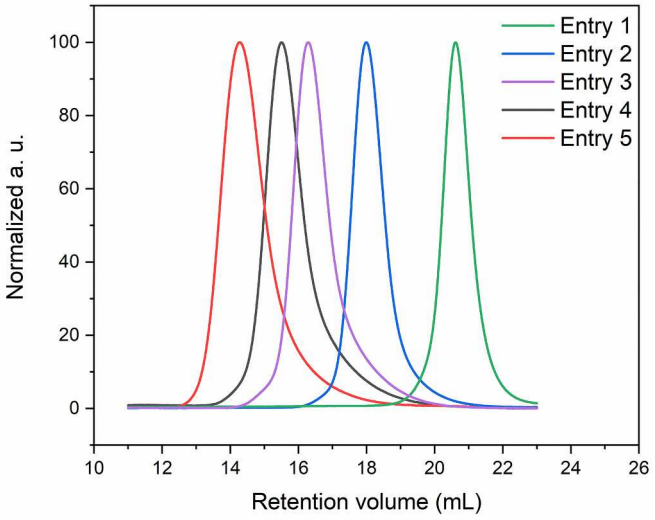

Fig. 2. SEC elugrams (RI traces) from the SEC-LS analyses of poly(HEMA) obtained via Cu(0)-RDRP in dioxane at different M/I ratios. Numbering of the traces corresponds to Table 2.

EGDMA and other impurities [10,16,20] while others used only distillation or did not purify the monomer at all [11–14,17,18]. Since we purified the monomer used in the initial experiments only by vacuum distillation, we hypothesized that the high-MW fraction observed at higher M/I ratios could be due to limited crosslinking reactions caused by the residual EGDMA. Indeed, such events would be more probable for higher-MW polymers bearing statistically higher number of EGDMA-borne polymerizable double bonds in their structure. To verify this hypothesis, we purified the monomer according to an established protocol [42], which brought the EGDMA concentration from 0.1 wt% down to 0.01 wt% as determined by a GC analysis. Indeed, upon repeating the polymerizations at M/I = 400:1 and 1000:1 with the purified monomer, SEC elugrams devoid of the previously observed high-MW shoulders were obtained (Fig. 2, see also **Fig. S3** and **Fig. S4** for an overlay comparison). Importantly, still quite high conversion values were obtained within 60 min when the polymerizations were terminated due to inefficient stirring (entries 2 and 3, Table 2). Moreover, the process was well-controlled in both cases as indicated by the low dispersity values. For the 400:1 ratio, this was further confirmed by performing a kinetic experiment that exhibited the standard characteristics of a controlled process (**Fig. S5**). Interestingly, the apparent rate constant of propagation (k_p^{app}) value obtained from the semilogarithmic plot (0.041 min^{-1}) is an order of magnitude higher than the values observed in Cu(0)-RDRP

of HEMA in DMSO [20], which highlights the high polymerization rate in the present system. Increased k_p values for radical polymerization conducted in non-polar solvents have been observed previously for various hydroxyl-bearing monomers [48].

Finally, to investigate the applicability of the method to the preparation of ultrahigh-MW poly(HEMA), we used the elevated M/I ratios of 2000:1 and 5000:1 in the subsequent experiments (entries 4 and 5, Table 2). Pleasingly, very good polymerization control and rapid polymerization rates were retained, obtaining poly(HEMA) of MW of approximately 500,000 within 150 min in the latter experiment while keeping the dispersity at 1.25. This represents a significant improvement over the current Cu-RDRP protocols for HEMA polymerization as, to the best of our knowledge, the preparation of poly(HEMA) of $M_n > 100{,}000$ and $Đ < 1.30$ via Cu-RDRP methods (and probably also by other RDRP methods) has not been reported before. Note that the content of the $CuCl_2$ deactivator was increased to 0.5 eq. (for the 1000:1 and 2000:1 ratios) and 1.25 eq. (for the 5000:1 ratio) for practical reasons as it became difficult to accurately weigh the progressively diminishing amounts while keeping the polymerization scale the same. The obvious limitation of the current protocol is the high viscosity of the polymerization mixtures when high-MW products are targeted, which limits the conversions achievable before the mixtures turn solid. The high viscosity was a limiting factor also in the study by Nguyen et al. who prepared ultrahigh-MW poly(HEMA) by Cu(0)-RDRP in DMSO [20]. Nevertheless, it should be mentioned that in that report, the polymerization control was gradually lost when aiming for higher MWs, with reported $Đ \geq 1.39$ for MWs of approximately 150,000 (based on poly(MMA) SEC calibration) and higher. In comparison, the control is retained with our method even for high M/I ratios, and even higher MWs than reported here should be, in principle, accessible. It is also noteworthy that high initiation efficiency values of 70 to 80% (calculated by comparing M_n (theor.) to M_n (SEC)) were generally obtained for the high-MW polymers (entries 2 to 5, Table 2) in our system. These values are comparable to those reported previously for the Cu(0)-RDRP of various methacrylates using the methyl α-chlorophenylacetate/PMDETA system [27].

3.3. Direct copolymerization of HEMA with non-polar comonomers

To exemplify the utility of using a non-polar medium for HEMA polymerization, we conducted a copolymerization of HEMA with an equimolar amount of a non-polar comonomers (EHMA) and a highly lipophilic comonomer (LMA), yielding amphiphilic poly(HEMA-*co*-EHMA) and poly(HEMA-*co*-LMA) copolymers, respectively. Both the copolymerizations were performed using the standard conditions developed for HEMA above (HEMA/comonomer/ECPA/PMDETA/$CuCl_2$ = 50:50:1:1:0.2, 5 cm of copper wire, monomers/dioxane = 1:1 *v*/v, 85 °C).

Pleasingly, the polymerization mixtures were homogeneous throughout the polymerization course, and virtually quantitative monomer conversions were obtained within 3 h as judged from the almost complete disappearance of the monomeric vinylic signals around 6 ppm in the ^{1}H NMR spectra of the crude polymerization mixtures (**Figs. S6 and S7**). Moreover, the SEC-LS analysis revealed that copolymers of very low dispersity (1.13 and 1.09 for the EHMA and LMA copolymerization, respectively) were obtained (Fig. 3), indicating that an excellent degree of control was retained even in these systems. The small high-MW fraction, apparent particularly for the poly(HEMA-*co*-EHMA) copolymer, is ascribed to termination reactions. For comparison, we performed HEMA copolymerization with LMA using the conditions reported by Percec's group for the homopolymerization of HEMA by Cu(0)-RDRP in DMSO (HEMA/LMA/MBPA/Me_6TREN/$CuBr_2$ = 50:50:1:0.1:0.05, 5 cm of copper wire, monomers/DMSO = 1:1 *v*/v, r.t.) [20]. While high monomer conversion was apparently achieved, the polymerization mixture was heterogeneous, which was possibly reflected in the characteristics of the resulting copolymer. The product was not completely soluble in the DMAc/LiBr mobile phase we used for SEC-LS; however, we managed to obtain at least relative MW values from the SEC analysis in THF with poly(methyl methacrylate) calibration. A bimodal SEC trace was observed (**Fig. S8**), with the major peak corresponding to a very high-MW product (M_n = 357,000) of high dispersity ($Đ$ = 2.35). Taken together, these results indicate that the polymerization conditions developed in this study should be of a great use in constructing various amphiphilic HEMA-based copolymers without the risk of obtaining heterogeneous polymerization mixtures that may negatively impact on the polymerization control.

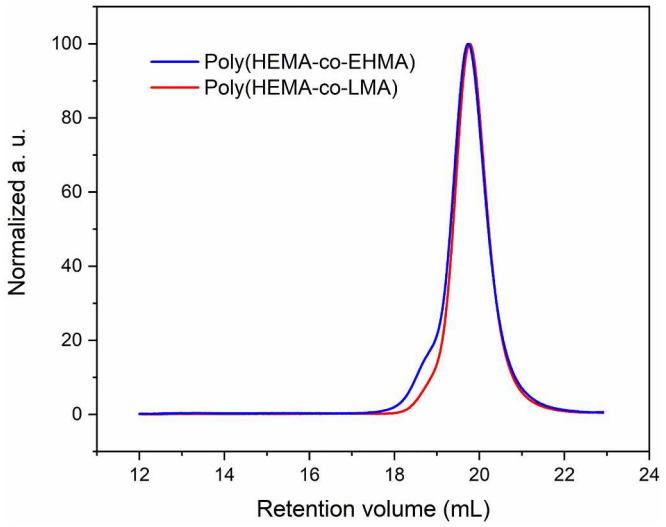

Fig. 3. SEC elugrams (RI traces) from the SEC-LS analyses of poly(HEMA-*co*-EHMA) (blue) and poly(HEMA-*co*-LMA) (red) obtained via Cu(0)-RDRP in dioxane under optimized conditions (HEMA/comonomer/ECPA/PMDETA/$CuCl_2$ = 50:50:1:1:0.2, 5 cm of copper wire, monomers/dioxane = 1:1 v/v, 85 °C, 3 h). Poly(HEMA-*co*-EHMA) characteristics: M_n = 26,900, $Đ$ = 1.13; poly(HEMA-*co*-LMA) characteristics: M_n = 30,700, $Đ$ = 1.09. (For interpretation of the references to colour in this figure legend, the reader is referred to the web version of this article.)

4. Conclusions

In conclusion, our data show that Cu(0)-RDRP in dioxane using a chlorine-based initiation/catalytic system is a method that is superior to the previous Cu-RDRP protocols applied to HEMA (co)polymerization. With purified HEMA, our method provides a rapid access to well-defined poly(HEMA) in an unprecedently wide range of MWs without the risk of solvent transesterification side-reactions. Additionally, we demonstrated that the developed conditions will be particularly useful for HEMA copolymerization with non-polar/lipophilic monomers where the current protocols (using highly polar solvents) may face compatibility problems. Well-defined HEMA-rich amphiphilic copolymers thus become readily accessible. This study also represents the first application of Cu(0)-RDRP in a non-polar solvent to a polar monomer, suggesting that the scope of this methodology might be broader than previously anticipated.

CRediT authorship contribution statement

Sachin Gupta: Methodology, Validation, Formal analysis, Investigation, Data curation, Writing – review & editing, Visualization. **Vladimír Raus:** Conceptualization, Methodology, Writing – original draft, Writing – review & editing, Supervision, Project administration, Funding acquisition.

Declaration of Competing Interest

The authors declare that they have no known competing financial interests or personal relationships that could have appeared to influence the work reported in this paper.

Data availability

Data will be made available on request.

Acknowledgements

The authors thank Dr. Lívia Kanizsová for performing the GC analysis of HEMA monomers and to Ms. Eva Čadová for performing the SEC analysis in THF. Sachin Gupta is a PhD student at Charles University, Prague, Czech Republic.

Appendix A. Supplementary data

Supplementary data to this article can be found online at https://doi.org/10.1016/j.reactfunctpolym.2023.105509.

References

[1] O. Wichterle, D. Lím, Hydrophilic gels for biological use, Nature 185 (4706) (1960) 117–118.
[2] J. Kopecek, Hydrogels: from soft contact lenses and implants to self-assembled nanomaterials, J. Polym. Sci., Part A: Polym. Chem. 47 (22) (2009) 5929–5946.
[3] M. Dreifus, O. Wichterle, Clinical experiences with hydrogel contact lenses, Cesk. Oftalmol. 20 (1964) 393–399.
[4] R. Menapace, C. Skorpik, M. Juchem, W. Scheidel, R. Schranz, Evaluation of the first 60 cases of poly HEMA posterior chamber lenses implanted in the sulcus, J Cataract Refract Surg 15 (3) (1989) 264–271.
[5] L. Krejci, R. Harrison, O. Wichterle, Hydroxyethyl methacrylate capillary strip: animal trials with a new Glaucoma drainage device, Arch. Ophthalmol. 84 (1) (1970) 76–82.
[6] D. Horák, H. Hlídková, J. Hradil, M. Lapčíková, M. Šlouf, Superporous poly(2-hydroxyethyl methacrylate) based scaffolds: preparation and characterization, Polymer 49 (8) (2008) 2046–2054.
[7] L. Poláková, V. Raus, L. Kostka, A. Braunová, J. Pilař, V. Lobaz, J. Pánek, Z. Sedláková, Antioxidant properties of 2-hydroxyethyl methacrylate-based copolymers with incorporated sterically hindered amine, Biomacromolecules 16 (9) (2015) 2726–2734.
[8] L. Poláková, V. Raus, L. Cuchalová, R. Poręba, M. Hrubý, J. Kučka, D. Větvička, O. Trhlíková, Z. Sedláková, SHARP hydrogel for the treatment of inflammatory bowel disease, Int. J. Pharm. 613 (2022), 121392.
[9] H. Kakwere, S. Perrier, Design of complex polymeric architectures and nanostructured materials/hybrids by living radical polymerization of hydroxylated monomers, Polym. Chem. 2 (2) (2011) 270–288.
[10] K.L. Beers, S. Boo, S.G. Gaynor, K. Matyjaszewski, Atom transfer radical polymerization of 2-hydroxyethyl methacrylate, Macromolecules 32 (18) (1999) 5772–5776.
[11] K.L. Robinson, M.A. Khan, M.V. de Paz Báñez, X.S. Wang, S.P. Armes, Controlled polymerization of 2-hydroxyethyl methacrylate by ATRP at ambient temperature, Macromolecules 34 (10) (2001) 3155–3158.
[12] J.V.M. Weaver, I. Bannister, K.L. Robinson, X. Bories-Azeau, S.P. Armes, M. Smallridge, P. McKenna, Stimulus-responsive water-soluble polymers based on 2-hydroxyethyl methacrylate, Macromolecules 37 (7) (2004) 2395–2403.
[13] P.D. Topham, N. Sandon, E.S. Read, J. Madsen, A.J. Ryan, S.P. Armes, Facile synthesis of well-defined hydrophilic methacrylic macromonomers using ATRP and click chemistry, Macromolecules 41 (24) (2008) 9542–9547.
[14] P. Yang, S.P. Armes, Preparation of well-defined poly(2-hydroxyethyl methacrylate) macromonomers via atom transfer radical polymerization, Macromol. Rapid Commun. 35 (2) (2014) 242–248.
[15] B. Reining, H. Keul, H. Höcker, Block copolymers comprising poly(ethylene oxide) and poly(hydroxyethyl methacrylate) blocks: synthesis and characterization, Polymer 43 (11) (2002) 3139–3145.
[16] C. Hou, S. Lin, F. Liu, J. Hu, G. Zhang, G. Liu, Y. Tu, H. Zou, H. Luo, Synthesis of poly(2-hydroxyethyl methacrylate) end-capped with asymmetric functional groups via atom transfer radical polymerization, New J. Chem. 38 (6) (2014) 2538–2547.
[17] J.K. Oh, K. Matyjaszewski, Synthesis of poly(2-hydroxyethyl methacrylate) in protic media through atom transfer radical polymerization using activators generated by electron transfer, J. Polym. Sci., Part A: Polym. Chem. 44 (12) (2006) 3787–3796.
[18] S.M. Paterson, D.H. Brown, T.V. Chirila, I. Keen, A.K. Whittaker, M.V. Baker, The synthesis of water-soluble PHEMA via ARGET ATRP in protic media, J. Polym. Sci., Part A: Polym. Chem. 48 (18) (2010) 4084–4092.
[19] L.S. Connell, J.R. Jones, J.V.M. Weaver, Transesterification of functional methacrylate monomers during alcoholic copper-catalyzed atom transfer radical polymerization: formation of compositional and architectural side products, Polym. Chem. 3 (10) (2012) 2735–2738.
[20] N.H. Nguyen, X. Leng, V. Percec, Synthesis of ultrahigh molar mass poly(2-hydroxyethyl methacrylate) by single-electron transfer living radical polymerization, Polym. Chem. 4 (9) (2013) 2760–2766.
[21] L. Yuan, W. Chen, J. Li, J. Hu, J. Yan, D. Yang, PEG-b-PtBA-b-PHEMA well-defined amphiphilic triblock copolymer: synthesis, self-assembly, and application in drug delivery, J. Polym. Sci., Part A: Polym. Chem. 50 (21) (2012) 4579–4588.
[22] P. Ritz, P. Látalová, J. Kříž, J. Genzer, P. Vlček, Statistical copolymers of 2-(trimethylsilyloxy)ethyl methacrylate and methyl methacrylate synthesized by ATRP, J. Polym. Sci., Part A: Polym. Chem. 46 (5) (2008) 1919–1923.
[23] P. Liu, L. Jin, J. Hu, C. Wang, Synthesis of well-defined comb-like amphiphilic copolymers with protonizable units in the pendent chains: 1. Preparation of narrow polydispersity copolymers of methyl methacrylate and 2-hydroxyethyl methacrylate by atom-transfer radical polymerization, Polym. Int. 53 (2) (2004) 136–141.
[24] V. Percec, T. Guliashvili, J.S. Ladislaw, A. Wistrand, A. Stjerndahl, M. J. Sienkowska, M.J. Monteiro, S. Sahoo, Ultrafast synthesis of ultrahigh molar mass polymers by metal-catalyzed living radical polymerization of acrylates, methacrylates, and vinyl chloride mediated by SET at 25 °C, J. Am. Chem. Soc. 128 (43) (2006) 14156–14165.
[25] B.M. Rosen, V. Percec, Single-electron transfer and single-electron transfer degenerative chain transfer living radical polymerization, Chem. Rev. 109 (11) (2009) 5069–5119.
[26] Y. Zhang, Y. Wang, C.-H. Peng, M. Zhong, W. Zhu, D. Konkolewicz, K. Matyjaszewski, Copper-mediated CRP of methyl acrylate in the presence of metallic copper: effect of ligand structure on reaction kinetics, Macromolecules 45 (1) (2012) 78–86.
[27] R. Whitfield, A. Anastasaki, V. Nikolaou, G.R. Jones, N.G. Engelis, E.H. Discekici, C. Fleischmann, J. Willenbacher, C.J. Hawker, D.M. Haddleton, Universal conditions for the controlled polymerization of acrylates, methacrylates, and styrene via cu(0)-RDRP, J. Am. Chem. Soc. 139 (2) (2017) 1003–1010.
[28] A. Anastasaki, V. Nikolaou, G. Nurumbetov, P. Wilson, K. Kempe, J.F. Quinn, T. P. Davis, M.R. Whittaker, D.M. Haddleton, Cu(0)-mediated living radical polymerization: a versatile tool for materials synthesis, Chem. Rev. 116 (3) (2016) 835–877.
[29] G.R. Jones, A. Anastasaki, R. Whitfield, N. Engelis, E. Liarou, D.M. Haddleton, Copper-mediated reversible deactivation radical polymerization in aqueous media, Angew. Chem. Int. Ed. 57 (33) (2018) 10468–10482.
[30] Q. Zhang, P. Wilson, Z. Li, R. McHale, J. Godfrey, A. Anastasaki, C. Waldron, D. M. Haddleton, Aqueous copper-mediated living polymerization: exploiting rapid disproportionation of CuBr with Me6TREN, J. Am. Chem. Soc. 135 (19) (2013) 7355–7363.
[31] V. Raus, L. Kostka, Optimizing the Cu-RDRP of N-(2-hydroxypropyl) methacrylamide toward biomedical applications, Polym. Chem. 10 (5) (2019) 564–568.
[32] V. Raus, A. Hološ, J. Kronek, J. Mosnáček, Well-defined linear and grafted poly(2-isopropenyl-2-oxazoline)s prepared via copper-mediated reversible-deactivation radical polymerization methods, Macromolecules 53 (6) (2020) 2077–2087.
[33] M.J. Monteiro, T. Guliashvili, V. Percec, Kinetic simulation of single electron transfer–living radical polymerization of methyl acrylate at 25 °C, J. Polym. Sci., Part A: Polym. Chem. 45 (10) (2007) 1835–1847.
[34] G. Lligadas, V. Percec, A comparative analysis of SET-LRP of MA in solvents mediating different degrees of disproportionation of Cu(I)Br, J. Polym. Sci., Part A: Polym. Chem. 46 (20) (2008) 6880–6895.
[35] P.M. Wright, G. Mantovani, D.M. Haddleton, Polymerization of methyl acrylate mediated by copper(0)/Me6-TREN in hydrophobic media enhanced by phenols; single electron transfer-living radical polymerization, J. Polym. Sci., Part A: Polym. Chem. 46 (22) (2008) 7376–7385.
[36] J. Tom, B. Hornby, A. West, S. Harrisson, S. Perrier, Copper(0)-mediated living radical polymerization of styrene, Polym. Chem. 1 (4) (2010).
[37] B.D. Hornby, A.G. West, J.C. Tom, C. Waterson, S. Harrisson, S. Perrier, Copper(0)-mediated living radical polymerization of methyl methacrylate in a non-polar solvent, Macromol. Rapid Commun. 31 (14) (2010) 1276–1280.
[38] A.G. West, B. Hornby, J. Tom, V. Ladmiral, S. Harrisson, S. Perrier, Origin of initial uncontrolled polymerization and its suppression in the copper(0)-mediated living radical polymerization of methyl acrylate in a nonpolar solvent, Macromolecules 44 (20) (2011) 8034–8041.
[39] Y.-P. Miao, J. Lyu, H.-Y. Yong, S. A, Y.-S. Gao, W.-X. Wang, Controlled polymerization of methyl methacrylate and styrene via Cu(0)-mediated RDRP by selecting the optimal reaction conditions, Chin. J. Polym. Sci. 37 (6) (2019) 591–597.
[40] V. Raus, M. Janata, E. Čadová, Copper wire–catalyzed RDRP in nonpolar media as a route to ultrahigh molecular weight organic–inorganic hybrid polymers, Macromol. Chem. Phys. 219 (14) (2018) 1800141.
[41] G.J.P. Britovsek, J. England, A.J.P. White, Non-heme Iron(II) complexes containing tripodal tetradentate nitrogen ligands and their application in alkane oxidation catalysis, Inorg. Chem. 44 (22) (2005) 8125–8134.
[42] O. Wichterle, R. Chromeček, Polymerization of ethylene glycol monomethacrylate in the presence of solvents, J. Polym. Sci., Part C: Polym. Symp. 16 (8) (1967) 4677–4686.
[43] C. Reichardt, Empirical parameters of solvent polarity as linear free-energy relationships, Angew. Chem. Int. Ed. Eng. 18 (2) (1979) 98–110.
[44] G. Cinacchi, F. Ingrosso, A. Tani, Solvation dynamics by computer simulation: coumarin C153 in 1,4-dioxane, J. Phys. Chem. B 110 (27) (2006) 13633–13641.

[45] W. Tang, Y. Kwak, W. Braunecker, N.V. Tsarevsky, M.L. Coote, K. Matyjaszewski, Understanding atom transfer radical polymerization: effect of ligand and initiator structures on the equilibrium constants, J. Am. Chem. Soc. 130 (32) (2008) 10702–10713.
[46] K. Matyjaszewski, W. Jakubowski, K. Min, W. Tang, J. Huang, W.A. Braunecker, N. V. Tsarevsky, Diminishing catalyst concentration in atom transfer radical polymerization with reducing agents, Proc. Natl. Acad. Sci. U. S. A. 103 (42) (2006) 15309.
[47] W. Jakubowski, K. Matyjaszewski, Activators regenerated by electron transfer for atom-transfer radical polymerization of (meth)acrylates and related block copolymers, Angew. Chem. Int. Ed. 45 (27) (2006) 4482–4486.
[48] T.R. Rooney, R.A. Hutchinson, Monomer structure and solvent effects on copolymer composition in (meth)acrylate radical copolymerization, Ind. Eng. Chem. Res. 57 (15) (2018) 5215–5227.

Supporting Information for:

Cu(0)-RDRP of 2-hydroxyethyl methacrylate in a non-polar solvent enables rapid synthesis of high-molecular weight homopolymers and direct access to amphiphilic copolymers

Sachin Gupta and Vladimír Raus*

Institute of Macromolecular Chemistry, Czech Academy of Sciences, Heyrovského nám. 2, 162 06 Prague 6, Czech Republic

*email: raus@imc.cas.cz

EXPERIMENTAL

Determination of the dn/dc value of poly(HEMA)

The dn/dc value for poly(HEMA) was obtained by an on-line determination assuming 100% sample recovery. Since crude polymerization mixtures were analyzed in this work, the actual concentration of poly(HEMA) in each SEC sample was calculated using the known monomer content in the polymerization mixture and the monomer conversion determined by ^{1}H NMR. The dn/dc value of 0.078 ± 0.003 mL/g was determined as an average of multiple measurements and subsequently employed in the MW determination for all the reported samples analyzed by SEC-LS. Properly stabilized samples of the polymerization mixtures were used for this determination (see the discussion accompanying the experimental procedure in the main text). Note that we also attempted on an external determination of an isolated poly(HEMA) sample using a Brookhaven Instruments BI-DNDC differential refractometer in a batch mode (in DMAc/LiBr (5 g/L) at 55 °C); however, considerably lower dn/dc value (0.051 mL/g) was obtained, probably due to the impurities present in the sample, which led to inflated MW values when applying this dn/dc value. We presume that the dn/dc value determined by the former (on-line) method is considerably more accurate as the influence of impurities (e.g. water and solvents used for polymerization mixture dilution and polymer precipitation) is largely eliminated. This observation should be relevant for a range of polar monomers that are often difficult to dry completely and that often show a strong affinity to organic solvents.[1] It is noteworthy that the dn/dc value determined through the preferred on-line method is close to that for poly(HEMA) measured in DMF as reported in Polymer Handbook (0.076 mL/g).[2]

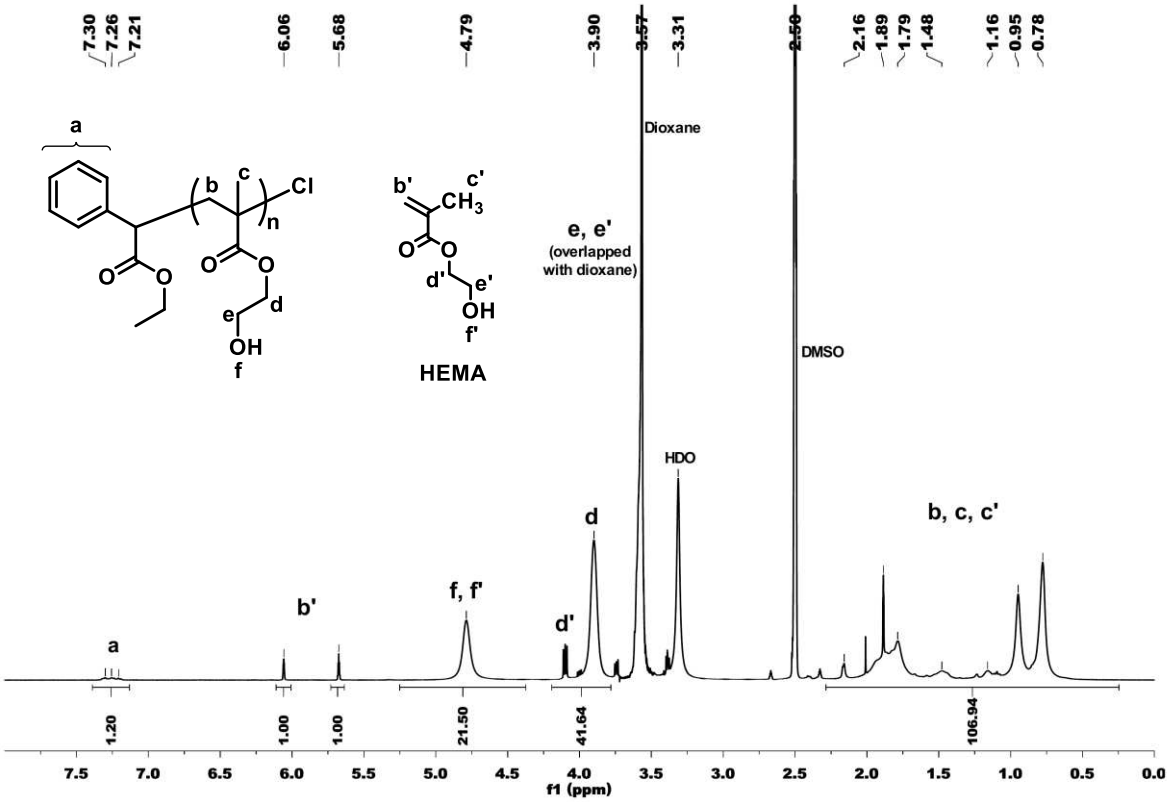

Figure S1. A typical ^{1}H NMR spectrum of a crude polymerization mixture from Cu(0)-RDRP of HEMA in dioxane (the experiment from entry 4, Table 1). The analysis was performed in DMSO-*d6*. Monomer conversion was calculated based on the intensity of the signals corresponding to the unreacted monomer at 5.68 and 6.06 ppm and the monomer/polymer signals between 0.5 ppm to 2.2 ppm.

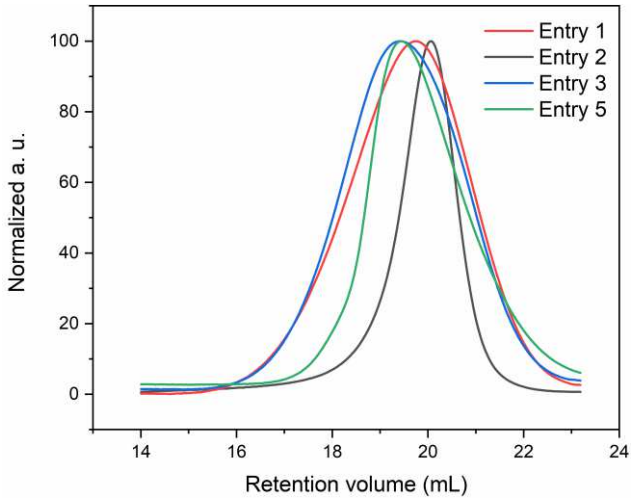

Figure S2. SEC elugrams (RI traces) of poly(HEMA) obtained via Cu(0)-RDRP in dioxane under different conditions. Numbering of the traces corresponds to Table 1 where experimental details can be found.

Table S1. Additional experiments for Cu(0)-RDRP of HEMA in dioxane[a]

Entry	M/I	$CuCl_2$ (eq.)	Time (min)	Conv. (%)[b]	M_n (theor.)[c]	M_n (SEC)[d]	Đ[d]
1	400:1	0.2	60	87	45 300	68 000	1.28
2	1000:1	0.5	90	75	97 600	169 400	1.53
3	400:1	0.5	60	92	47 900	70 000	1.47

[a] Standard polymerization conditions: ECPA/PMDETA = 1:1, 5 cm of activated copper wire, dioxane/HEMA = 1:1 (v/v). HEMA monomer purified only by distillation, containing 0.1 wt.% of residual EGDMA crosslinker, was used.

[b] Monomer conversion as determined by a ^1H NMR analysis.

[c] Theoretical M_n calculated from the M/I ratio and conversion.

[d] Determined by SEC with LS detection.

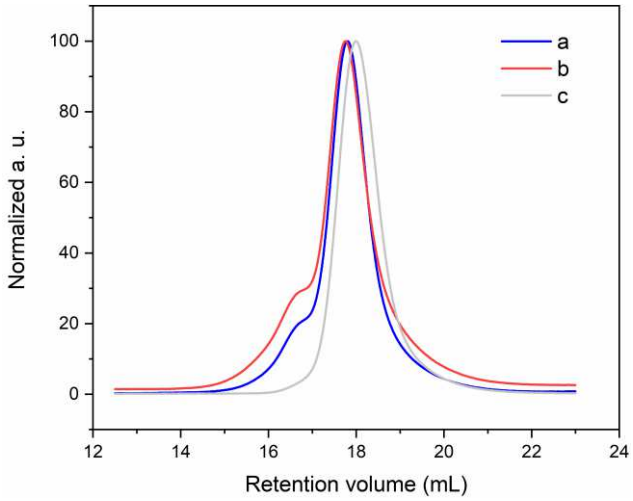

Figure S3. SEC elugrams (RI traces) of poly(HEMA) obtained at the M/I = 400:1 ratio via Cu(0)-RDRP of non-purified HEMA using (a) 0.2 eq. of $CuCl_2$ (entry 1, Table S1), and (b) 0.5 eq. $CuCl_2$ (entry 3, Table S1). Data for the experiment where purified HEMA with minimized EGDMA content, using 0.2 eq. of $CuCl_2$ (entry 2, Table 2) is displayed for a comparison (c).

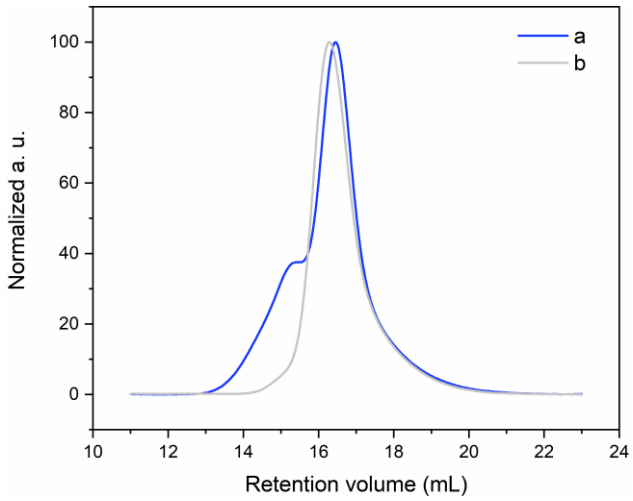

Figure S4. SEC elugrams (RI traces) of poly(HEMA) obtained at the M/I = 1000:1 ratio via Cu(0)-RDRP of non-purified HEMA (entry 2, Table S1) (a). Data for the experiment where purified HEMA with minimized EGDMA content was used (entry 3, Table 2) is displayed for a comparison (b).

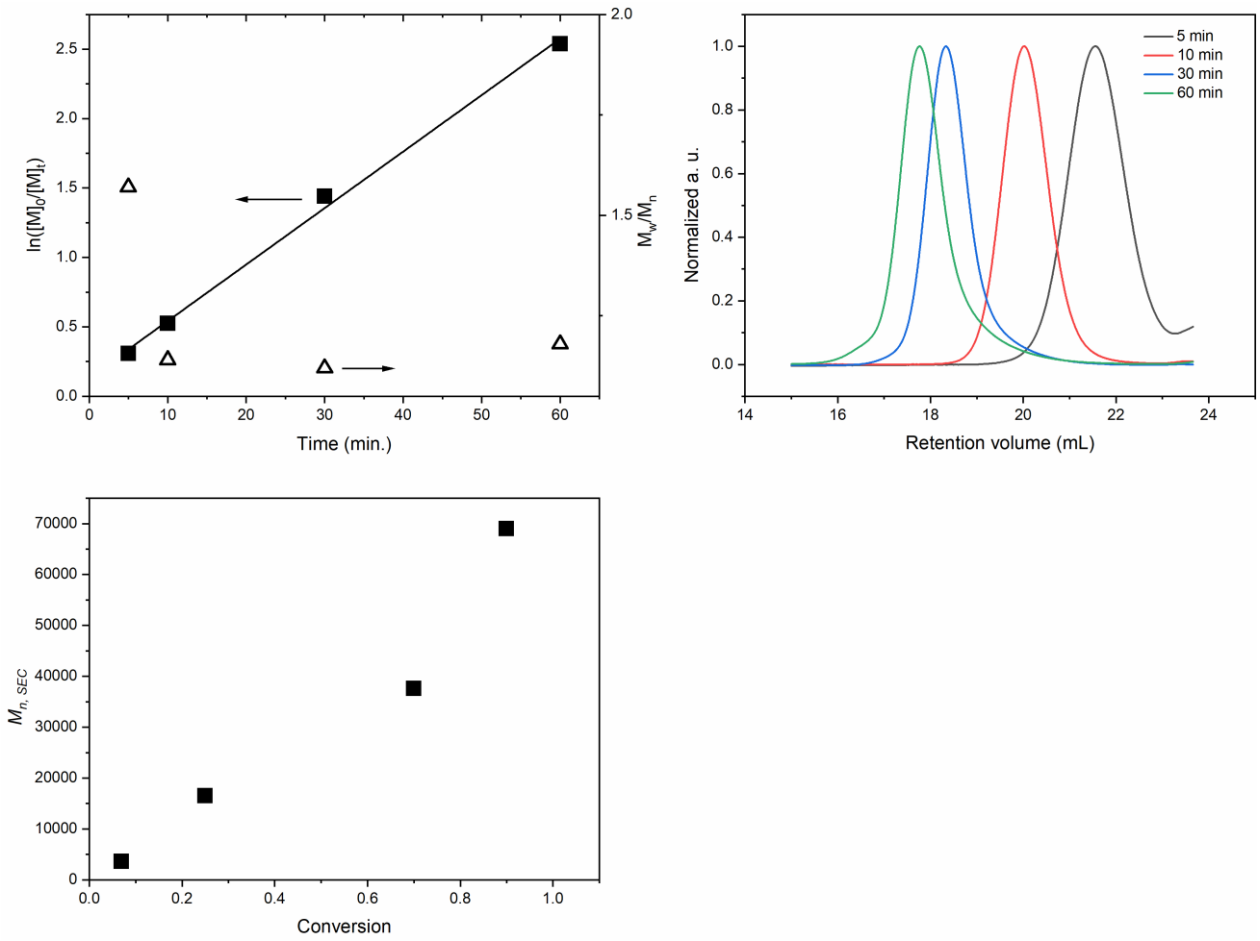

Figure S5. Kinetics of Cu(0)-RDRP of HEMA at M/I = 400:1 (for experimental conditions and sample analysis see Table S2). Top, left: the semilogarithmic plot and the development of dispersity; the full line represents a linear fit of the semilogarithmic plot. Bottom, left: the development of M_n (as measured by SEC-LS) with conversion. Top, right: SEC elugrams (RI traces) of the kinetic samples.

Table S2. Experimental data for the kinetics of HEMA homopolymerization at M/I of 400:1 (Figure S5)[a]

Sample	Time (min)	Conv. (%)[b]	M_n (theor.)[c]	M_n (SEC)[d]	Đ[d]
1	5	7	3600	3600	1.57
2	10	25	13000	16500	1.14
3	30	70	36500	50000	1.12
4	60	90	47000	69000	1.18

[a] Polymerization conditions: ECPA/PMDETA/$CuCl_2$ = 1:1:0.2, 5 cm of activated copper wire, dioxane/HEMA = 1:1 (v/v), purified monomer with minimized EGDMA content.

[b] Monomer conversion as determined by a ^{1}H NMR analysis.

[c] Theoretical M_n calculated from the M/I ratio and conversion.

[d] Determined by SEC with LS detection.

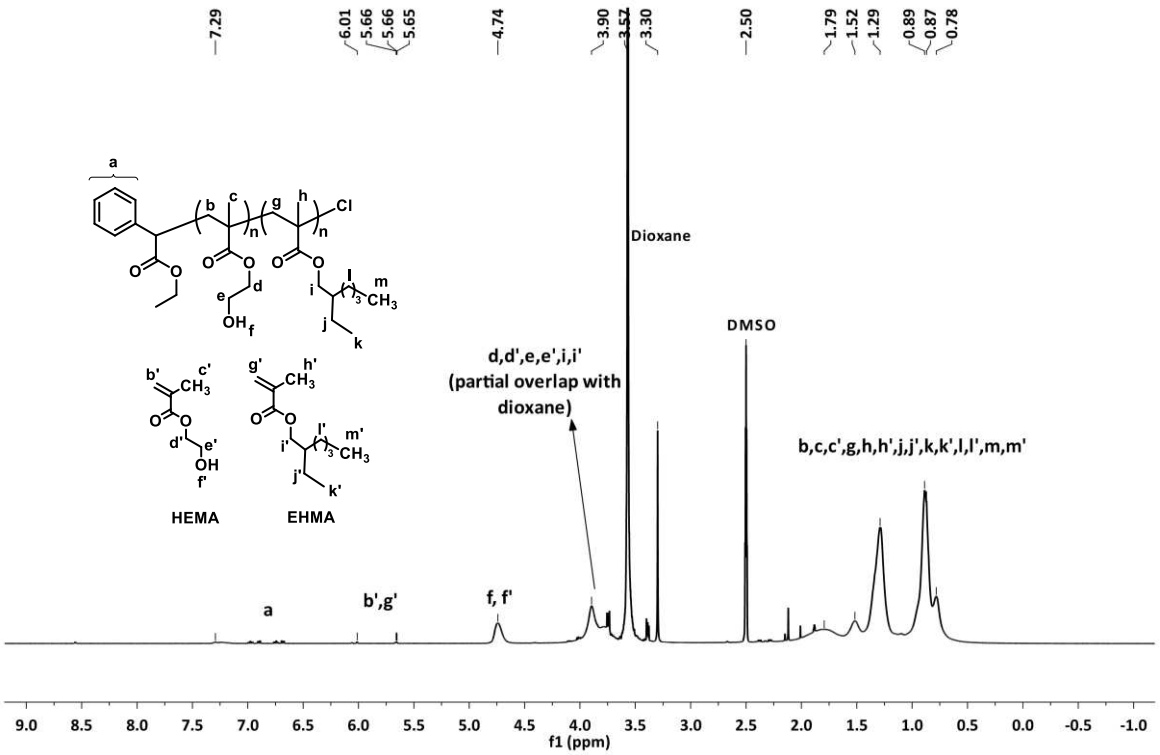

Figure S6. ^{1}H NMR spectrum of a crude polymerization mixture from the copolymerization of HEMA and EHMA via Cu(0)-RDRP in dioxane (HEMA/EHMA/ECPA/PMDETA/$CuCl_2$ = 50:50:1:1:0.2, 5 cm of copper wire, monomers/dioxane = 1:1 v/v, 85°C). The analysis was performed in DMSO-*d6*.

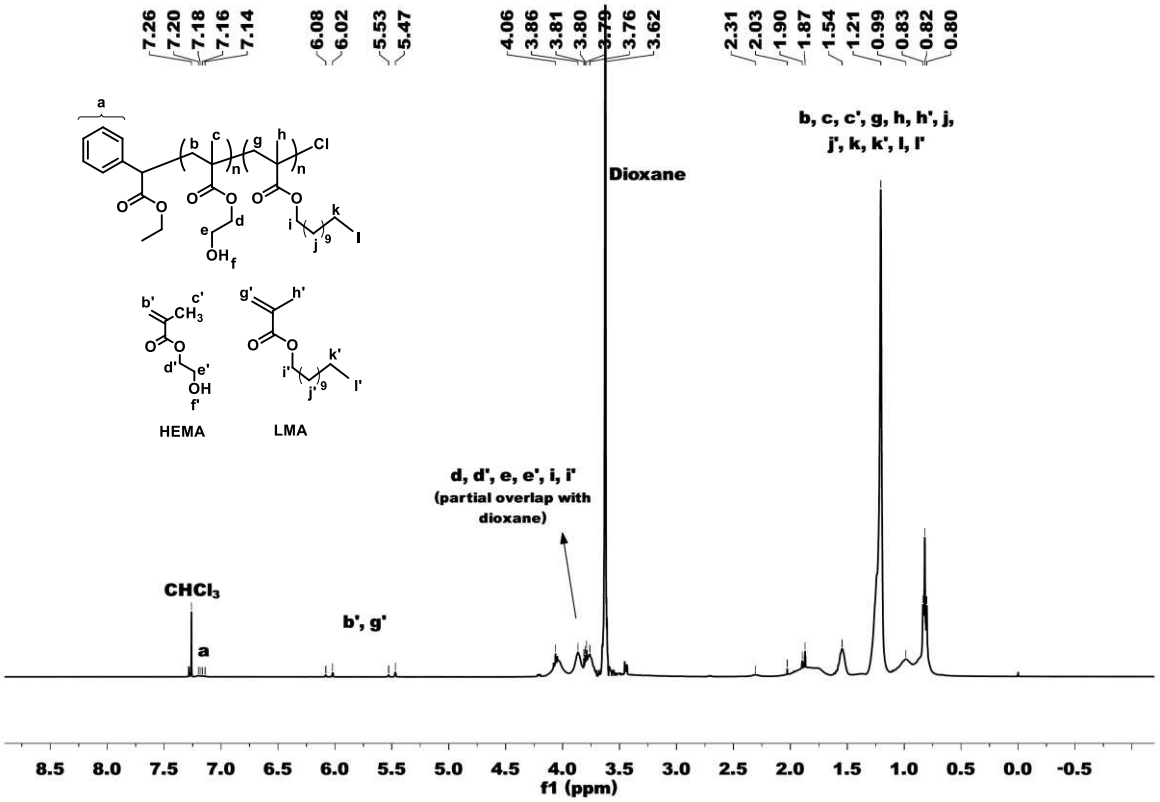

Figure S7. ^{1}H NMR spectrum of a crude polymerization mixture from the copolymerization of HEMA and LMA via Cu(0)-RDRP in dioxane (HEMA/LMA/ECPA/PMDETA/$CuCl_2$ = 50:50:1:1:0.2, 5 cm of copper wire, monomers/dioxane = 1:1 v/v, 85°C). The analysis was performed in $CDCl_3$.

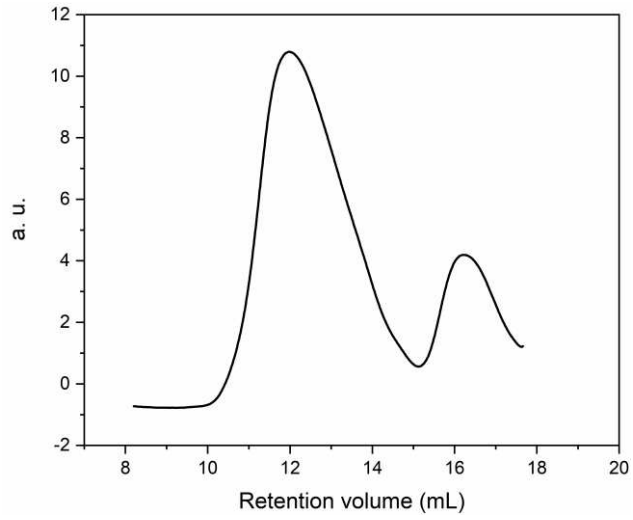

Figure S8. SEC elugram (RI trace) of poly(HEMA-*co*-LMA) obtained via Cu(0)-RDRP in DMSO according to a published procedure (HEMA/LMA/MBPA/Me_6TREN/$CuBr_2$ = 50:50:1:0.1:0.05, 5 cm of copper wire, monomers/DMSO = 1:1 v/v, r.t.).[3] The analysis was performed in THF with poly(methyl methacrylate) calibration; the obtained values (M_n = 357 000 and Đ = 2.35 for the main peak) are thus relative.

REFERENCES

1. Raus, V.; Hološ, A.; Kronek, J.; Mosnáček, J. Well-Defined Linear and Grafted Poly(2-isopropenyl-2-oxazoline)s Prepared via Copper-Mediated Reversible-Deactivation Radical Polymerization Methods. *Macromolecules* **2020,** 53 (6), 2077-2087.
2. Michielsen, S., Polymer handbook. In *Polymer handbook*, 4th ed ed.; Brandrup, J.; Immergut, E. H.; Grulke, E. A., Eds. Wiley: New York, 2004; p 547.
3. Nguyen, N. H.; Leng, X.; Percec, V. Synthesis of ultrahigh molar mass poly(2-hydroxyethyl methacrylate) by single-electron transfer living radical polymerization. *Polym. Chem.* **2013,** 4 (9), 2760-2766.

Straightforward synthesis of complex polymeric architectures with ultra-high chain density

*Sachin Gupta, Miroslav Janata, Eva Čadová, and Vladimír Raus**

Institute of Macromolecular Chemistry, Czech Academy of Sciences, Heyrovského nám. 2, 162 06, Prague 6, Czech Republic

E-mail: raus@imc.cas.cz

ABSTRACT

Synthesis of complex polymeric architectures (CPAs) via reversible-deactivation radical polymerization (RDRP) currently relies on the rather inefficient attachment of monofunctional initiation/transfer sites onto CPA precursors. This drawback seriously limits the overall functionality of the resulting (macro)initiators and, consequently, also the total number of installable polymeric chains, which represents a significant bottleneck in the design of new polymeric materials. Here, we show that the (macro)initiator functionality can be substantially amplified by using trichloroacetyl isocyanate as a highly efficient vehicle for the rapid and clean introduction of trichloroacetyl groups (TAGs) into diverse precursors. Through extensive screening of polymerization conditions and comprehensive NMR and triple-detection SEC studies, we demonstrate that TAGs function as universal trifunctional initiators of copper-mediated RDRP of different monomer classes, affording low-dispersity polymers in a wide molecular weight range. We thus unlock an access to a whole new group of ultra-high chain density CPAs previously inaccessible via simple RDRP protocols. We highlight new opportunities in CPA synthesis through numerous examples, including the *de novo* one-pot synthesis of a novel "star-on-star" CPA, the preparation of β-cyclodextrin-based 45-arm star polymers, and facile grafting from otherwise problematic cellulose substrates both in solution and from surface, obtaining effortlessly ultra-dense, ultra-high-molecular weight bottle-brush copolymers and thick spatially-controlled polymeric coatings, respectively.

INTRODUCTION

Complex polymeric architectures (CPAs), such as star,[1] dendrimer,[2] graft,[3] bottle-brush,[4] or hyperbranched[5] (co)polymers, are characterized by an additional layer of intricacy endowing these polymeric objects with unique physical properties and an ability to self-assemble into higher-order structures. Owing to their intriguing features, CPAs have found multiple applications in diverse fields, including drug delivery,[6-9] bioimaging,[10] catalysis,[11] nanotemplating,[12-14] photonics,[15] or super-elastomers.[16-18]

Reversible-deactivation radical polymerization (RDRP) methods, and particularly copper-mediated RDRP (Cu-RDRP) and reversible addition-fragmentation chain transfer (RAFT), represent powerful tools for precisely controlling composition, functionality, and topology of polymeric chains, enabling thus a straightforward access to unique CPAs otherwise unattainable with conventional polymerization techniques.[19,20] In the key step of CPA synthesis via RDRP, a CPA precursor is decorated with specific functionalities, such as initiators in Cu-RDRP or transfer agents in RAFT, that predetermine the sites of the future polymer chain attachment or growth. The concentration and distribution of these sites within the precursor is essential for determining key CPA characteristics, such as grafting density in graft copolymers or the number of arms in star polymers, and thus the (co)polymer's macroscopic

properties and application prospects.[3] Importantly, the current implementation of the RDRP strategy operates almost exclusively with monofunctional initiation/transfer sites, allowing for a maximum of one polymeric chain per site. Unfortunately, this inherent limitation is often further exacerbated by the inefficiency of the reactions used for the initiation/transfer site attachment and by the decreased initiation efficiency (IE) observed in some Cu-RDRP systems.[21] Collectively, these shortcomings impose significant limitations on the total number of polymeric chains that could be installed onto a given CPA precursor, which is detrimental in applications relying on high grafting density[14,22] and generally represents a clear bottle-neck in macromolecular design.

Cu-RDRP can potentially provide an elegant solution to some of these drawbacks in the form of multifunctional initiation sites. In multifunctional Cu-RDRP initiators (e.g., CCl_4 or α-di/trichloro esters), more than one of the present carbon-halogen bonds can theoretically undergo activation by a copper catalyst, initiating the growth of multiple polymeric chains from a single carbon atom. In the case of CPA synthesis, bi- or trifunctional initiation sites could possibly be employed, providing instantaneous amplification of the functionality of the precursor-derived (macro)initiator. Interestingly, multifunctional initiators have been considered since the early days of Cu-RDRP but never achieved a widespread use.[23-25] This can be ascribed to the uncertainty about the actual functionality of these compounds and also the field's rapid adoption of active (monofunctional) brominated initiators, such as those containing 2-bromoisobutyryl (BriB) group, that became the preferred choice in many Cu-RDRP scenarios, including CPA synthesis.[14,26-30] A rare example of multifunctional Cu-RDRP initiator usage in CPA synthesis was the grafting from cellulose esters decorated with bifunctional dichloroacetate initiation sites reported by Vlček et al.[31,32] However, while these pioneering efforts resulted in a comparatively higher grafting density, they suffered from two serious limitations. Firstly, the dichloroacetate initiator lacked universality, being successfully used for methacrylates only. More importantly, the grafting density was still seriously diminished by the typical inefficiency of the initiation site attachment that traditionally relies on the acylation of precursor's hydroxyl or amino groups with an α-haloacyl halide, whereby only relatively little initiator is often introduced despite using a large excess of the acylation reagent.[14,31,33,34] While this issue is also relevant to small-molecule CPA precursors,[34] it is particularly pronounced for macromolecular substrates such as cellulose where the supramolecular structure significantly diminishes the acylation efficiency,[14,30,33] necessitating the development of elaborate, multi-step strategies to prepare densely-grafted products.[14] Furthermore, the standard acylation protocols generate byproducts that need to be removed in a separate step via recrystallization/chromatography (for small molecules)[34-36] or precipitation/extraction (for macromolecular precursors).[14,32,33,37] In addition, long reaction times ranging from several hours up to a week are typically used in these transformations.[13,14,35,38] Collectively, the described limitations have so far prevented the macromolecular community from exploiting the full potential of multifunctional Cu-RDRP initiating sites in CPA synthesis.

Clearly, several criteria have to be met in order to successfully amplify the (macro)initiator functionality through multifunctional Cu-RDRP initiation sites and enable thus the synthesis of CPAs with a severalfold higher number of polymeric chains as compared to current protocols. Firstly, the multifunctional initiation sites must be sufficiently universal, that is, applicable to different monomer classes, ideally under diverse polymerization conditions. Further, the IE should be sufficiently high with respect to both the entire (macro)initiator and the individual multifunctional initiation sites where activation of all the available carbon-halogen bonds should be feasible. Finally, the introduction of multifunctional initiation sites into CPA precursors must be considerably more efficient than with the contemporary acylation protocols.

Herein, we hypothesize that adducts of trichloroacetyl isocyanate (TAI) can potentially meet all these criteria. TAI is a commercially available *in situ* derivatizing reagent used in NMR spectroscopy to facilitate structural assignment of compounds bearing hydroxy,[39-42] thio,[43] and amino[40] groups. In most cases, these moieties undergo rapid, quantitative, and uncomplicated 1,2-addition reactions with TAI, affording carbamate, thiocarbamate, and urea derivatives, respectively. The TAI method is also routinely applied for end-groups analysis in polymer chemistry.[44-48] Besides 1,2-additions, TAI can take part in other reactions, which increases the diversity of CPA precursors it can modify (**Scheme 1a**).[39,49] We propose here that TAI can be repurposed as a highly efficient vehicle for installing trichloroacetyl groups (TAGs) onto a variety of small-molecule- and macromolecular CPA precursors, avoiding the limitations of the traditional acylation approach. Importantly, several studies used TAG-bearing compounds as initiators for transition metal-catalyzed RDRP of different monomers,[23,24,50-54] and there is limited evidence that TAGs can act as bi- or trifunctional initiators.[23,53] Additionally, the utility of halo-isocyanates as initiating site precursors in the block and graft copolymer synthesis via free-radical polymerization has been recognized already in 1980s by Bamford and coworkers.[55-59] As visualized in **Scheme 1b**, the unique combination of TAI reactivity and TAG multifunctionality could effectively amplify the CPA (macro)initiator functionality and provide thus an access to a whole new group of CPAs characterized by dramatically increased chain density and, potentially, new properties and applications.

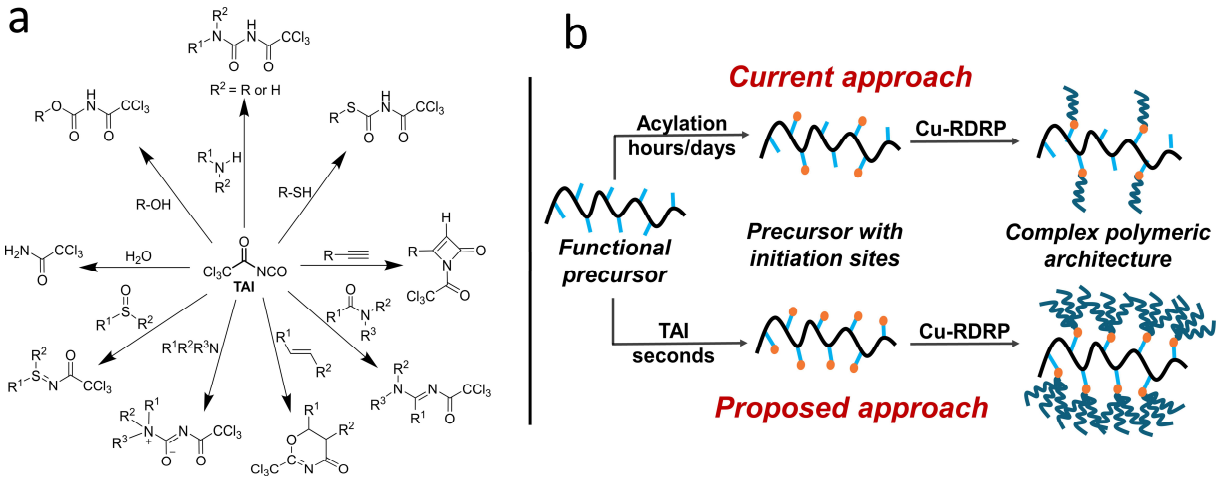

Scheme 1. (a) Selected reactions of TAI deemed as relevant to polymer chemistry; (b) a scheme contrasting the number of chains installed onto a CPA precursor using the current and the newly proposed (TAI-based) approach.

In this study, we strived to firmly establish the TAI-based Cu-RDRP strategy as a powerful yet simple tool in CPA synthesis. To this end, we investigated and confirmed the considerable universality of TAI-derived initiators by identifying the polymerization conditions under which well-controlled Cu-RDRP of different monomer classes can be achieved. Subsequently, we used ^{1}H NMR spectroscopy and triple-detection size-exclusion chromatography (TD-SEC) to prove conclusively that the TAI-derived TAGs act as inherently trifunctional initiators, which has a profound impact on the topology of the attained polymeric architectures and distinguishes the TAI-based strategy from earlier RDRP approaches. Finally, we provide examples documenting the strong points of the new strategy in various relevant scenarios such as the (one-pot) synthesis of star-shaped and branched CPAs, including a novel "star-on-star" graft copolymer topology, and the modification of otherwise problematic cellulose substrates

yielding ultra-high-MW ultra-dense bottle-brush copolymers and diverse surface-grafted "2D" and 3D objects with unprecedented ease.

RESULTS AND DISCUSSION

Developing conditions for Cu-RDRP initiated by TAI adducts

In order to probe the universality of TAI-derived initiators, we conducted an extensive screening of multiple polymerization parameters, seeking conditions under which well-controlled Cu-RDRP, characterized by low dispersity and pre-determined MWs of products, can be achieved for monomers from different classes: styrene, acrylates, and methacrylates (**Scheme 2**).

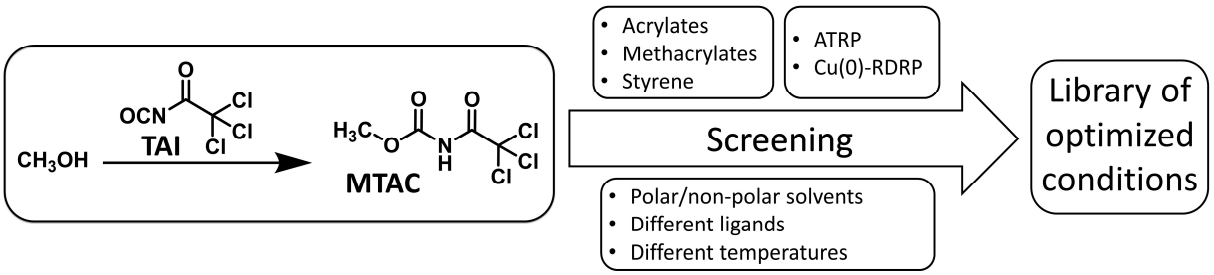

Scheme 2. The workflow of the polymerization conditions screening.

In the optimization study, we used methyl acrylate (MA), methyl methacrylate (MMA), and styrene as model monomers together with a model initiator, methyl *N*-trichloroacetyl carbamate (MTAC), that was readily obtained by the addition of TAI into dry methanol, followed by the evaporation of the methanol excess (**Scheme 2**, **Figure S1**). We investigated two Cu-RDRP approaches, namely (conventional) atom transfer radical polymerization (ATRP)[26,60] and Cu(0)-mediated RDRP [Cu(0)-RDRP],[61] employing Cu(I) salts (CuBr or CuCl) and Cu(0) (activated copper wire) as catalysts, respectively. Note that Cu(0)-RDRP is sometimes denoted as single-electron transfer living radical polymerization (SET-LRP)[62,63] or supplemental activation reducing agent (SARA) ATRP[64,65] with reference to the expected polymerization mechanism; since we do not address the mechanism in this study, we opted for the generic term Cu(0)-RDRP. Me_6TREN and PMDETA were used as ligands at different ligand/initiator ratios. Solvents of different polarity were tested to enable future application of the developed strategy to CPA precursors of different solubility. Temperatures ranging from r.t. to 110 °C were utilized depending on the targeted monomer. The monomer/initiator (M/I) ratio of 200:1 was used in optimization runs, with other M/I ratios subsequently employed under selected conditions. MW and dispersity values were obtained through size-exclusion chromatography (SEC) calibrated with appropriate standards.

In **Table 1**, we summarize the selected optimized polymerization conditions for performing MTAC-initiated Cu-RDRP of the model monomers, selected mainly on the basis of achieving high monomer conversion, low dispersity, and a reasonably good match between theoretical and experimental MWs. Numerous additional experimental conditions tested during the extensive screening process are then collected in Supporting Information (**Table S1**, **Table S2**, **Table S3**) and might be of use in specific cases, e.g., when a particular ligand/solvent combination is desired.

Table 1. Selected optimized conditions for MTAC-initiated Cu-RDRP of model monomers[a]

Entry	Mon.	Cat.	Solvent	Ligand (eq.)	M/I	T (°C)	Time (h)	Conv. (%)[b]	M_n (theor.)[c]	M_n (SEC)[d]	$Đ$[d]
1	MA	Cu(0)	DMSO	PMDETA (0.2)	200	60	4	96	16 500	22 200	1.19
2	MA	Cu(0)	DMAc	PMDETA (0.2)	200	60	24	98	17 000	21 100	1.27
3	MA	Cu(0)	DMSO	Me_6TREN (0.5)	200	60	5	91	15 700	21 800	1.17
4	MA	Cu(0)	DMSO	Me_6TREN (0.5)	200	r.t.	24	95	16 400	20 400	1.12
5	MA	Cu(0)	dioxane	Me_6TREN (0.5)	200	60	24	99	17 000	22 000	1.19
6	MA	Cu(0)	toluene	Me_6TREN (0.5)	200	60	24	89	15 300	18 600	1.19
7	MA	Cu(0)	DMSO	Me_6TREN (0.5)	50	60	5	80	3 700	4 900	1.22
8	MA	Cu(0)	DMSO	Me_6TREN (0.5)	100	60	5	89	7 800	10 500	1.18
9	MA	Cu(0)	DMSO	Me_6TREN (0.5)	400	60	7	97	33 500	48 200	1.20
10	MMA	Cu(0)	DMSO	PMDETA (0.2)	200	85	3	87	17 600	24 700	1.27
11	MMA	Cu(0)	DMSO	Me_6TREN (0.2)	200	85	4	85	17 200	23 000	1.20
12	MMA	Cu(0)	DMSO	Me_6TREN (0.2)	200	r.t.	24	91	18 400	25 900	1.19
13	MMA	Cu(0)	dioxane	PMDETA (1.0)	200	85	5	90	18 200	26 600	1.16
14	MMA	Cu(0)	toluene	PMDETA (1.0)	200	85	24	95	19 200	19 600	1.12
15	MMA	Cu(0)	DMSO	Me_6TREN (0.2)	50	85	4	>99	5 200	5 900	1.27
16	MMA	Cu(0)	DMSO	Me_6TREN (0.2)	100	85	4	90	9 200	10 900	1.25
17	MMA	Cu(0)	DMSO	Me_6TREN (0.2)	400	85	7	93	37 400	43 700	1.20
18	MMA	Cu(0)	toluene	PMDETA (1.0)	50	85	18	>99	5 200	5 100	1.26
19	MMA	Cu(0)	toluene	PMDETA (1.0)	100	85	18	96	9 800	10 800	1.22
20	MMA	Cu(0)	toluene	PMDETA (1.0)	400	85	45	92	37 000	33 000	1.12
21	MMA	CuBr	toluene	PMDETA (1.0)	200	85	22	90	18 200	15 500	1.12
22	MMA	CuBr	dioxane	PMDETA (1.0)	200	85	24	88	17 800	18 200	1.09
23	MMA	CuBr	dioxane	PMDETA (1.0)	50	85	18	>99	5 200	5 000	1.21
24	MMA	CuBr	dioxane	PMDETA (1.0)	100	85	18	85	8 700	9 500	1.13
25	MMA	CuBr	dioxane	PMDETA (1.0)	400	85	45	70	28 200	29 700	1.11
26	styrene	Cu(0)	toluene	Me_6TREN (0.2)	200	90	24	45	9 700	10 400	1.19
27	styrene	CuBr	-	Me_6TREN (1.0)	400	110	21	95	40 000	45 300	1.25
28[e]	styrene	CuBr	-	Me_6TREN (1.2)	50	110	2	89	4 900	6 000	1.30
29	styrene	CuBr	-	Me_6TREN (1.0)	100	110	6	84	9 000	10 500	1.26
30	styrene	CuBr	-	Me_6TREN (1.0)	200	110	6	86	18 100	21 100	1.21
31	styrene	CuBr	-	Me_6TREN (1.0)	800	110	24	92	77 000	75 200	1.34

[a] Standard polymerization conditions: MTAC initiator; catalyst (Cat.): 10 cm of activated copper wire in Cu(0)-RDRP, CuBr (1 eq.) in ATRP; ligands: tris[2-(dimethylamino)ethyl]amine (Me_6TREN) and *N,N,N′,N″,N‴*-pentamethyldiethylenetriamine (PMDETA); solvent/monomer (Mon.) = 1:1 (v/v).

[b] Monomer conversion determined by ^{1}H NMR (for MA, **Figure S2**) or gravimetrically (for MMA and styrene).

[c] Theoretical M_n calculated from the M/I ratio and conversion, assuming 100% IE.

[d] Determined by SEC with poly(MMA) calibration (for MA and MMA) or polystyrene calibration (for styrene).

[e] $CuBr_2$ (0.2 eq.) was added as a deactivator, and the concentration of ligand was increased to account for this addition.

Our screening showed that MTAC-initiated ATRP (CuBr or CuCl as a catalyst) of MA was largely unsuccessful. Under host of different polymerization conditions, including different solvents, ligands, and temperatures, no polymerization was observed, or the achieved conversions were very low (entries 1 – 15, **Table S1**). On the other hand, Cu(0)-RDRP catalyzed by Cu wire yielded low-dispersity polymers at high conversion under a range of polymerization conditions, including both polar and non-polar solvents (entries 1 – 9, **Table 1**; additional experiments in **Table S1**). SEC elugrams of obtained polymers are provided in **Figure 1** and **Figure S3**; a kinetic experiment documenting the good polymerization control is shown in **Figure S4**.

Further, we demonstrated that the MTAC initiator works remarkably well for MMA, affording high conversions and low-dispersity products under a range of conditions, including both ATRP and Cu(0)-RDRP methods, different temperatures and solvents of different polarity (entries 10 – 25, **Table 1**, and **Table S2**; for SEC elugrams see **Figure 1** and **Figure S5**). A well-controlled character of the polymerization under the developed conditions was confirmed by kinetic experiments (**Figure S6,**

Figure S7, and **Figure S8**). The high chain-end fidelity of poly(MMA) prepared via MTAC-initiated ATRP in dioxane was demonstrated by chain-extension experiments. To this end, poly(MMA) prepared at high conversion (M_n = 9 500, Đ = 1.13; entry 24, **Table 1**) was successfully used as a macroinitiator to initiate chain-extension with MMA and block-copolymerization with styrene, which is visualized by clear shifts of the corresponding SEC elugrams and the significant increases in MWs (**Figure S9**).

Finally, styrene was polymerized at 90 °C through a well-controlled Cu(0)-RDRP (in DMSO and toluene) and ATRP (in toluene); however, the process was rather slow (ca 50% conversions reached). High conversions were achieved via ATRP in bulk at 110 °C (entries 26 – 31, **Table 1**; **Table S3**; for SEC traces see **Figure 1** and **Figure S10**; for kinetics see **Figure S11**). It is of note that Cu(0)-RDRP of styrene in DMSO and DMAc was plagued by gel formation on the copper wire. Such gel formation has been described previously for other Cu(0)-RDRP systems.[62,66,67] Collectively, it is rather remarkable that MTAC is able to initiate well-controlled Cu(0)-RDRP of all three studied model monomers in toluene or dioxane because reports on successful Cu(0)-RDRP in non-polar solvents are extremely rare in literature.[68-70]

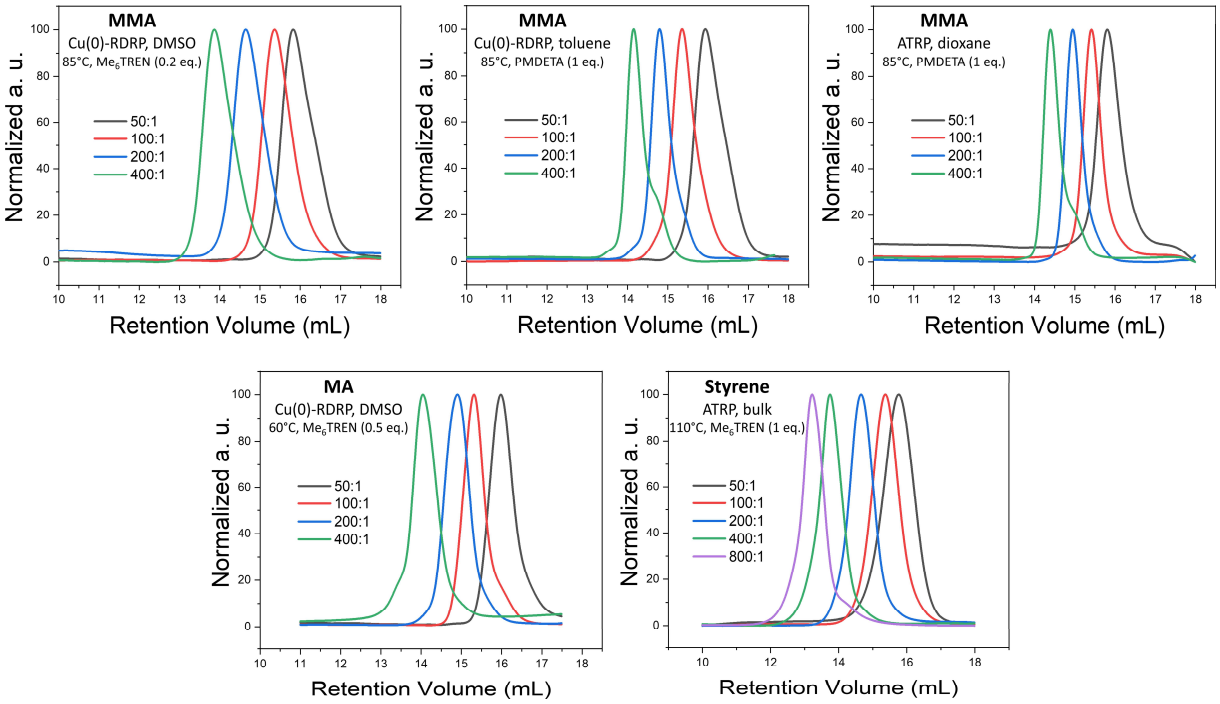

Figure 1. SEC elugrams of selected polymers prepared by MTAC-initiated Cu-RDRP at different M/I ratios. Product characteristics are provided in **Table 1**. The noticeable low-MW shoulder in the SEC elugrams of the polymers synthesized at the highest M/I ratios (400:1 or 800:1) in non-polar solvents/bulk are ascribed to the products of early termination or competing transfer reactions that tend to be more pronounced when aiming for high-MW products.[70]

Next, to verify that the Cu-RDRP conditions established using MTAC are usable also for TAI adducts with other functional groups, we synthesized *N,N*-diisopropylamine/TAI adduct, 1,1-diisopropyl-3-(2,2,2-trichloroacetyl)-urea (DTAU) (**Figure S12**). DTAU-initiated Cu-RDRP of styrene, MMA, and MA was then performed under the optimized conditions from our library. The experimental results together with the corresponding SEC traces, collected in **Figure S13**, prove that very similar polymers are obtained irrespective of the linker connecting the initiating TAG fragment to the CPA precursor.

This finding suggests that the developed library of Cu-RDRP conditions will be applicable to a variety of CPA precursors bearing TAI-reactive functions.

Having successfully identified polymerization protocols for model monomers, we next sought to investigate the universality of the developed conditions with respect to other monomers from the same class, including some important functional variants.[71-73] To this end, we applied selected conditions to other (meth)acrylates, including functional ones (**Table 2**, **Figure S14**). Although some of the (meth)acrylate analogues (expectedly) did not behave identically as the model monomers, we could easily identify conditions in our library providing well-defined products, which highlights the utility of the extensive screening approach we employed in this study. For example, butyl acrylate (BA) polymerized poorly in toluene (entry 1, **Table 2**) while quickly affording a well-defined product at quantitative conversion in a bi-phasic system[35] in DMSO (entry 2, **Table 2**). Similarly, Cu(0)-RDRP of 2-hydroxyethyl methacrylate (HEMA) was uncontrolled in DMSO while affording a well-defined product in dioxane[74] (cf. entries 7 and 8, **Table 2**). Further, for 2-hydroxyethyl acrylate (HEA), we obtained a well-defined polymer by using a lower ligand loading (cf. entries 3 and 4, **Table 2**). On the other hand, conditions originally developed for MMA could be directly applied to butyl methacrylate (BMA) and glycidyl methacrylate (GMA) without any changes (entries 5 and 6, **Table 2**). Taken together, the results confirm the considerable universality of TAI-derived initiators and manifest that our library of optimized conditions (**Tables 1**) can serve as an excellent starting point when polymerizing other (meth)acrylates.

Table 2. MTAC-initiated Cu-RDRP of other (meth)acrylates[a]

Entry	Monomer	Solvent	Ligand (eq.)	T (°C)	Time (h)	Conv. (%)[b]	M_n (theor.)[c]	M_n (SEC)[d]	$Đ$[d]
1	BA	toluene	Me_6TREN (0.5)	60	24	16	4 200	4 600	1.45
2[e]	BA	DMSO	Me_6TREN (0.5)	60	7	97	25 100	35 100	1.25
3	HEA	DMSO	Me_6TREN (0.5)	60	8	50	11 800	46 500	1.37
4	HEA	DMSO	Me_6TREN (0.2)	60	24	42	10 000	15 000	1.18
5	BMA	toluene	PMDETA (1.0)	85	24	84	24 000	20 400	1.15
6	GMA	DMSO	Me_6TREN (0.2)	85	2	80	23 000	21 400	1.23
7[f]	HEMA	DMSO	Me_6TREN (0.2)	85	24	99	13 100	20 000	1.85
8[f]	HEMA	dioxane	PMDETA (1.0)	85	1	99	13 100	17 200	1.28

[a] Standard polymerization conditions: MTAC initiator, M/I = 200:1, 10 cm of activated copper wire, monomer/solvent = 1:1 (v/v).

[b] Monomer conversion determined by ^{1}H NMR.

[c] Theoretical M_n calculated from the M/I ratio and conversion, assuming 100% IE.

[d] Determined by SEC with poly(MMA) calibration [directly (BA, BMA, GMA) or after acetylation[75] (HEMA)] or by TD-SEC (HEA).

[e] Biphasic polymerization mixture.

[f] M/I = 100:1 and 5 cm of activated copper wire were used.

To complement the results on TAG-initiated Cu-RDRP, we also performed a preliminary investigation into the hydrolytic stability of the TAI-derived carbamate linker present in most (macro)initiators used in this study. It can be expected that different TAI-derived linkers, connecting the initiating TAGs with the derivatized precursor, may show different hydrolytic stability/pH sensitivity. We envisage that the properties of these linkers could be potentially exploited in fields such as drug delivery where, for example, the use of CPAs featuring a pH-sensitive carbamate linker has already been established.[76-78] Nevertheless, the situation can be rather complex as organic carbamates show very varied hydrolytic stability depending on their structure and experimental conditions.[79-82] To get a preliminary insight, we studied hydrolytic stability of in-chain carbamate linkers in a poly(HEA) star polymer. As shown in

Figure S15 and in the accompanying discussion, the carbamate linker showed to be considerably resistant to hydrolysis in a wide pH range.

Functionality of TAI-based initiation groups

The functionality of TAG(s) introduced into CPA precursors by the reaction with TAI represents a key parameter defining the final polymeric architecture and distinguishes the TAI-based strategy from previous approaches based on monofunctional initiation sites such as BriB. Surprisingly, the functionality of TAG-containing Cu-RDRP initiators has been addressed only rarely in literature. In their seminal paper, Destarac et al. concluded based on NMR data that the studied methyl trichloroacetate acts as – at least – a bifunctional initiator in ATRP of styrene.[23] Additionally, Lorandi et al. have recently reported that trichloroacetic acid behaves as a trifunctional initiator in ATRP of acrylic acid,[53] maintaining that, upon initiation, the remaining chlorine(s) of the original TAG are increasingly prone to activation (and, subsequently, initiation) due to the penultimate effect.[83] Considering these limited previous results, we decided to perform an in-depth investigation into the functionality of the TAI-derived TAGs under our developed polymerization conditions.

First, we used ^{1}H NMR spectroscopy to evaluate the initiator functionality for model low-MW poly(MA), poly(MMA), and polystyrene prepared by MTAC-initiated Cu-RDRP. In the respective spectra, we identified the characteristic signals of the initiator fragment (the $–OCH_3$ group) and the terminal (chlorine-bearing) and in-chain monomeric units. We then used the relative intensities of these signals, together with the polymer M_n value determined by SEC, to calculate initiator functionality, obtaining values close to 3 in all cases (for details see **Figures S17-S19** and the accompanying discussion). It is of note that the used poly(MMA) sample was obtained at quantitative conversion (entry 23, **Table 1**), confirming the high end-chain fidelity attained under the used conditions. Overall, our findings suggest that the MTAC-initiated polymers have the topology of three-arm stars. Consequently, our reported MW values obtained by SEC with relative calibration are slightly underestimated due to the smaller hydrodynamic volume of branched polymers. Additionally, the poly(MMA)-*b*-polystyrene synthesized above in the chain-extension experiment (**Figure S9**) should be considered as a 3-arm star with diblock arms.

Next, we wanted to verify that the trifunctionality of TAI-derived TAGs is retained also for high-MW CPAs (i.e. a real-world scenario). Since high-MW polymers are not amenable to the simple end-group analysis applied above, we selected a different approach based on the viscometric analysis of the initiation site-related branching using TD-SEC. We reasoned that a standalone TAG provides branching only if the initiator acts as trifunctional while its mono- and bifunctionality leads to a linear polymer.

As model CPAs, we prepared star-shaped poly(MMA) and polystyrene via Cu-RDRP initiated by the pentaerythritol/TAI adduct, pentaerythritol tetrakis((2,2,2-trichloroacetyl) carbamate) (PTAC) (**Figure 2**, **Figure S20**). Using TD-SEC, we then analyzed the parent star polymers as well as the individual TAG-initiated polymeric segments released from the pentaerythritol core via alkaline hydrolysis[33] of carbamate linkers (**Figure 2**). As seen from the data summarized in **Table S4**, the poly(MMA) star showed low dispersity of 1.21, with the SEC elugram (**Figure 2b**) featuring only a small high-MW shoulder, indicating negligible extent of star-star coupling despite the high monomer conversion of 92 %. On the other hand, the polystyrene variant was comparatively less well-defined ($Đ$ = 1.69), probably due to the presence of both the coupling products and free segments as suggested by the SEC elugram shape (**Figure 2c**). Nevertheless, the low dispersity of the hydrolytically released star segments/arms indicated that well-controlled polymerization was achieved for both monomers.

Figure 2d,e shows Mark-Houwink (M-H) plots for both the parent multi-arm star polymers and the hydrolytically released segments, alongside the data for broad linear poly(MMA) and polystyrene

standards. In addition, the determined M-H α constants, which provide a good measure of polymer branching, are also displayed. While the broad linear standards provided the expected α ≈ 0.6, the considerably lower α value of approximately 0.4 obtained for the released segments confirmed branched character of these polymers and, thus, the TAG trifunctionality.[84] Finally, the α values for the parent polymers, presumably 12-arm stars, are even lower (≈ 0.2), as expected for the comparatively denser polymeric architecture.[84]

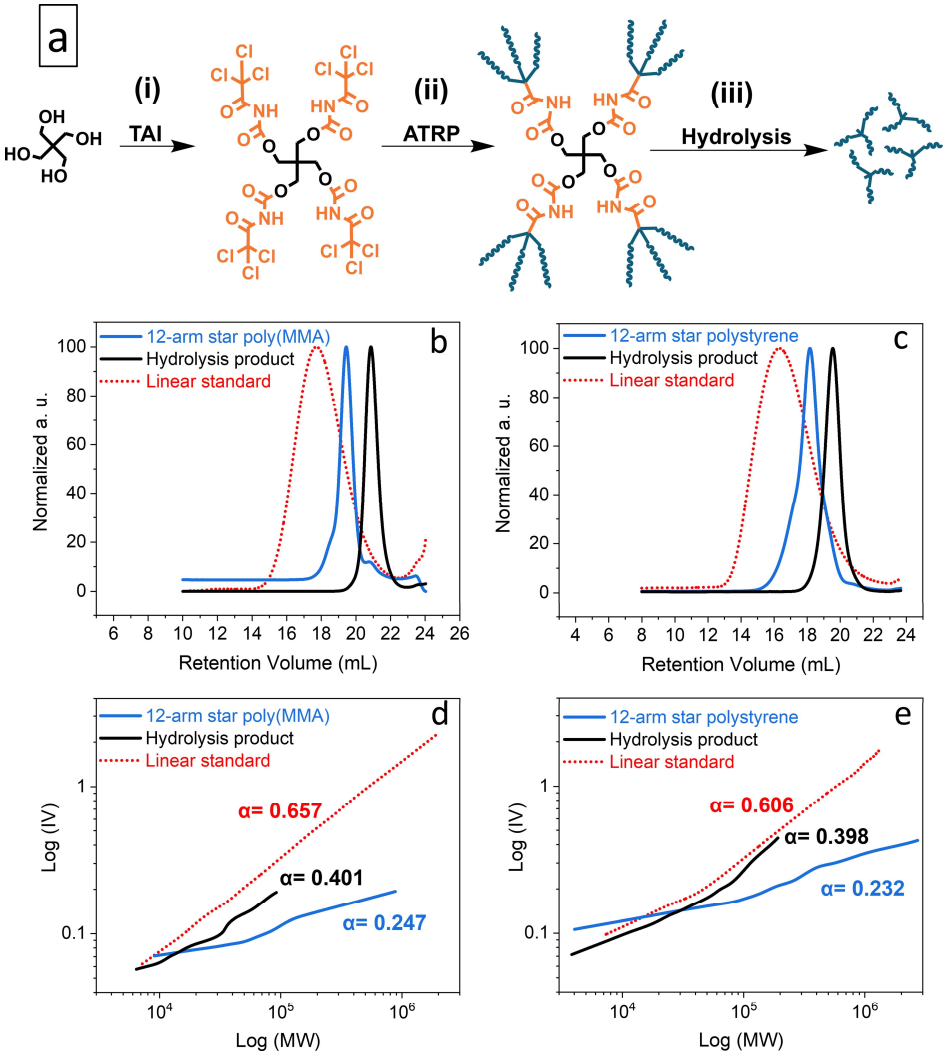

Figure 2. TAG functionality study: general scheme of the synthesis of model multi-arm stars based on a pentaerythritol core (a); elugrams – RI traces (b, c) and M-H plots (d, e) from the TD-SEC analysis of the synthesized poly(MMA) (b, d) and polystyrene (c, e) multi-arm star polymers and of products of their alkaline hydrolysis. Data for broad linear poly(MMA) and polystyrene standards are shown for comparison. See **Table S4** for experimental conditions and results.

Note that we performed also PTAC-initiated polymerization of MA (**Table S4**); however, we were unable to cleanly release the individual segments using our alkaline hydrolysis method in this case. Therefore, in **Figure S21**, we provide only the TD-SEC analysis of the parent star polymer together with the comparison data for a broad linear poly(MA)standard. The same α constant as for the poly(MMA)

star above (≈ 0.25) was obtained from the M-H analysis indicating a similar number of star arms and hence TAG trifunctionality also in this case.

Applications of the TAI-based strategy

Having successfully established that TAI functions as an efficient vehicle for introducing universal multifunctional initiation sites into different precursors, we highlight in this section some of the advantages that this new strategy brings to CPA synthesis.

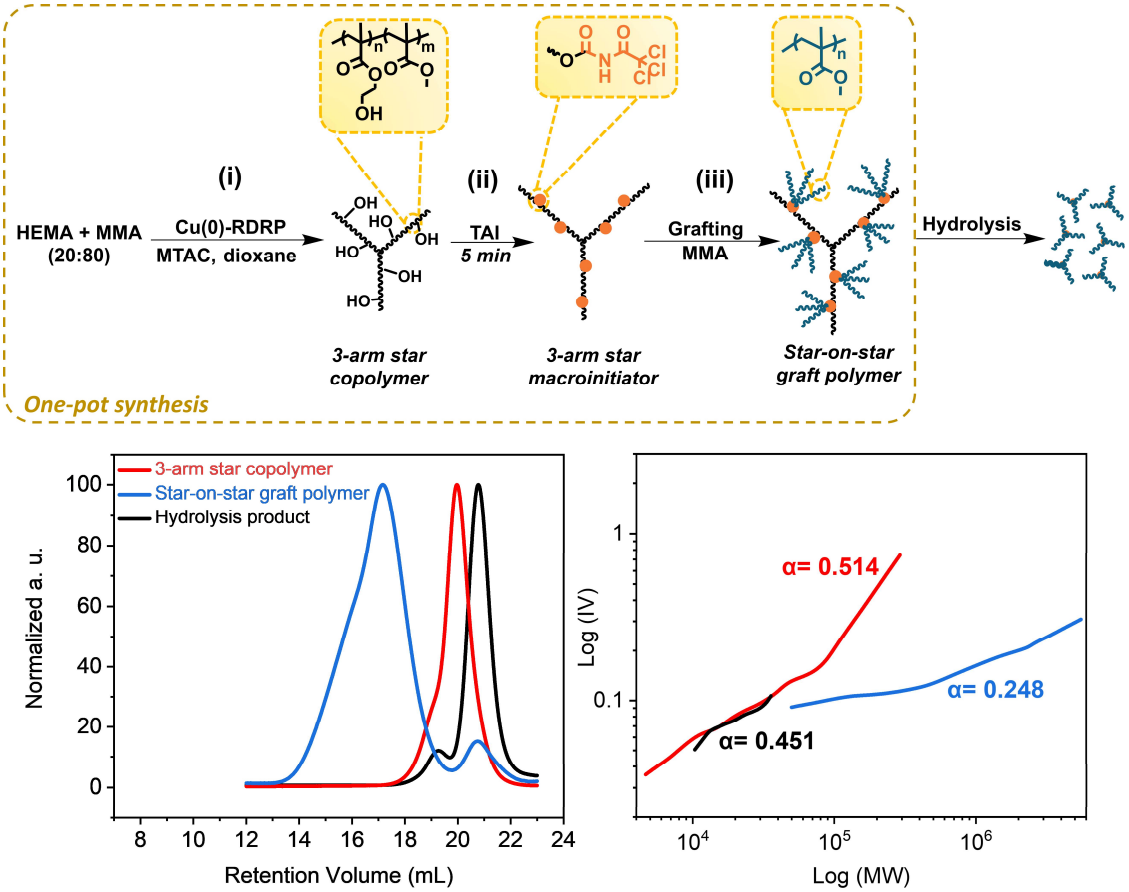

Figure 3. *De novo* one-pot synthesis of the poly(HEMA-*co*-MMA)-*graft*-poly(MMA) hybrid star/graft copolymer of "star-on-star" topology. Top: general reaction scheme; for experimental conditions see **Table S5**. Bottom: TD-SEC analysis of products at individual stages – elugrams (left) and M-H plots (right).

First, we show that the strategy allows for the clean *in situ* introduction of initiation sites in multi-step protocols without intermediate isolation, which enables the one-pot *de novo* synthesis of graft copolymers that avoids the isolation/purification steps typical for standard approaches.[14,32,33] To this end, we conducted a three-step protocol depicted in **Figure 3**; for experimental details and results see **Table S5**. First, we performed a MTAC-initiated copolymerization of HEMA and MMA (20/80 mol %) by Cu(0)-RDRP in dioxane, yielding a well-defined poly(HEMA-*co*-MMA) copolymer (M_n = 23 400, Đ = 1.23) at quantitative conversion (**Figure S22**, top). Subsequently, we *in situ* modified part of the pendent hydroxyl groups in HEMA units by adding TAI (**Figure S22**, bottom). Finally, upon the addition of another batch of MMA and solvent, we continued the polymerization to yield the final graft copolymer

(**Figure S23**). Owing to the TAG trifunctionality, the copolymer involves three-arm stars grafted from a three-arm star backbone, i.e., "star-on-star" architecture – apparently a novel type of CPA that structurally represents a hybrid between a star and a graft copolymer. The inflated dispersity of the final product (1.95) is mainly ascribed to the recombination reactions at the macroinitiator preparation stage where quantitative conversion was targeted (a high-MW shoulder in the SEC elugram of the macroinitiator supports this assumption). Nevertheless, TD-SEC analysis showed that the poly(MMA) grafts, removed by alkaline hydrolysis,[33] were extremely well defined ($Đ$ = 1.05), indicating a high degree of polymerization control in the grafting step. Note that there is a small lower-MW signal in the SEC chromatogram of the star-on-star copolymer. This signal is ascribed to the polymer initiated by the products of TAI reaction with present impurities (e.g., water). The M-H plots provided in **Figure 3** showed α values consistent with the expected topology of three-arm stars (for the macroinitiator precursor and cleaved grafts) and with the highly branched final star-on-star copolymer. Collectively, these results illustrate well that the TAI strategy opens avenues for unconventional approaches to the synthesis of graft and hyper-branched (co)polymers and enables designing of new CPA topologies.

In order to highlight the utility of the TAI-based initiator functionality amplification strategy in the synthesis of previously inaccessible multi-arm star-shaped polymers, we conducted polymerization of MMA initiated by a β-cyclodextrin (β-CD)/TAI adduct (**Figure 4**). The adduct was prepared by the reaction of pre-dried β-CD with an excess of TAI whereby the unreacted TAI was quenched with DMSO. The ^{1}H NMR spectrum of the reaction mixture (**Figure S24**) confirms the full modification of the β-CD hydroxyl groups as well as the presence of the DMSO/TAI adduct and trichloroacetamide originating from TAI reaction with residual water. The latter two compounds served as low-MW sacrificial initiators.[26,33,85] The SEC elugrams of the starting β-CD and the β-CD/TAI adduct displayed in **Figure S25a** show a clear shift of the sharp β-CD peak to higher MWs upon TAI modification. Afterward, the (macro)initiator solution was used to initiate ATRP of MMA in dioxane. Finally, the arms of the isolated star polymer were removed via alkaline hydrolysis for further analysis.

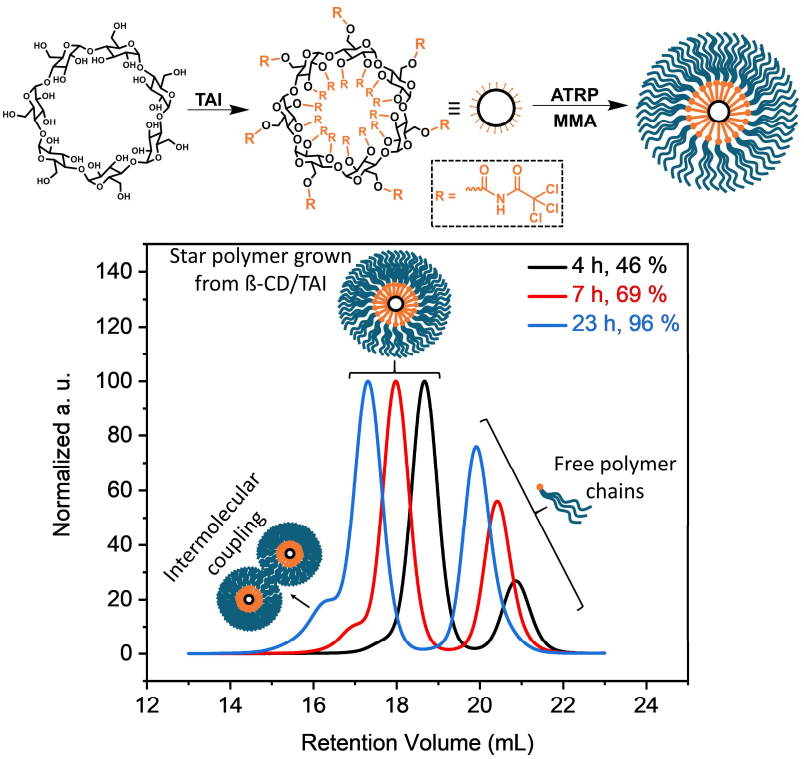

Figure 4. Synthesis of multi-arm poly(MMA) stars through ATRP initiated by the β-CD/TAI adduct. Top: general reaction scheme; bottom: TD-SEC analysis (elugrams – RI traces) of samples taken at different polymerization stages. Experimental details are provided in **Table S6**.

The data shown in **Figure 4**, **Figure S25b**, and **Table S6** confirmed that the use of a sacrificial initiator represents an efficient strategy[33] for suppressing the formation of intermolecular coupling products (visible as high-MW shoulders in SEC elugrams) even at the almost quantitative monomer conversion reached here. Both the star polymers and cleaved arms/free-growing chains were exceptionally well-defined throughout the polymerization course ($Đ$ = 1.15 and 1.05, respectively, at 96% conversion). Additionally, there was an excellent match in M_n and $Đ$ values evaluated for the free-growing chains (the low-MW signal in the SEC of the isolated products) and the mixture of the free-growing chains and the star arms obtained after hydrolysis (**Table S6**, **Figure S25b**), proving that both the star arms and free chains grew at a similar rate. At the same time, the determined M_n values were considerably higher than the theoretical ones calculated from conversion and the MMA/TAI ratio. Collectively, these observations suggest that a part of the TAGs on the β-CD/TAI adduct did not initiate polymerization due to the extreme steric crowding at the TAI-modified β-CD while the remaining TAGs acted as trifunctional initiators, owing to the increased reactivity of the chlorine atoms remaining at TAGs that underwent initiation.[53] Nevertheless, a simple comparison of the M_n values obtained for the final multi-arm star polymer and for the arms released therefrom suggests that one β-CD core bears approximately 15 poly(MMA) segments that actually are 3-arm stars on their own. Therefore, the product can be considered as a 45-arm star polymer, highlighting the clear advantage of the new strategy over the previous approaches based on monofunctional initiators that yield, at best, 21 arms from the same precursor in a much more laborious process.[34,37]

Next, we presumed that the high TAI reactivity will make the new strategy particularly useful in the synthesis of CPAs based on difficult-to-modify substrates. Herein, this is exemplified by the modification of cellulose that has been previously shown to be resistant to the introduction of high concentrations of Cu-RDRP initiation sites using standard acylation protocols.[14,33] First, we studied the reactivity of cellulose (microcrystalline AVICEL PH-101) toward TAI in different solvents. We found that cellulose, dissolved in the traditional cellulose solvent DMAc/LiCl,[86] could be easily fully modified with a slight excess of TAI (4 eq. toward the anhydroglucose units of cellulose) as documented by the ^{1}H and ^{13}C NMR spectra of the isolated adduct (**Figure S26**). Furthermore, overnight stirring of dioxane-activated cellulose[86] in dioxane containing 4 eq. of TAI led to complete cellulose modification and dissolution. Similarly, the dioxane-activated cellulose afforded a clear solution of the cellulose/TAI adduct after 2 h of reaction with 6 eq. of TAI in THF. Moreover, we found that pre-dried, non-activated cellulose could be fully modified and dissolved when reacted with TAI (6 eq.) in acetonitrile for 4 days. Most importantly, we also revealed that cellulose becomes highly reactive toward TAI when the modification is conducted in DMSO, i.e., a solvent that strongly swells cellulose and increases its accessibility and reactivity.[87] When 5 eq. of TAI were added to a suspension of non-dried (or pre-dried and soaked in DMSO overnight) cellulose in DMSO, a clear solution was obtained within 1 min. This finding is remarkable considering the reactivity of TAI toward DMSO and confirms that the modification of substrates in TAI-reactive solvents (e.g., DMSO or DMAc), as proposed by Samek et al.,[39] is possible also for heterogeneous reactions with polymeric substrates. While we did not focus here on testing the universality of this modification protocol with respect to different cellulose types, we can confirm that the same rapid modification in DMSO was obtained also for a considerably higher-MW cellulose Sigmacell type 101. We thus envisage that this protocol may find important applications in the field of

cellulose characterization where a similar but considerably more laborious approach based on cellulose modification with phenyl isocyanate is used for cellulose MW determination by SEC.[88]

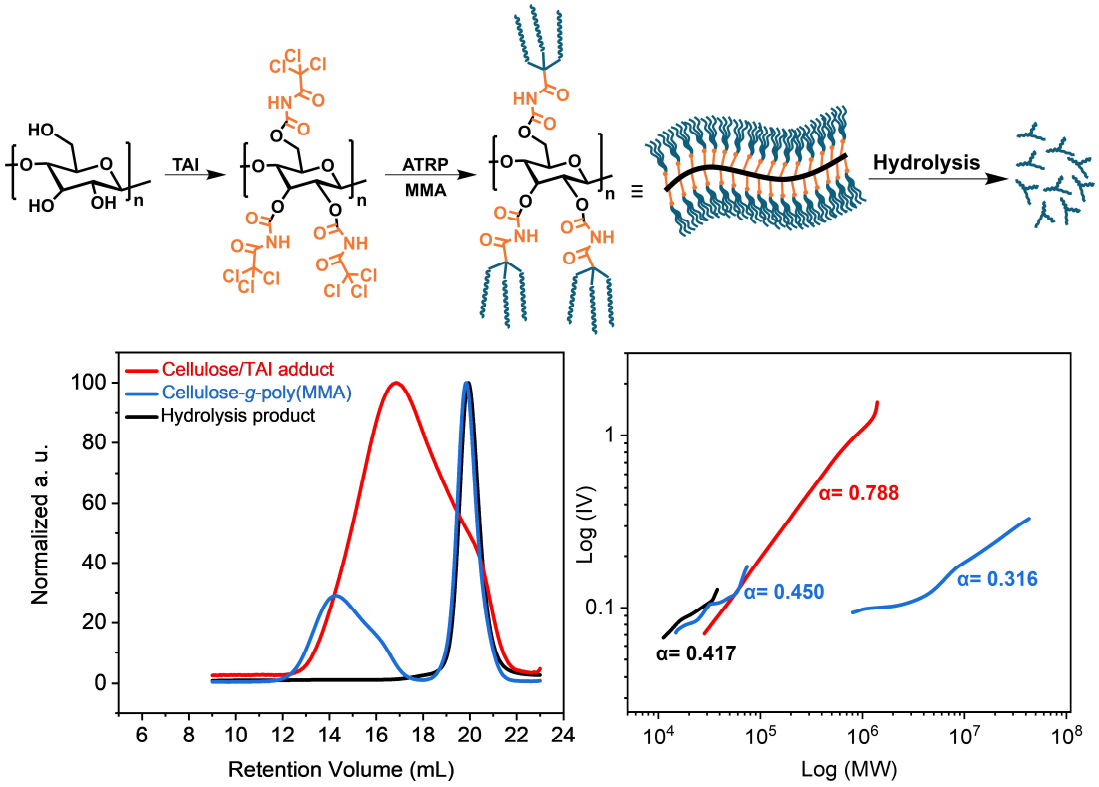

Figure 5. Synthesis of the ultra-dense bottle-brush cellulose-*g*-poly(MMA) graft copolymer via ATRP of MMA initiated by the cellulose/TAI adduct. Top: general reaction scheme; bottom: TD-SEC analysis (left – RI elugrams; right – M-H plots) of the cellulose/TAI macroinitiator, the copolymer obtained after 5 h, and poly(MMA) obtained after alkaline hydrolysis of the isolated product. Experimental details are provided in **Table S7**.

Cellulose fully modified with TAI represents a unique macroinitiator that can potentially give rise to 9 polymeric chains per one backbone repeat unit, affording, upon graft copolymerization, extremely dense bottle-brush copolymers. To investigate this option, we synthesized a cellulose-*graft*-poly(MMA) copolymer via ATRP initiated by a cellulose/TAI adduct (**Figure 5**). We first prepared a stock solution containing the cellulose/TAI adduct and MTAC as a low-MW sacrificial initiator by reacting cellulose (AVICEL) with 6 eq. of TAI in acetonitrile and subsequently quenching the excess of TAI by methanol. The TD-SEC analysis of the adduct revealed M_n of 106 700 and dispersity of 2.17 consistent with the characteristics of the cellulose precursor (**Figure 5**).[86] Subsequently, we used the obtained (macro)initiator solution to initiate ATRP of MMA in dioxane. As can be seen from the experimental data collected in **Table S7**, 27% conversion was reached in 5 h, which corresponds to the M_n(theor.) of 9 644 000, as calculated from the macroinitiator number-average degree of polymerization (DP_n) of 147, assuming three TAI-modified hydroxyl groups per a repeat unit that initiate polymerization. After 24 h, 72% conversion was attained, corresponding to M_n(theor.) of 25 539 000. In this context, it is rather remarkable how the application of a sacrificial initiator effectively suppresses intermolecular crosslinking reactions even for such an ultra-dense bottle-brush at very high monomer conversion.[33]

It is known that SEC of high-MW bottle-brushes is challenging due to the non-SEC elution behavior of high-MW fractions.[16,89] Indeed, we observed delayed elution of high-MW polymer fraction(s), which obscured the MW analysis (for details see **Figure S27** and the accompanying discussion). Nevertheless, for the 5 h sample, we were able to obtain, using universal calibration, rather realistic M_n of 28 300 for the free-growing chains initiated by the sacrificial initiator (**Table S7**). This value agreed well with that for the mixture of grafts and free-growing chains acquired through the alkaline hydrolysis of the isolated product (M_n = 24 400), confirming that the polymer grew at a similar rate from both the cellulose backbone-attached and free initiation sites. The close match between the experimental M_n values and the M_n(theor.), calculated based on the monomer conversion and the MMA/TAG ratio (considering all forms of TAI adducts), indicates that the much lower than theoretical M_n of the graft copolymer determined by TD-SEC (3 174 000) is severely underestimated due to the effects discussed above. The high compactness of the prepared bottle-brush copolymer is well-illustrated by the low α constant obtained from the M-H plot (**Figure 5**). Further, even though we were unable to obtain any MW values from the TD-SEC analysis of the 24 h sample, we note that a good match between the M_n(theor.) and M_n(SEC) values of the hydrolysis product was retained also in this case (**Table S7**). Additionally, the unimodal character of the SEC signals (data not shown) together with the low obtained $Đ$ of 1.11 suggested that the M_n of grafts was similar as that determined for the hydrolysate. Altogether, the obtained data point to the extreme MW of the final cellulose-*graft*-poly(MMA) copolymer despite the rather low-MW cellulose backbone employed. We predict that truly giant cellulose-based graft copolymers with MWs in the order of hundreds of millions should be readily accessible using this strategy when starting from regular cellulose substrates having MWs in hundreds of thousands.

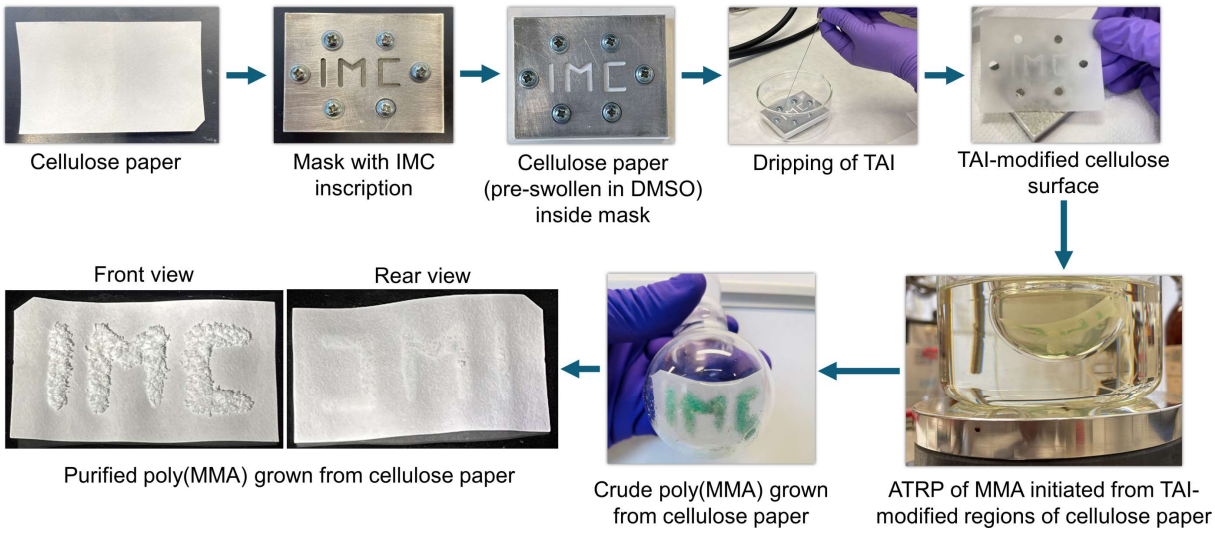

Figure 6. Spatial control in the modification of Whatman filter paper with TAI and subsequent ATRP SI grafting of MMA from the modified cellulose surface.

In the last part of this study, we highlight that the use of TAI-derived multifunctional initiation groups can have a much broader impact in the cellulose field as it can be easily adapted for the surface modification of diverse cellulose-based precursors. In the first example, we took advantage of the extremely high reactivity of DMSO-swollen cellulose toward TAI to demonstrate the possibility of spatial control in surface-initiated (SI) grafting from flat cellulose/TAI substrates. To this end, we placed

a DMSO-wetted cellulose filter paper (Whatman) into a metallic mask and applied TAI into the mask opening. We then used the purified TAI-modified paper to initiate ATRP of MMA, obtaining within 30 min a thick, macroscopic layer of polymer bound to the regions of the paper surface originally exposed to TAI (**Figure 6**). Notably, there was virtually no polymer growth from the rear side of the paper, confirming the instantaneous TAI reaction with the DMSO-wetted paper. We thus envisage that this strategy could be applicable to the fabrication of Janus-type fabrics.[90]

In another experiment, 5 cm of a thick cotton thread was surface-modified with TAI in DMSO and subsequently used to trigger MMA polymerization, which led to the complete coverage of the thread with a thick polymer layer (**Figure 7**, **Figure S28**). In the close-up picture, the disentanglement of the individual strands at the thread ends and the efficient modification of the smallest thread features is well-visible. Finally, to illustrate the feasibility of this strategy also for more complex (cellulose-based) natural substrates, we successfully grafted a polymer layer from TAI-modified pine tree cone in the same way (**Figure 7**, **Figure S29**). The non-modified areas visible on the cone scales correspond to the places where seeds blocked the access of TAI during the modification step (the seeds got released during the polymerization step). This further demonstrates the spatial control in the TAI-based SI grafting strategy. Altogether, these preliminary results show the great potential of the TAI-based strategy in both homogeneous and heterogeneous SI grafting from natural polymeric substrates with efficiency and grafting density unparalleled by the traditional protocols.[30,91]

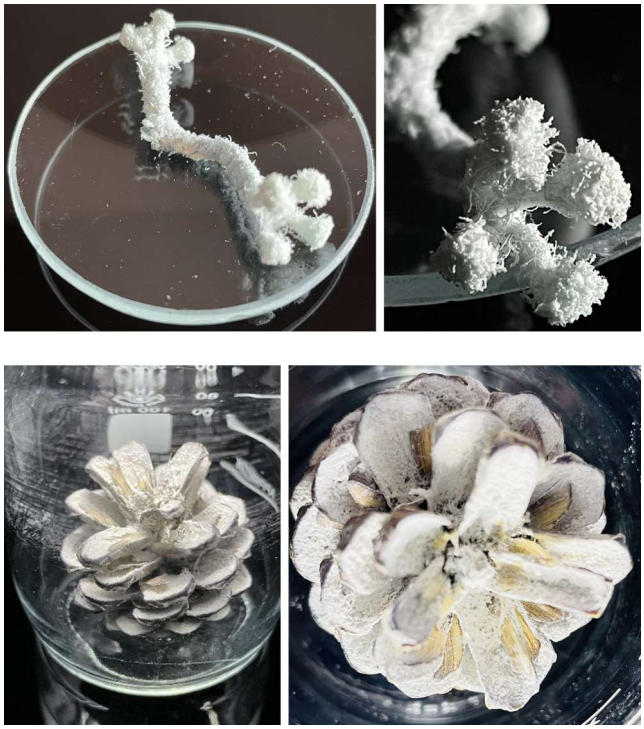

Figure 7. A cotton thread (top) and a pine tree cone (bottom) grafted with poly(MMA) *via* the two step TAI-modification/ATRP-grafting strategy.

CONCLUSIONS

In conclusion, we showed in this study that the application of universal multifunctional TAI-based Cu-RDRP initiation sites can significantly extend the “toolset” of synthetic polymer chemists aspiring at

constructing CPAs of novel architectures and properties. To assist with this task, we provided here an extensive library of optimized conditions for conducting well-controlled TAG-initiated Cu-RDRP of different monomers. The unique synergistic combination of TAI trifunctionality and extreme reactivity allows for rapid amplification of the functionality of CPA precursor-derived (macro)initiators. As a result, an unprecedently high number of polymeric chains can be easily installed onto CPA precursors, in stark contrast to earlier approaches based on monofunctional initiation sites introduced into precursors via inefficient acylations. Resulting opportunities in CPA synthesis were illustrated on multiple relevant scenarios yielding CPAs of novel qualities in uncomplicated protocols.

We envisage that in future the scope of the presented strategy will be significantly extended. For example, the broad reactivity of TAI will extend the range of functional substrates that could serve as CPA precursors; moreover, the different reactivity (stability) of linkers through which precursors are connected to the initiating TAGs could be exploited in programmed CPA decomposition. Furthermore, synthesis of miktoarm star polymers based on telechelic precursors or preparation of ultra-dense polymeric brushes with controlled thickness[92] represent some of the expected future applications. Last but not least, the study of the physico-chemical properties of the new multi-chain CPAs can be desirable from the viewpoint of future applications of these materials.

AUTHOR CONTRIBUTIONS

SG: investigation, validation, visualization, writing – original draft; MJ: funding acquisition, investigation; EČ: investigation; VR: conceptualization, funding acquisition, investigation, methodology, project administration, supervision, visualization, writing – original draft, writing – review & editing.

ACKNOWLEDGMENT

The financial support from the Institute of Macromolecular Chemistry, CAS, is greatly appreciated. The authors thank Mrs. Jana Rovenská for her experimental work. Sachin Gupta is a PhD student at Charles University, Prague, Czech Republic.

CONFLICT OF INTEREST

The authors declare no conflict of interest.

DATA AVAILABILITY

Data supporting this article have been included in ESI: used materials, synthetic protocols, instrumentation and methods, additional experimental and characterization data, additional figures and images.

REFERENCES

1. J. M. Ren, T. G. McKenzie, Q. Fu, E. H. H. Wong, J. Xu, Z. An, S. Shanmugam, T. P. Davis, C. Boyer and G. G. Qiao, Star Polymers, *Chem. Rev.*, 2016, **116**, 6743-6836.

2. A. W. Bosman, H. M. Janssen and E. W. Meijer, About Dendrimers: Structure, Physical Properties, and Applications, *Chem. Rev.*, 1999, **99**, 1665-1688.
3. C. Feng, Y. Li, D. Yang, J. Hu, X. Zhang and X. Huang, Well-defined graft copolymers: from controlled synthesis to multipurpose applications, *Chem. Soc. Rev.*, 2011, **40**, 1282-1295.
4. S. S. Sheiko, B. S. Sumerlin and K. Matyjaszewski, Cylindrical molecular brushes: Synthesis, characterization, and properties, *Prog. Polym. Sci.*, 2008, **33**, 759-785.
5. K. Kapil, G. Szczepaniak, M. R. Martinez, H. Murata, A. M. Jazani, J. Jeong, S. R. Das and K. Matyjaszewski, Visible-Light-Mediated Controlled Radical Branching Polymerization in Water, *Angew. Chem. Int. Ed.*, 2023, **62**, e202217658.
6. A. Kakkar, G. Traverso, O. C. Farokhzad, R. Weissleder and R. Langer, Evolution of macromolecular complexity in drug delivery systems, *Nat. Rev. Chem.*, 2017, **1**, 0063.
7. A. Detappe, H. V. T. Nguyen, Y. Jiang, M. P. Agius, W. Wang, C. Mathieu, N. K. Su, S. L. Kristufek, D. J. Lundberg, S. Bhagchandani, I. M. Ghobrial, P. P. Ghoroghchian and J. A. Johnson, Molecular bottlebrush prodrugs as mono- and triplex combination therapies for multiple myeloma, *Nat. Nanotechnol.*, 2023, **18**, 184-192.
8. J. A. Johnson, Y. Y. Lu, A. O. Burts, Y.-H. Lim, M. G. Finn, J. T. Koberstein, N. J. Turro, D. A. Tirrell and R. H. Grubbs, Core-Clickable PEG-Branch-Azide Bivalent-Bottle-Brush Polymers by ROMP: Grafting-Through and Clicking-To, *J. Am. Chem. Soc.*, 2011, **133**, 559-566.
9. B. Newland, Y. Zheng, Y. Jin, M. Abu-Rub, H. Cao, W. Wang and A. Pandit, Single Cyclized Molecule Versus Single Branched Molecule: A Simple and Efficient 3D "Knot" Polymer Structure for Nonviral Gene Delivery, *J. Am. Chem. Soc.*, 2012, **134**, 4782-4789.
10. M. A. Sowers, J. R. McCombs, Y. Wang, J. T. Paletta, S. W. Morton, E. C. Dreaden, M. D. Boska, M. F. Ottaviani, P. T. Hammond, A. Rajca and J. A. Johnson, Redox-responsive branched-bottlebrush polymers for in vivo MRI and fluorescence imaging, *Nat. Commun.*, 2014, **5**, 5460.
11. T. Terashima, M. Kamigaito, K.-Y. Baek, T. Ando and M. Sawamoto, Polymer Catalysts from Polymerization Catalysts: Direct Encapsulation of Metal Catalyst into Star Polymer Core during Metal-Catalyzed Living Radical Polymerization, *J. Am. Chem. Soc.*, 2003, **125**, 5288-5289.
12. K. Huang and J. Rzayev, Well-Defined Organic Nanotubes from Multicomponent Bottlebrush Copolymers, *J. Am. Chem. Soc.*, 2009, **131**, 6880-6885.
13. Y. He, Y. J. Yoon, Y. W. Harn, G. V. Biesold-McGee, S. Liang, C. H. Lin, V. V. Tsukruk, N. Thadhani, Z. Kang and Z. Lin, Unconventional route to dual-shelled organolead halide perovskite nanocrystals with controlled dimensions, surface chemistry, and stabilities, *Sci. Adv.*, 2019, **5**, eaax4424.
14. X. Pang, Y. He, J. Jung and Z. Lin, 1D nanocrystals with precisely controlled dimensions, compositions, and architectures, *Science*, 2016, **353**, 1268-1272.
15. B. R. Sveinbjörnsson, R. A. Weitekamp, G. M. Miyake, Y. Xia, H. A. Atwater and R. H. Grubbs, Rapid self-assembly of brush block copolymers to photonic crystals, *Proc. Natl. Acad. Sci. U. S. A.*, 2012, **109**, 14332-14336.
16. W. F. M. Daniel, J. Burdyńska, M. Vatankhah-Varnoosfaderani, K. Matyjaszewski, J. Paturej, M. Rubinstein, A. V. Dobrynin and S. S. Sheiko, Solvent-free, supersoft and superelastic bottlebrush melts and networks, *Nat. Mater.*, 2016, **15**, 183-189.
17. M. Vatankhah-Varnosfaderani, W. F. M. Daniel, M. H. Everhart, A. A. Pandya, H. Liang, K. Matyjaszewski, A. V. Dobrynin and S. S. Sheiko, Mimicking biological stress–strain behaviour with synthetic elastomers, *Nature*, 2017, **549**, 497-501.
18. M. Vatankhah-Varnosfaderani, A. N. Keith, Y. Cong, H. Liang, M. Rosenthal, M. Sztucki, C. Clair, S. Magonov, D. A. Ivanov, A. V. Dobrynin and S. S. Sheiko, Chameleon-like elastomers with molecularly encoded strain-adaptive stiffening and coloration, *Science*, 2018, **359**, 1509-1513.
19. W. Braunecker and K. Matyjaszewski, Controlled/living radical polymerization: Features, developments, and perspectives, *Prog. Polym. Sci.*, 2007, **32**, 93-146.

20. N. Corrigan, K. Jung, G. Moad, C. J. Hawker, K. Matyjaszewski and C. Boyer, Reversible-deactivation radical polymerization (Controlled/living radical polymerization): From discovery to materials design and applications, *Prog. Polym. Sci.*, 2020, **111**, 101311.
21. B. S. Sumerlin, D. Neugebauer and K. Matyjaszewski, Initiation Efficiency in the Synthesis of Molecular Brushes by Grafting from via Atom Transfer Radical Polymerization, *Macromolecules*, 2005, **38**, 702-708.
22. J. O. Zoppe, N. C. Ataman, P. Mocny, J. Wang, J. Moraes and H.-A. Klok, Surface-Initiated Controlled Radical Polymerization: State-of-the-Art, Opportunities, and Challenges in Surface and Interface Engineering with Polymer Brushes, *Chem. Rev.*, 2017, **117**, 1105-1318.
23. M. Destarac, J.-M. Bessiere and B. Boutevin, Atom transfer radical polymerization of styrene initiated by polychloroalkanes and catalyzed by CuCl/2,2'-bipyridine: A kinetic and mechanistic study, *J. Polym. Sci., Part A: Polym. Chem.*, 1998, **36**, 2933-2947.
24. M. Destarac, K. Matyjaszewski and B. Boutevin, Polychloroalkane initiators in copper-catalyzed atom transfer radical polymerization of (meth)acrylates, *Macromol. Chem. Phys.*, 2000, **201**, 265-272.
25. M. Destarac, B. Boutevin and K. Matyjaszewski, in *Controlled/Living Radical Polymerization*, American Chemical Society, 2000, vol. 768, ch. 17, pp. 234-247.
26. K. Matyjaszewski and N. V. Tsarevsky, Nanostructured functional materials prepared by atom transfer radical polymerization, *Nat. Chem.*, 2009, **1**, 276.
27. K. Matyjaszewski, Advanced Materials by Atom Transfer Radical Polymerization, *Adv. Mater.*, 2018, **30**, 1706441.
28. Y. Chen, D. Yang, Y. J. Yoon, X. Pang, Z. Wang, J. Jung, Y. He, Y. W. Harn, M. He, S. Zhang, G. Zhang and Z. Lin, Hairy Uniform Permanently Ligated Hollow Nanoparticles with Precise Dimension Control and Tunable Optical Properties, *J. Am. Chem. Soc.*, 2017, **139**, 12956-12967.
29. J. Burdyńska, Y. Li, A. V. Aggarwal, S. Höger, S. S. Sheiko and K. Matyjaszewski, Synthesis and Arm Dissociation in Molecular Stars with a Spoked Wheel Core and Bottlebrush Arms, *J. Am. Chem. Soc.*, 2014, **136**, 12762-12770.
30. A. Carlmark and E. Malmström, Atom Transfer Radical Polymerization from Cellulose Fibers at Ambient Temperature, *J. Am. Chem. Soc.*, 2002, **124**, 900-901.
31. P. Vlček, M. Janata, P. Látalová, J. Kríž, E. Čadová and L. Toman, Controlled grafting of cellulose diacetate, *Polymer*, 2006, **47**, 2587-2595.
32. P. Vlček, V. Raus, M. Janata, J. Kříž and A. Sikora, Controlled grafting of cellulose esters using SET-LRP process, *J. Polym. Sci., Part A: Polym. Chem.*, 2011, **49**, 164-173.
33. V. Raus, M. Štěpánek, M. Uchman, M. Šlouf, P. Látalová, E. Čadová, M. Netopilík, J. Kříž, J. Dybal and P. Vlček, Cellulose-based graft copolymers with controlled architecture prepared in a homogeneous phase, *J. Polym. Sci., Part A: Polym. Chem.*, 2011, **49**, 4353-4367.
34. F. Li, M. Cao, Y. Feng, R. Liang, X. Fu and M. Zhong, Site-Specifically Initiated Controlled/Living Branching Radical Polymerization: A Synthetic Route toward Hierarchically Branched Architectures, *J. Am. Chem. Soc.*, 2019, **141**, 794-799.
35. C. Boyer, A. Atme, C. Waldron, A. Anastasaki, P. Wilson, P. B. Zetterlund, D. Haddleton and M. R. Whittaker, Copper(0)-mediated radical polymerisation in a self-generating biphasic system, *Polym. Chem.*, 2013, **4**, 106-112.
36. R. Aksakal, M. Resmini and C. R. Becer, SET-LRP of acrylates catalyzed by a 1 penny copper coin, *Polym. Chem.*, 2016, **7**, 6564-6569.
37. X. Pang, L. Zhao, M. Akinc, J. K. Kim and Z. Lin, Novel Amphiphilic Multi-Arm, Star-Like Block Copolymers as Unimolecular Micelles, *Macromolecules*, 2011, **44**, 3746-3752.
38. I. Zaborniak, P. Chmielarz, K. Wolski, G. Grześ, Z. Wang, A. Górska, K. Pielichowska and K. Matyjaszewski, Maltotriose-based star polymers as self-healing materials, *Eur. Polym. J.*, 2022, **164**, 110972.

39. Z. Samek and M. Buděšínský, In situ reactions with trichloroacetyl isocyanate and their application to structural assignment of hydroxy compounds by 1H NMR spectroscopy. A general comment, *Collect. Czech. Chem. Commun.*, 1979, **44**, 558-588.
40. A. K. Bose and P. R. Srinivasan, NMR spectral studies—XII, *Tetrahedron*, 1975, **31**, 3025-3029.
41. V. W. Goodlett, Use of In Situ Reactions for Characterization of Alcohols and Glycols by Nuclear Magnetic Resonance, *Anal. Chem.*, 1965, **37**, 431-432.
42. M. Buděšínský, Z. Samek and M. Tichý, In situ reactions of amines and amino alcohols and their application to structural assignment by 1H NMR spectroscopy, *Collect. Czech. Chem. Commun.*, 1980, **45**, 2784-2803.
43. P. E. Butler and W. H. Mueller, Simplification of Thiol Nuclear Magnetic Resonance Spectra by in Situ Derivatization, *Anal. Chem.*, 1966, **38**, 1407-1408.
44. J. Loccufier, M. Van Bos and E. Schacht, Convenient method for the analysis of primary and secondary hydroxyl end groups in polyethers, *Polym. Bull.*, 1991, **27**, 201-204.
45. I. Fallais, J. Devaux and R. Jérôme, End-capping of polystyrene by aliphatic primary amine by derivatization of precursor hydroxyl end group, *J. Polym. Sci., Part A: Polym. Chem.*, 2000, **38**, 1618-1629.
46. A. R. Donovan and G. Moad, A novel method for determination of polyester end-groups by NMR spectroscopy, *Polymer*, 2005, **46**, 5005-5011.
47. A. Postma, T. P. Davis, A. R. Donovan, G. Li, G. Moad, R. Mulder and M. S. O'Shea, A simple method for determining protic end-groups of synthetic polymers by 1H NMR spectroscopy, *Polymer*, 2006, **47**, 1899-1911.
48. L. Cao, B. Cao, C. Lu, G. Wang, L. Yu and J. Ding, An injectable hydrogel formed by in situ cross-linking of glycol chitosan and multi-benzaldehyde functionalized PEG analogues for cartilage tissue engineering, *J. Mater. Chem. B*, 2015, **3**, 1268-1280.
49. J. C. Martin, J. L. Chitwood and P. G. Gott, Reactions of trichloroacetyl isocyanate with unsaturated ethers, *J. Org. Chem.*, 1971, **36**, 2228-2232.
50. T. Ando, M. Kamigaito and M. Sawamoto, Design of initiators for living radical polymerization of methyl methacrylate mediated by ruthenium(II) complex, *Tetrahedron*, 1997, **53**, 15445-15457.
51. Y. Shen, S. Zhu, F. Zeng and R. Pelton, Versatile Initiators for Macromonomer Syntheses of Acrylates, Methacrylates, and Styrene by Atom Transfer Radical Polymerization, *Macromolecules*, 2000, **33**, 5399-5404.
52. G. Soriano-Moro, J. Percino, M. Cerón, A. Bañuelos, V. M. Chapela and M. E. Castro, Using of Novel Halides in the ATRP Polymerization. Estimation of Polymer Molecular Mass, *Macromol. Symp.*, 2014, **339**, 112-121.
53. F. Lorandi, M. Fantin, Y. Wang, A. A. Isse, A. Gennaro and K. Matyjaszewski, Atom Transfer Radical Polymerization of Acrylic and Methacrylic Acids: Preparation of Acidic Polymers with Various Architectures, *ACS Macro Lett.*, 2020, **9**, 693-699.
54. S. Alkan, L. Toppare, Y. Hepuzer and Y. Yagci, Block copolymers of thiophene-capped poly(methyl methacrylate) with pyrrole, *J. Polym. Sci., Part A: Polym. Chem.*, 1999, **37**, 4218-4225.
55. C. H. Bamford, I. P. Middleton, K. G. Ai-Lamee and J. Paprotny, Halo-isocyanates as 'transformation' reagents, *Br. Polym. J.*, 1987, **19**, 269-274.
56. Y. Shirai, K. Kawatsura and N. Tsubokawa, Graft polymerization of vinyl monomers from initiating groups introduced onto polymethylsiloxane-coated titanium dioxide modified with alcoholic hydroxyl groups, *Prog. Org. Coat.*, 1999, **36**, 217-224.
57. Y. Shirai, K. Shirai and N. Tsubokawa, Effective grafting of polymers onto ultrafine silica surface: Photopolymerization of vinyl monomers initiated by the system consisting of trichloroacetyl groups on the surface and Mn2(CO)10, *J. Polym. Sci., Part A: Polym. Chem.*, 2001, **39**, 2157-2163.
58. Y. Shirai and N. Tsubokawa, Grafting of polymers onto ultrafine inorganic particle surface: graft polymerization of vinyl monomers initiated by the system consisting of trichloroacetyl

groups on the surface and molybdenum hexacarbonyl, *React. Funct. Polym.*, 1997, **32**, 153-160.
59. G. Wei, K. Shirai, K. Fujiki, H. Saitoh, T. Yamauchi and N. Tsubokawa, Grafting of vinyl polymers onto VGCF surface and the electric properties of the polymer-grafted VGCF, *Carbon*, 2004, **42**, 1923-1929.
60. F. Lorandi, M. Fantin and K. Matyjaszewski, Atom Transfer Radical Polymerization: A Mechanistic Perspective, *J. Am. Chem. Soc.*, 2022, **144**, 15413-15430.
61. A. Anastasaki, V. Nikolaou, G. Nurumbetov, P. Wilson, K. Kempe, J. F. Quinn, T. P. Davis, M. R. Whittaker and D. M. Haddleton, Cu(0)-Mediated Living Radical Polymerization: A Versatile Tool for Materials Synthesis, *Chem. Rev.*, 2016, **116**, 835-877.
62. V. Percec, T. Guliashvili, J. S. Ladislaw, A. Wistrand, A. Stjerndahl, M. J. Sienkowska, M. J. Monteiro and S. Sahoo, Ultrafast Synthesis of Ultrahigh Molar Mass Polymers by Metal-Catalyzed Living Radical Polymerization of Acrylates, Methacrylates, and Vinyl Chloride Mediated by SET at 25 °C, *J. Am. Chem. Soc.*, 2006, **128**, 14156-14165.
63. B. M. Rosen and V. Percec, Single-Electron Transfer and Single-Electron Transfer Degenerative Chain Transfer Living Radical Polymerization, *Chem. Rev.*, 2009, **109**, 5069-5119.
64. Y. Zhang, Y. Wang and K. Matyjaszewski, ATRP of Methyl Acrylate with Metallic Zinc, Magnesium, and Iron as Reducing Agents and Supplemental Activators, *Macromolecules*, 2011, **44**, 683-685.
65. Y. Zhang, Y. Wang, C.-h. Peng, M. Zhong, W. Zhu, D. Konkolewicz and K. Matyjaszewski, Copper-Mediated CRP of Methyl Acrylate in the Presence of Metallic Copper: Effect of Ligand Structure on Reaction Kinetics, *Macromolecules*, 2012, **45**, 78-86.
66. X. Leng, N. H. Nguyen, B. van Beusekom, D. A. Wilson and V. Percec, SET-LRP of 2-hydroxyethyl acrylate in protic and dipolar aprotic solvents, *Polym. Chem.*, 2013, **4**, 2995-3004.
67. M. Zhang, M. F. Cunningham and R. A. Hutchinson, Aqueous copper(0) mediated reversible deactivation radical polymerization of 2-hydroxyethyl acrylate, *Polym. Chem.*, 2015, **6**, 6509-6518.
68. A. G. West, B. Hornby, J. Tom, V. Ladmiral, S. Harrisson and S. Perrier, Origin of Initial Uncontrolled Polymerization and Its Suppression in the Copper(0)-Mediated Living Radical Polymerization of Methyl Acrylate in a Nonpolar Solvent, *Macromolecules*, 2011, **44**, 8034-8041.
69. B. D. Hornby, A. G. West, J. C. Tom, C. Waterson, S. Harrisson and S. Perrier, Copper(0)-Mediated Living Radical Polymerization of Methyl Methacrylate in a Non-polar Solvent, *Macromol. Rapid Commun.*, 2010, **31**, 1276-1280.
70. V. Raus, M. Janata and E. Čadová, Copper Wire–Catalyzed RDRP in Nonpolar Media as a Route to Ultrahigh Molecular Weight Organic–Inorganic Hybrid Polymers, *Macromol. Chem. Phys.*, 2018, **219**, 1800141.
71. L. Poláková, V. Raus, L. Kostka, A. Braunová, J. Pilař, V. Lobaz, J. Pánek and Z. Sedláková, Antioxidant Properties of 2-Hydroxyethyl Methacrylate-Based Copolymers with Incorporated Sterically Hindered Amine, *Biomacromolecules*, 2015, **16**, 2726-2734.
72. L. Poláková, V. Raus, L. Cuchalová, R. Poręba, M. Hrubý, J. Kučka, D. Větvička, O. Trhlíková and Z. Sedláková, SHARP hydrogel for the treatment of inflammatory bowel disease, *Int. J. Pharm.*, 2022, **613**, 121392.
73. M. Janata, E. Čadová, J. W. Johnson and V. Raus, Diminishing the catalyst concentration in the Cu(0)-RDRP and ATRP synthesis of well-defined low-molecular weight poly(glycidyl methacrylate), *J. Polym. Sci.*, 2023, **61**, 1348-1359.
74. S. Gupta and V. Raus, Cu(0)-RDRP of 2-hydroxyethyl methacrylate in a non-polar solvent enables rapid synthesis of high-molecular weight homopolymers and direct access to amphiphilic copolymers, *React. Funct. Polym.*, 2023, **183**, 105509.

75. N. H. Nguyen, X. Leng and V. Percec, Synthesis of ultrahigh molar mass poly(2-hydroxyethyl methacrylate) by single-electron transfer living radical polymerization, *Polym. Chem.*, 2013, **4**, 2760-2766.
76. T. Liu, X. Li, Y. Qian, X. Hu and S. Liu, Multifunctional pH-Disintegrable micellar nanoparticles of asymmetrically functionalized β-cyclodextrin-Based star copolymer covalently conjugated with doxorubicin and DOTA-Gd moieties, *Biomaterials*, 2012, **33**, 2521-2531.
77. X. Hu, S. Liu, Y. Huang, X. Chen and X. Jing, Biodegradable Block Copolymer-Doxorubicin Conjugates via Different Linkages: Preparation, Characterization, and In Vitro Evaluation, *Biomacromolecules*, 2010, **11**, 2094-2102.
78. B.-S. Kim, H.-i. Lee, Y. Min, Z. Poon and P. T. Hammond, Hydrogen-bonded multilayer of pH-responsive polymeric micelles with tannic acid for surface drug delivery, *Chem. Commun.*, 2009, DOI: 10.1039/B908688A, 4194-4196.
79. L. W. Dittert and T. Higuchi, Rates of Hydrolysis of Carbamate and Carbonate Esters in Alkaline Solution, *J. Pharm. Sci.*, 1963, **52**, 852-857.
80. T. Vontor and M. Vecera, Carbamates .4. Kinetics and Mechanism of Hydrolysis of Substituted Phenyl N-Methylcarbamates in Strongly Alkaline and Acid-Media, *Collect. Czech. Chem. Commun.*, 1973, **38**, 3139-3145.
81. O. Vandenabeele-Trambouze, L. Garrelly, L. Mion, L. Boiteau and A. Commeyras, Key parameters for carbamate stability in dilute aqueous–organic solution, *Adv. Environ. Res.*, 2001, **6**, 67-80.
82. A. K. Ghosh and M. Brindisi, Organic Carbamates in Drug Design and Medicinal Chemistry, *J. Med. Chem.*, 2015, **58**, 2895-2940.
83. C. Y. Lin, M. L. Coote, A. Petit, P. Richard, R. Poli and K. Matyjaszewski, Ab Initio Study of the Penultimate Effect for the ATRP Activation Step Using Propylene, Methyl Acrylate, and Methyl Methacrylate Monomers, *Macromolecules*, 2007, **40**, 5985-5994.
84. M. S. Rolph, A. Pitto-Barry and R. K. O'Reilly, The hydrolytic behavior of N,N'-(dimethylamino)ethyl acrylate-functionalized polymeric stars, *Polym. Chem.*, 2017, **8**, 5060-5070.
85. Z. Zheng, J. Ling and A. H. E. Müller, Revival of the R-Group Approach: A "CTA-shuttled" Grafting from Approach for Well-Defined Cylindrical Polymer Brushes via RAFT Polymerization, *Macromol. Rapid Commun.*, 2014, **35**, 234-241.
86. V. Raus, A. Sturcova, J. Dybal, M. Slouf, T. Vackova, P. Salek, L. Kobera and P. Vlcek, Activation of cellulose by 1,4-dioxane for dissolution in N,N-dimethylacetamide/LiCl, *Cellulose*, 2012, **19**, 1893-1906.
87. D. Klemm, B. Heublein, H.-P. Fink and A. Bohn, Cellulose: Fascinating Biopolymer and Sustainable Raw Material, *Angew. Chem. Int. Ed.*, 2005, **44**, 3358-3393.
88. A. Potthast, S. Radosta, B. Saake, S. Lebioda, T. Heinze, U. Henniges, A. Isogai, A. Koschella, P. Kosma, T. Rosenau, S. Schiehser, H. Sixta, M. Strlič, G. Strobin, W. Vorwerg and H. Wetzel, Comparison testing of methods for gel permeation chromatography of cellulose: coming closer to a standard protocol, *Cellulose*, 2015, **22**, 1591-1613.
89. M. Gerle, K. Fischer, S. Roos, A. H. E. Müller, M. Schmidt, S. S. Sheiko, S. Prokhorova and M. Möller, Main Chain Conformation and Anomalous Elution Behavior of Cylindrical Brushes As Revealed by GPC/MALLS, Light Scattering, and SFM, *Macromolecules*, 1999, **32**, 2629-2637.
90. Q. Xu, J. Yang, X. Zhang, X. Wen, M. Yamada, F. Fu, H. Diao and X. Liu, A "grafting through" strategy for constructing Janus cotton fabric by mist polymerization, *J. Mater. Chem. A*, 2020, **8**, 24553-24562.
91. I. Zaborniak and P. Chmielarz, Polymer-modified regenerated cellulose membranes: following the atom transfer radical polymerization concepts consistent with the principles of green chemistry, *Cellulose*, 2023, **30**, 1-38.
92. S. Sant and H.-A. Klok, Linear, Y- and Ψ-shaped poly(2-(dimethylamino)ethyl methacrylate) and poly(methyl methacrylate) brushes prepared by surface-initiated polymerization from a homologous series of ATRP initiators, *Eur. Polym. J.*, 2024, **205**, 112706.

Electronic supplementary information for

Straightforward synthesis of complex polymeric architectures with ultra-high chain density

*Sachin Gupta, Miroslav Janata, Eva Čadová, and Vladimír Raus**

Institute of Macromolecular Chemistry, Czech Academy of Sciences, Heyrovského nám. 2, 162 06, Prague 6, Czech Republic

E-mail: raus@imc.cas.cz

EXPERIMENTAL

Materials

Trichloroacetyl isocyanate (TAI; Acros Organics, NMR grade, >97%), CuBr (Fluka, >98%), $CuBr_2$ (Sigma Aldrich, 98%) CuCl (Sigma-Aldrich, >99%), $CuCl_2$ (Sigma-Aldrich, 99%), and phenothiazine (Sigma-Aldrich, 98%) were used as received. Cu-wire (Sigma-Aldrich, diameter=0.64 mm) was activated before each polymerization by conc. HCl using the procedure provided below. Lithium chloride (Fluka) was vacuum dried at 190 °C for 8 h prior the use. *N,N,N′,N″,N‴*-Pentamethyldiethylenetriamine (PMDETA; Sigma-Aldrich, 99%) was vacuum distilled and stored under argon at 4 °C. Tris[2-(dimethylamino)ethyl]amine (Me_6TREN) was synthesized using a literature protocol[1] and stored under argon at 4 °C. Solvents, i.e. dimethyl sulfoxide (DMSO; Acros Organics, 99.7+%), dimethylacetamide (DMAc; Acros Organics, 99.5+%), 1,4-dioxane (Lach-Ner, p.a.), toluene (Lach-Ner, p.a.), isopropyl alcohol (IPA; Lach-Ner, p.a.), methanol (Lach-Ner, p.a), acetonitrile (Lach-Ner, p.a.), dichloromethane (Lach-Ner, p.a.), tetrahydrofuran (THF; Lach-Ner, p.a.), and acetone (Lach-Ner, p.a.), were either used as received or dried using 3Å molecular sieves and purged with argon for 1 h (when used for polymerization) or dried using 3Å molecular sieves and stored under argon (when used for TAI modifications). Hydrochloric acid (Lach-Ner, 35-38%) was used as received.

N,N-Dimethylacetamide (DMAc; VWR; HPLC Grade, 99.5 %) and lithium bromide (Sigma-Aldrich, 99%) were used for the preparation of the mobile phase for SEC with triple detection (TD-SEC); the prepared mobile phase was filtered through a 0.22 µm polyamide filter before use. THF used for SEC with relative calibration (Lach-Ner, p.a.) was distilled before use.

Methyl acrylate (MA; Sigma-Aldrich, 99%), methyl methacrylate (MMA; Acros Organics, 99%), styrene (Fluka, 99.5%), *n*-butyl acrylate (BA; Fluka, 99%), glycidyl methacrylate (GMA; Fluka, 99.5%), 2-hydroxyethyl methacrylate (HEMA; Sigma-Aldrich, 97%), and *n*-butyl methacrylate (BMA; Fluka, 99%) were distilled under high vacuum to remove the inhibitor and stored under argon atmosphere at -20°C. 2-Hydroxyethyl acrylate (HEA; Sigma-Aldrich, 96%) was used as received.

Pentaerythritol (Sigma-Aldrich, 98%), ethylene glycol (Fluka, >99.5%), *N,N*-diisopropylamine (DIPA; Sigma-Aldrich, >99.5%), cellulose Avicel PH-101 (Fluka) and Sigmacell type 101 (Sigma), filter paper Whatman 1450-917, cotton thread Catania (Schachenmayr smc, 100% cotton), and ß-cyclodextrin (Sigma-Aldrich, ≥97%) were treated before the reaction with TAI as detailed in the experimental protocols.

Characterization

The number-average molecular weights (M_n), weight-average molecular weights (M_w), and dispersity ($Đ$) of the (co)polymers were determined by SEC.

Most of the analyses during the optimization of polymerization conditions were performed using an SEC system consisting of the SDS 150 pump (Watrex, Czech Republic), an RI detector (RI-101; Shodex, Japan), and two PLgel MIXED-C columns (300 × 7.5 mm, SDV gel with particle size 5µm; Agilent, USA). Tetrahydrofuran was used as the mobile phase at 25 °C with a flow rate of 1 mL/min. The molecular weight (MW) values were calculated using the Clarity software (Dataapex, Czech Republic). Calibrations with polystyrene standards (PSS, Germany) in the molecular weight range of 580 and

1 820 000 and with poly(MMA) standards (PSS, Germany) in the MW range of 2 200 to 1 220 000 were used.

Advanced polymer characterization was done using the Malvern Panalytical OMNISEC triple detection SEC (TD-SEC) system consisting of OMNISEC Resolve and OMNISEC Reveal units. Two PSS GRAM analytical linear columns with the dimensions of 8 x 300 mm and the particle size of 10 µm were used. Triple detection with the following detectors was performed: differential refractive index (RI) detector, right-angle light scattering (RALS) + low-angle light scattering (LALS) measuring at an angle of 7° to the incident beam (laser wavelength of 640 nm), and a 4-capillary Wheatstone bridge viscometer. The columns and detectors were held at 55 °C. Dimethylacetamide with 5g/L LiBr was used as an eluent at a flow rate of 1 mL/min. OMNISEC software from Malvern Panalytical was used for online monitoring and processing of the data. In some cases, universal calibration was used for the MW determination; in this case, the calibration was performed using the polystyrene standards (PSS, Germany) in the MW range of 1,930 to 990,500. All sample solutions were filtered through 0.2 µm PTFE filters prior to injection.

^{1}H NMR and ^{13}C NMR spectra were recorded on a Bruker Avance NEO 400 spectrometer operating at 400.13 MHz at 300 K or Bruker AVANCE-III operating at 600 MHz at 298 K.

Procedures

Note: All reactions with TAI as well as polymerizations were conducted using a Schlenk-type technique in inert atmosphere (under argon) unless stated otherwise.

Activation of Cu wire

The wire was placed into ca. 5 mL of conc. HCl for 5 min, removed and washed with water, and returned to conc. HCl for another 10 min. Afterwards, the activated wire was successively washed with water and acetone, dried in an argon stream, and kept under argon until use.

Methyl(trichloroacetyl)carbamate (MTAC)

Into a 50 mL reaction flask equipped with a magnetic stirring bar and a three-way stopcock connected to an argon/vacuum inlet, dry methanol (20 mL) was added, and the flask was cooled in an ice bath. Upon dropwise addition of TAI (6.325 mL, 53.08 mmol), the flask was removed from the ice bath, and the mixture was left to stir at r.t. for 1 h. Thereafter, unreacted methanol was evaporated to afford a white solid (11.3 g, 97% yield) that was stored at 4 °C and used as a Cu-RDRP initiator without any further purification.

1,1-Diisopropyl-3-(2,2,2-trichloroacetyl)-urea (DTAU)

Into a 25 mL two-necked round-bottomed flask equipped with a magnetic stirring bar and connected via a distillation bridge to another flask having an argon/vacuum inlet, dried CH_2Cl_2 (5 mL) and *N,N*-diisopropylamine (0.420 mL, 0.2965 mmol, pre-dried using 3Å molecular sieves) were added. The flask

was placed in an ice bath, and TAI (0.442 mL, 0.3706 mmol) was added dropwise. Once the addition of TAI was complete, the flask was removed from the ice bath, and the mixture was left to stir at r. t. for 20 minutes during which the solution turned slight yellow. Thereafter, CH_2Cl_2 and the excess of TAI were distilled off under high vacuum, affording a slightly yellow solid (0.834 g, 97% yield) that was further dried under vacuum and stored at 4 °C. The product was used as a Cu-RDRP initiator without any further purification.

Pentaerythritol tetrakis((2,2,2-trichloroacetyl)carbamate) (PTAC)

In a 50 mL two-necked round-bottomed flask equipped with a magnetic stirring bar and connected via a distillation bridge to another flask having an argon/vacuum inlet, pentaerythritol (0.25 g, 1.836 mmol, pre-dried under vacuum at 80 °C overnight) was mixed with dried dioxane (10 mL). Then, TAI (1.1 mL, 9.231 mmol) was added dropwise, which led to the dissolution of the solids. After 20 min, dioxane and the excess of TAI were distilled off under high vacuum, affording a white solid (1.513 g, 93% yield) that was further dried under vacuum and stored at 4 °C. The product was used as a Cu-RDRP initiator without any further purification.

Ethane-1,2-diyl bis((2,2,2-trichloroacetyl)carbamate) (ETAC)

Into a 25 mL two-necked round-bottomed flask equipped with a magnetic stirring bar and connected via a distillation bridge to another flask having an argon/vacuum inlet, dried CH_2Cl_2 (5 mL) and ethylene glycol (0.112 mL, 0.2014 mmol, pre-dried using 3Å molecular sieves) were added. The flask was placed in an ice bath, and TAI (0.600 mL, 0.5035 mmol) was added dropwise. Once the addition of TAI was complete, the flask was removed from the ice bath, and the mixture was left to stir at r. t. for 20 min. Thereafter, CH_2Cl_2 and the excess of TAI were distilled off under the high vacuum, affording a white solid (0.865 g, 98% yield) that was further dried under vacuum and stored at 4 °C. The product was used as a Cu-RDRP initiator without any further purification.

Polymerization experiments

During the optimization of polymerization conditions, Cu-RDRP experiments were conducted in a similar way regardless of the monomer used. Generally, the experimental scale was kept the same, i.e., 5 mL of a monomer and 5 mL of a solvent were used, with the amount of initiator adjusted based on the targeted M/I ratio. In the bulk polymerization of styrene, 10 mL of the monomer was used to keep a similar polymerization mixture volume. In Cu(0)-RDRP experiments, a fixed length of Cu wire (10 cm) was employed unless stated otherwise. Since the initiators used here are solids, in the polymerization protocols, we generally first deoxygenated the solid compounds (an initiator, Cu-salt(s), or Cu wire), added a solvent and a monomer, and finally started the polymerization by adding a ligand (and placing the flask into a heating bath if needed). Typically, the polymerization was stopped either when the viscosity of the polymerization mixture prevented efficient stirring or when 24 h elapsed. Monomer conversions were typically determined by gravimetry (for styrene and MMA) or using ^{1}H NMR (for other monomers). Below, we provide sample procedures for Cu(0)-RDRP and ATRP experiments.

Cu(0)-RDRP of MMA

MTAC (51.52 mg, 0.2337 mmol) and activated Cu wire (10 cm) were placed into a reaction flask equipped with a magnetic stirring bar and a three-way stopcock connected to an argon/vacuum inlet. After thorough deoxygenation by several vacuum-argon cycles, toluene (5 mL) was added, followed by the addition of MMA (5 mL, 46.74 mmol). Subsequently, the polymerization was started by the addition of PMDETA (49 µL, 0.2337 mmol), and the flask was placed into a stirred oil bath pre-heated to 85 °C. After 24 h, the experiment was ended, the flask was cooled down, the Cu-wire was removed, and the polymerization was quenched by adding a small amount of phenothiazine. Then, the mixture was diluted with THF and the product was precipitated in MeOH/water (4:1 v/v). The precipitate was collected on a glass frit, washed, and dried overnight under vacuum at 40 °C.

ATRP of styrene

CuBr (62.4 mg, 0.4349 mmol) and MTAC (96 mg, 0.4349 mmol) were placed into a reaction flask equipped with a magnetic stirring bar and a three-way stopcock connected to an argon/vacuum inlet. After thorough deoxygenation by several vacuum-argon cycles, styrene (10 mL, 86.98 mmol) was added. Subsequently, the polymerization was started by the addition of Me_6TREN (116 µL, 0.4349 mmol), and the flask was placed into a stirred oil bath pre-heated to 110 °C. After 6 h, the mixture was highly viscous, and so the experiment was ended, the flask was cooled down, and the polymerization was quenched by adding a small amount of phenothiazine. Then, the mixture was diluted with THF and the product was precipitated in MeOH. The precipitate was collected on a glass frit, washed, and dried overnight under vacuum at 40 °C.

Alkaline hydrolysis of star polymers and graft copolymers

Reactions were carried out according to the literature.[2] In a 25 mL flask equipped with a magnetic stirring bar, a (co)polymer (100 mg), THF (8 mL), and 1 M solution of KOH in methanol (4 mL) were mixed, and the reaction mixture was stirred for 3 days at r. t. Then, the mixture was neutralized with 1 M HCl, solvents were evaporated, and the residuum was extracted with THF (3 mL). The product was then precipitated by the addition of the extract into MeOH/water (4:1 v/v) in case of poly(MMA) or neat MeOH in case of polystyrene. The precipitates were filtered, washed, and dried in vacuum at 40 °C.

Hydrolytic stability of the TAI-based carbamate linker

Poly(2-hydroxyethyl) acrylate (poly(HEA)): The preparation of the poly(HEA) starting polymer for the stability study was performed via Cu(0)-RDRP in DMSO at 60 °C using the standard procedure detailed above. Upon termination of the polymerization, the reaction mixture was dialyzed against deionized water, and the product was obtained by freeze-drying.

Attempted hydrolysis of the carbamate linker in poly(HEA) at different pH: In a 20 mL vial equipped with a magnetic stirring bar, 20 mg of the synthesized poly(HEA) was dissolved in the selected buffer (4 mL; pH = 1, 3, 5, 7, 9, or 11), and the solution was stirred at 37 °C for 24 h. Afterward, the solution was dialyzed against deionized water (MWCO = 1 000) and freeze-dried. The obtained polymer was

analyzed by TD-SEC in DMAc/LiBr (dn/dc was calculated by the OMNISEC software considering 100% sample recovery).

De novo one-pot synthesis of poly(HEMA-co-MMA)-graft-poly(MMA) graft copolymer

Step 1: Activated Cu wire (4 cm) and MTAC (55.11 mg, 0.25 mmol) were placed into a reaction flask equipped with a magnetic stirring bar and a three-way stopcock connected to an argon/vacuum inlet. After thorough deoxygenation by several vacuum-argon cycles, dioxane (2.75 mL), HEMA (0.606 mL, 5.0 mmol), and MMA (2.14 mL, 20.0 mmol) were added. Subsequently, the polymerization was started by the addition of PMDETA (52.2 µL, 0.25 mmol), and the flask was placed into a stirred oil bath pre-heated to 85 °C. After 3 h, the flask was removed from the oil bath and cooled to r. t. A sample of the reaction mixture was withdrawn for SEC and NMR analysis.

Step 2: The polymerization mixture was diluted with dioxane (5 mL), which was followed by a dropwise addition of TAI (298 µL, 2.5 mmol, 0.5 eq. toward HEMA) under intensive stirring. The resulting mixture was further stirred at r. t. for 15 min. Then, 9 mL of the reaction mixture was removed from the flask: a sample was used for ^{1}H NMR analysis, and the rest was isolated by precipitation in MeOH/water (4:1 v/v). The 1.5 mL of reaction mixture that remained in the reaction flask was used as a macroinitiator in the following step.

Step 3: The macroinitiator solution was diluted with dioxane (5 mL), and MMA (15 mL, 140 mmol, 400 eq. toward present TAGs) and PMDETA (75 µL, 0.357 mmol, 1.0 eq. toward the present TAGs) were added, and the flask was placed into a stirred oil bath pre-heated to 85 °C. After 2 h, the experiment was ended, the flask was cooled down, the Cu-wire was removed, and the polymerization was quenched by adding a small amount of phenothiazine. Then, the mixture was diluted with THF and the product was precipitated in MeOH. The precipitate was collected on a glass frit, washed, and dried overnight under vacuum at 40 °C. A sample of the obtained product was further subjected to alkaline hydrolysis.

Synthesis of multi-arm poly(MMA) stars based on a ß-cyclodextrin core

Modification of ß-cyclodextrin with TAI: In a 5 mL round-bottomed flask equipped with a magnetic stirring bar and an argon/vacuum inlet, ß-CD (0.030 g, 0.0264 mmol, pre-dried under vacuum at 80 °C) was dispersed in dried acetonitrile (800 µL). Then, TAI (95 µL, 0.793 mmol) was added, and the mixture was stirred at r.t. for 16 h. Into the obtained clear solution of the ß-CD/TAI adduct, DMSO (~17 µL) was added to quench the excess of TAI. Samples were withdrawn for ^{1}H NMR and SEC analyses, and the remaining mixture was used as an initiator in the subsequent step.

ATRP of MMA initiated by the ß-CD/TAI adduct: CuBr (57 mg, 0.397 mmol) was placed into a reaction flask equipped with a magnetic stirring bar and a three-way stopcock connected to an argon/vacuum inlet. After thorough deoxygenation by several vacuum-argon cycles, dioxane (5.9 mL), MMA (5.9 mL, 55.15 mmol), and 400 µL of the solution of ß-CD/TAI adduct prepared in the previous step (0.397 mmol of TAGs) were added. Afterward, the polymerization was started by the addition of PMDETA (83 µL, 0.397 mmol), and the flask was placed into a stirred oil bath pre-heated to 85°C. Samples of the polymerization mixture, withdrawn at 4 h and 7 h timepoints, were quenched with phenothiazine.

diluted with THF, precipitated in MeOH, and used for SEC and NMR analyses. After 23 h, the experiment was ended, the flask was cooled down and opened to air, and the polymerization was quenched by adding a small amount of phenothiazine. The stabilized removed samples as well as the final mixture were analyzed by ^{1}H HMR (conversion determination). Products were isolated as follows: the mixture was diluted with THF, the polymer was precipitated in MeOH, the precipitate was collected on a glass frit, washed, and dried overnight under vacuum at 40 °C. Isolated samples were analyzed by TD-SEC.

Modification of powder cellulose with TAI

Modification in DMAc/LiCl (homogeneous modification): Cellulose AVICEL PH-101 was activated by dioxane according to the literature protocol (the full activation protocol finished with freeze drying).[3] In a 25 mL reaction flask, activated cellulose (0.1 g, 0.617 mmol of monomeric units) was dissolved in 7.7% DMAc/LiCl (10 mL; prepared under anhydrous conditions). To the stirred solution, TAI (294 µL, 2.467 mmol) was added dropwise. After 20 min, the excess of TAI was quenched with several drops of water, and the product was precipitated in IPA/water (1:1, v/v), collected on a glass frit, washed thoroughly with IPA, and dried in vacuum at 40 °C overnight. Product weight = 0.416 g (93% yield).

Modification in other solvents (heterogeneous modification): Modification of powder cellulose in other solvents was done in a similar way as described above, starting with the cellulose suspension in the respective solvent.

Synthesis of an ultra-dense bottle-brush graft copolymer by ATRP grafting of MMA from cellulose/TAI adduct

Preparation of the cellulose/TAI macroinitiator: Into a 10 mL round-bottomed flask, equipped with a magnetic stirring bar and an argon/vacuum inlet, containing the Avicel PH-101 (0.050 g, 0.3084 mmol, pre-dried in vacuum at 80 °C) suspension in dried acetonitrile (5 mL), TAI (0.221 mL, 1.8546 mmol) was added, and the mixture was left to stir at r. t. for 4 days. Then, MeOH (0.040 mL) was added into the homogeneous solution to quench any unreacted TAI. The prepared mixture was analyzed by SEC and used as a stock solution of the (macro)initiator in the subsequent polymerization step.

ATRP grafting of MMA from the cellulose/TAI adduct: CuBr (13.3 mg, 0.0927 mmol) was placed into a 50 mL reaction flask equipped with a magnetic stirring bar and a three-way stopcock connected to an argon/vacuum inlet. After thorough deoxygenation by several vacuum-argon cycles, dioxane (7.9 mL), MMA (7.9 mL, 74.2 mmol), and the (macro)initiator solution from the previous step (250 µL, 0.0927 mmol of TAGs) were added. Afterward, the polymerization was started by the addition of PMDETA (19.4 µL, 0.0927 mmol), and the flask was placed into a stirred oil bath pre-heated to 85°C. At 5 h, a sample of the polymerization mixture was withdrawn for conversion determination by ^{1}H NMR and for TD-SEC analysis (performed using the polymer isolated by precipitation into MeOH). At 24 h, the experiment was ended, the flask was cooled down and opened to air, and the polymerization was quenched by adding a small amount of phenothiazine. A sample was withdrawn for conversion determination via ^{1}H NMR. Then, the mixture was diluted with THF and the product was precipitated

in MeOH. The precipitate was collected on a glass frit, washed, and dried overnight in vacuum at 40 °C.

Surface-initiated grafting from TAI-modified filter paper

Modification of Whatman paper with TAI: Whatman paper (7 x 5.5 cm) was cut and soaked in dry DMSO for 3 days. Then, the paper was removed from DMSO, briefly dried with a paper towel, and placed on a customized mask (see picture below) with an "IMC" inscription. After closely tightening the paper inside the mask, TAI (100 µL, 0.8392 mmol) was dripped evenly onto the exposed paper surface in argon flow. Subsequently, the mask was immersed into a beaker containing IPA in order to quench the excess of TAI. The paper was then removed from the mask and washed excessively with methanol in order to remove any unbound TAI adducts and dried in vacuum at r.t.

ATRP grafting of MMA from the TAI-modified paper: CuBr (120.4 mg, 0.8392 mmol) and the TAI-modified Whatman paper were placed into a reaction flask equipped with a magnetic stirring bar and a three-way stopcock connected to an argon/vacuum inlet. After thorough deoxygenation by several vacuum-argon cycles, dioxane (17.5 mL) and MMA (17.5 mL, 163.6 mmol) were added. Afterward, the polymerization was started by the addition of PMDETA (175 µL, 0.8392 mmol), and the flask was placed into a stirred oil bath pre-heated to 85°C. After 30 min, the experiment was ended, the flask was cooled down, and the polymerization was quenched by adding a small amount of phenothiazine. The paper was removed, washed carefully first with THF to remove any free polymer and then with methanol to remove the catalytic complex residua, and finally dried in vacuum at r.t.

Surface-initiated grafting from TAI-modified cotton thread

Modification of cotton thread with TAI: 5 cm long cotton thread was placed into a reaction flask equipped with a magnetic stirring bar and a three-way stopcock connected to an argon/vacuum inlet. After inertization, dry DMSO (10 mL) was added, and the thread was left to soak for 5 minutes after which TAI (400 µL, 3.356 mmol) was added. After 15 minutes, the thread was removed from the flask, washed with an excess of methanol, and dried in vacuum at r.t.

ATRP grafting of MMA from the TAI-modified cotton thread: CuBr (34.4 mg, 0.2398 mmol) and TAI-modified cotton thread were placed into a reaction flask equipped with a magnetic stirring bar and a three-way stopcock connected to an argon/vacuum inlet. After thorough deoxygenation by several vacuum-argon cycles, dioxane (5 mL) and MMA (5 mL, 46.74 mmol) were added. Afterward, the polymerization was started by the addition of PMDETA (50 µL, 0.2398 mmol), and the flask was placed into a stirred oil bath pre-heated to 85°C. After 1 h, the experiment was ended, the flask was cooled down, and the polymerization was quenched by adding a small amount of phenothiazine. The thread was removed, washed thoroughly with THF and methanol, and dried in vacuum at 40 °C.

Surface-initiated grafting from TAI-modified pine cone

Modification of a pine cone with TAI: A pine cone was left to soak in dry DMSO (80 mL) overnight. The original (discolored) DMSO was then replaced with a fresh one, and 3Å molecular sieves were added. After 7 days, the cone was quickly transferred into a 100 mL wide-neck reagent bottle equipped with a magnetic stirring bar and fitted with a rubber septum pierced with a needle connected to an

argon/vacuum inlet. After inertization, dry DMSO (70 mL) was added, and the bottle was placed in an ice bath. TAI (2 mL, 16.78 mmol) was then added dropwise, and the mixture was then stirred for 15 minutes. Thereafter, the cone was removed from the flask, washed thoroughly with methanol, and dried in vacuum at r.t.

ATRP grafting of MMA from the TAI-modified pine cone: CuBr (137.4 mg, 0.958 mmol) and the TAI-modified cone were placed into a into a 100 mL wide-neck reagent bottle equipped with a magnetic stirring bar and fitted with a rubber septum pierced with a needle connected to an argon/vacuum inlet. After thorough deoxygenation, dioxane (40 mL) and MMA (40 mL, 374 mmol) were added. Afterward, the polymerization was started by the addition of PMDETA (200 µL, 0.958 mmol), and the flask was placed into a stirred oil bath pre-heated to 85°C. After 4 h, the experiment was ended, the flask was cooled down, and the polymerization was quenched by adding a small amount of phenothiazine. The cone was removed, washed thoroughly with THF and methanol, and dried in vacuum at 40 °C.

ADDITIONAL RESULTS

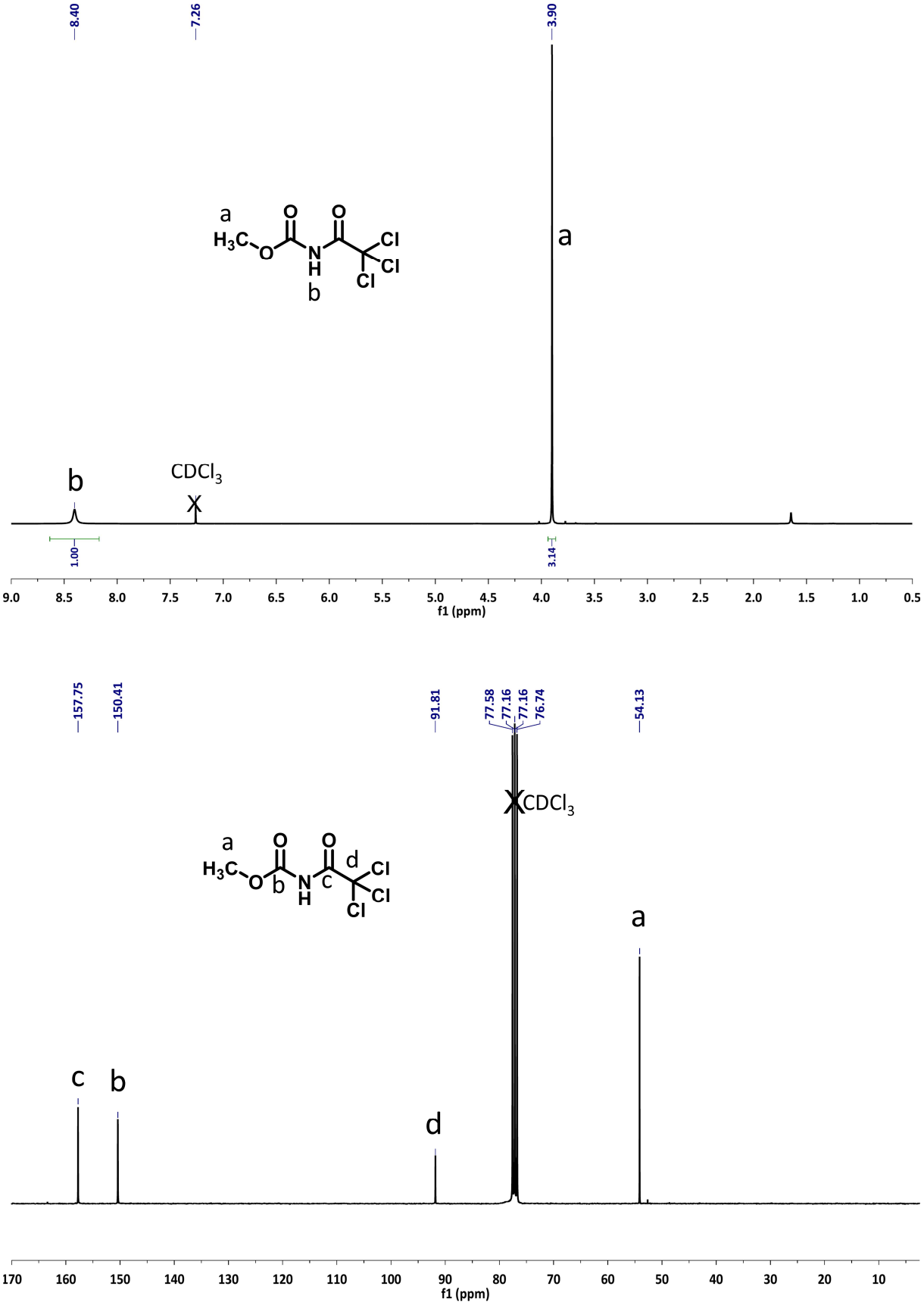

Figure S1. ^{1}H NMR (top) and ^{13}C NMR (bottom) spectra of methyl(trichloroacetyl)carbamate (MTAC) measured in $CDCl_3$.

Table S1. Additional results obtained during the optimization of polymerization conditions for MTAC-initiated Cu-RDRP of MA[a]

Entry	Cat.	Solvent	Ligand (eq.)	T (°C)	Time (h)	Conv. (%)[b]	M_n (theor.)[c]	M_n (SEC)[d]	$Đ$[d]
1	CuBr	DMSO	PMDETA (1.0)	r.t.	24	*no polymerization*			
2	CuBr	DMSO	Me_6TREN (1.0)	r.t.	24	*no polymerization*			
3	CuBr	DMSO	PMDETA (1.0)	60	24	*no polymerization*			
4	CuBr	DMSO	Me_6TREN (1.0)	60	24	*no polymerization*			
5	CuBr	DMAC	PMDETA (1.0)	r.t.	24	*no polymerization*			
6	CuBr	DMAC	Me_6TREN (1.0)	r.t.	24	*no polymerization*			
7	CuBr	DMAC	PMDETA (1.0)	60	24	*no polymerization*			
8	CuBr	DMAC	Me_6TREN (1.0)	60	24	*no polymerization*			
9	CuBr	toluene	PMDETA (1.0)	r.t.	24	*no polymerization*			
10	CuBr	toluene	Me_6TREN (1.0)	r.t.	24	*no polymerization*			
11	CuBr	toluene	PMDETA (1.0)	60	24	*no polymerization*			
12	CuBr	toluene	Me_6TREN (1.0)	60	24	36	6 300	6 100	2.51
13	CuBr	dioxane	PMDETA (1.0)	60	24	*no polymerization*			
14	CuBr	dioxane	Me_6TREN (1.0)	60	24	*no polymerization*			
15	CuCl[e]	dioxane	Me_6TREN (1.5)	60	24	*no polymerization*			
16	Cu(0)	DMAc	PMDETA (0.2)	r.t.	24	32	5 700	8 200	1.74
17	Cu(0)	DMAc	PMDETA (0.5)	r.t.	24	18	3 300	6 000	1.55
18	Cu(0)	DMAc	PMDETA (1.0)	r.t.	24	22	4 000	12 400	1.34
19	Cu(0)	DMAc	Me_6TREN (0.2)	r.t.	24	*no polymerization*			
20	Cu(0)	DMAc	Me_6TREN (0.5)	r.t.	24	29	5 100	5 300	1.23
21	Cu(0)	DMAc	Me_6TREN (1.0)	r.t.	24	71	12 300	18 700	1.24
22	Cu(0)	DMAc	Me_6TREN (0.2)	60	24	77	13 300	15 700	1.19
23	Cu(0)	DMSO	PMDETA (0.2)	r.t.	24	82	14 100	18 700	1.26
24	Cu(0)	DMSO	PMDETA (0.5)	r.t.	24	97	16 700	26 100	1.22
25	Cu(0)	DMSO	PMDETA (0.5)	60	4	99	17 100	24 800	1.25
26	Cu(0)	DMSO	PMDETA (1.0)	r.t.	1	36	6 300	6 900	6.49
27	Cu(0)	DMSO	Me_6TREN (0.2)	r.t.	24	*no polymerization*			
28	Cu(0)[f]	DMSO	Me_6TREN (0.2)	r.t.	24	22	4 000	4 600	1.29
29	Cu(0)	DMSO	Me_6TREN (0.2)	60	5	88	15 200	18 400	1.21
30	Cu(0)	DMSO	Me_6TREN (1.0)	r.t.	24	94	16 200	24 300	1.35
31	Cu(0)[f]	DMSO	Me_6TREN (1.0)	r.t.	24	94	16 200	25 500	1.25
32	Cu(0)	toluene	Me_6TREN (0.5)	r.t.	24	3	730	3 000	1.44
33	Cu(0)	toluene	PMDETA (0.5)	60	24	28	5 000	12 500	1.81
34	Cu(0)	dioxane	PMDETA (0.5)	60	24	18	3 300	10 000	1.82

[a] Standard polymerization conditions: M/I = 200:1; monomer/solvent = 1:1 (v/v), catalyst (Cat.): 10 cm of activated copper wire in Cu(0)-RDRP, 1 eq. of Cu(I) salt in ATRP.

[b] Monomer conversion determined by ^{1}H NMR.

[c] Theoretical M_n calculated from the M/I ratio and conversion, assuming 100% initiation efficiency.

[d] Determined by SEC with poly(MMA) calibration.

[e] $CuCl_2$ (0.5 eq.) was added as a deactivator.

[f] $CuCl_2$ (0.05 eq.) was added as a deactivator.

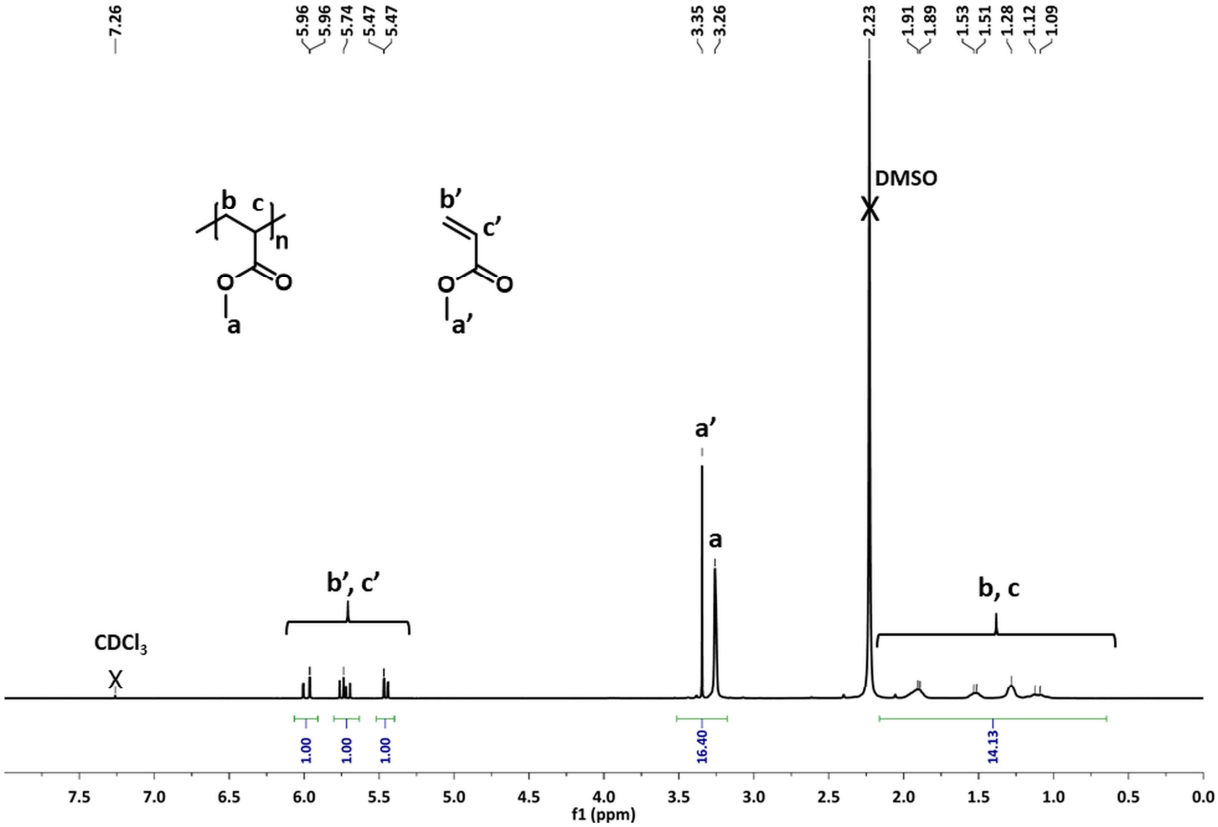

Figure S2. A representative ^{1}H NMR spectrum (measured in $CDCl_3$) of a reaction mixture from Cu(0)-RDRP of MA (entry 23, Table S1). Monomer conversion was calculated by comparing the intensity of the signals of unreacted monomer (b',c') to that of the combined signals of the monomer and polymer (a,a'): conversion (%) = $[1 - (I_{b',c'}/I_{a',a})] \times 100$

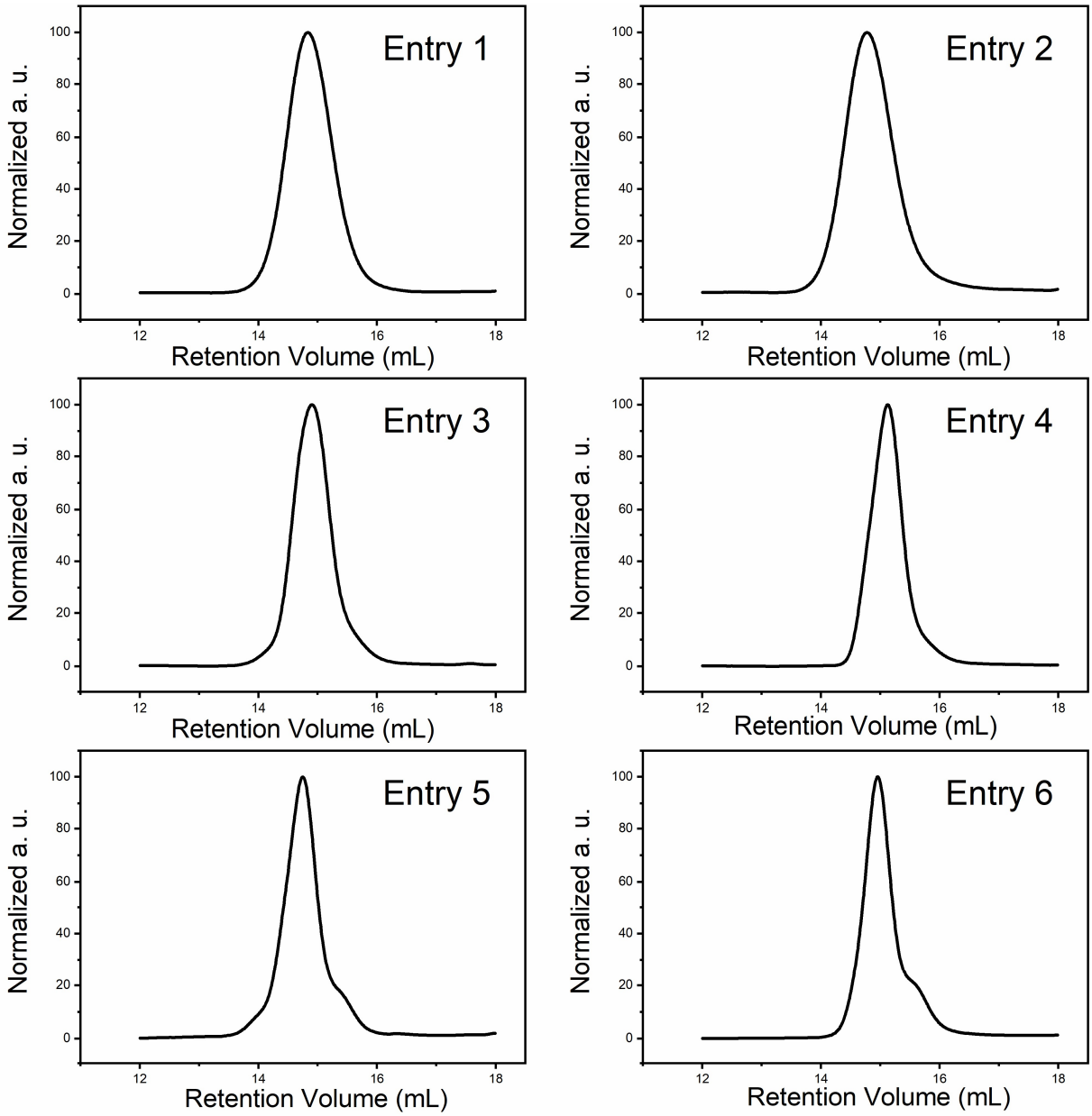

Figure S3. SEC elugrams (RI traces) for poly(MA) prepared by MTAC-initiated Cu(0)-RDRP at M/I = 200:1 under optimized conditions (description corresponds to Table 1).

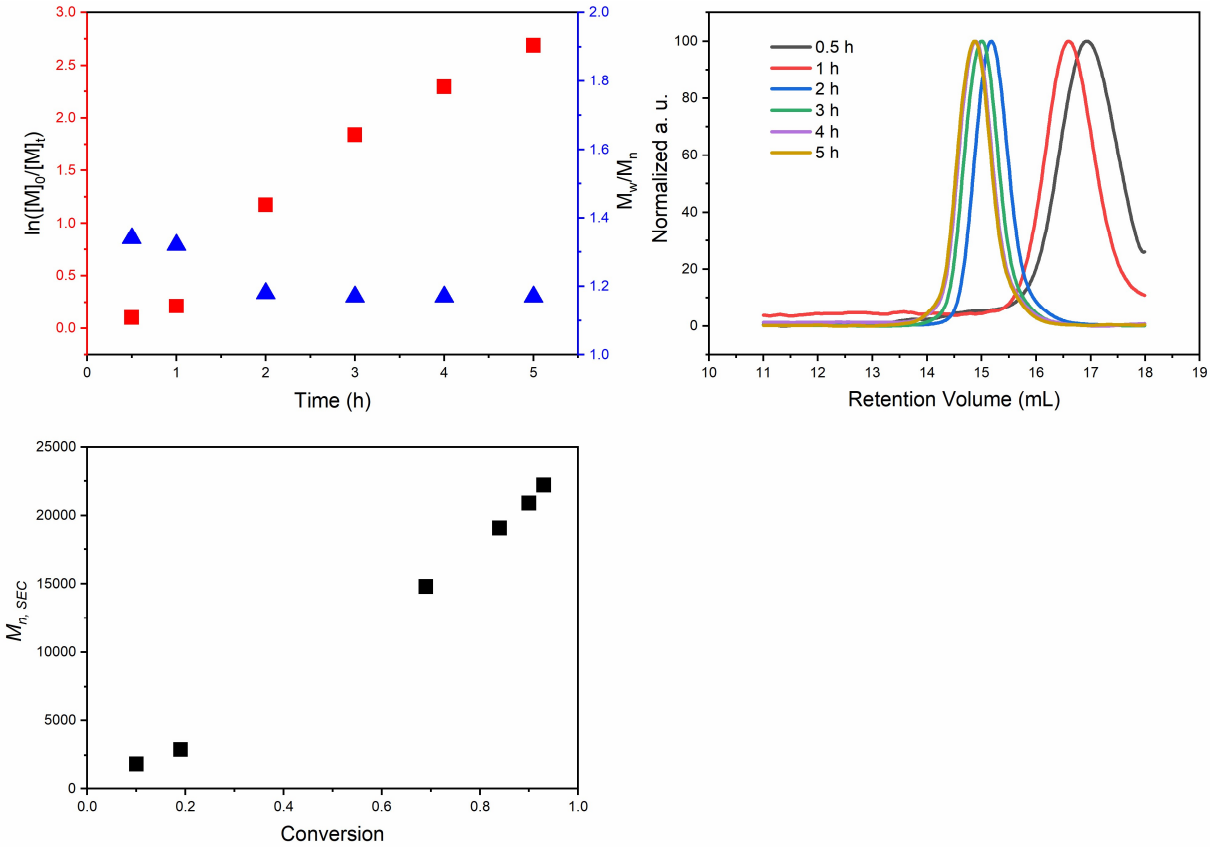

Time (h)	Conv. (%)[a]	M_n (theor.)[b]	M_n (SEC)[c]	$Đ$[c]
0.5	10	1 850	1 850	1.34
1	19	3 400	2 900	1.32
2	69	12 000	14 800	1.18
3	84	14 500	19 100	1.17
4	90	15 500	20 900	1.17
5	93	16 000	22 200	1.17

[a] Monomer conversion determined via ^{1}H NMR.

[b] Theoretical M_n calculated from the M/I ratio and conversion, assuming 100% initiation efficiency.

[c] Determined by SEC with poly(MMA) calibration.

Figure S4. Kinetics of MTAC-initiated Cu(0)-RDRP of MA. Experimental conditions: MA/MTAC/Me_6TREN = 200:1:0.5; MA/DMSO = 1:1 (v/v), 60 °C, 10 cm of activated Cu wire.

Table S2. Additional results obtained during the optimization of polymerization conditions for MTAC-initiated Cu-RDRP of MMA[a]

Entry	Cat.	Solvent	Ligand (eq.)	T (°C)	Time (h)	Conv. (%)[b]	M_n (theor.)[c]	M_n (SEC)[d]	$Đ$[d]
1	Cu(0)	DMAc	PMDETA (0.2)	r.t.	24	69	14 000	20 500	1.27
2	Cu(0)	DMAc	PMDETA (0.5)	r.t.	24	70	14 200	24 500	1.25
3	Cu(0)	DMAc	PMDETA (1.0)	r.t.	5	77	15 700	28 300	1.32
4	Cu(0)	DMAc	PMDETA (0.2)	85	6	87	17 600	23 600	1.21
5	Cu(0)	DMAc	Me_6TREN (0.2)	r.t.	24	39	8 100	12 900	1.18
6	Cu(0)	DMAc	Me_6TREN (0.5)	r.t.	9.5	73	14 800	20 900	1.28
7	Cu(0)	DMAc	Me_6TREN (1.0)	r.t.	7.5	71	14 500	21 400	1.31
8	Cu(0)	DMAc	Me_6TREN (0.2)	85	24	92	18 600	22 100	1.24
9	Cu(0)	DMSO	PMDETA (0.2)	r.t.	24	94	19 000	27 100	1.26
10	Cu(0)	DMSO	PMDETA (0.5)	r.t.	8.5	67	13 700	22 300	1.27
11	Cu(0)	DMSO	PMDETA (1.0)	r.t.	3.5	76	15 400	25 800	1.27
12	Cu(0)	DMSO	Me_6TREN (0.5)	r.t.	7.5	69	14 000	23 100	1.23
13	Cu(0)	DMSO	Me_6TREN (1.0)	r.t.	3.5	78	15 900	29 200	1.31
14	Cu(0)	dioxane	PMDETA (0.2)	85	24	*no polymerization*			
15	Cu(0)	dioxane	PMDETA (1.0)	r.t.	23	79	16 100	20 800	1.21
16	Cu(0)	dioxane	Me_6TREN (0.2)	85	24	87	17 600	23 000	1.14
17	Cu(0)	dioxane	Me_6TREN (1.0)	r.t.	24	69	13 900	28 100	1.62
18	Cu(0)	dioxane	Me_6TREN (1.0)	85	5	94	19 000	29 600	1.28
19	Cu(0)	toluene	Me_6TREN (1.0)	85	5	82	16 600	28 800	1.36
20	Cu(0)	IPA	PMDETA (0.2)	85	24	25	5 200	12 000	1.39
21	Cu(0)	IPA	PMDETA (1.0)	85	2	89	18 000	34 000	1.28
22	Cu(0)	IPA	Me_6TREN (0.2)	85	24	15	3 200	9 700	1.14
23	Cu(0)	IPA	Me_6TREN (1.0)	85	2	72	14 600	27 000	1.46
24	CuBr	DMSO	PMDETA (1.0)	85	24	*no polymerization*			
25	CuBr	DMSO	Me_6TREN (1.0)	85	24	*no polymerization*			
26	CuBr	DMAc	PMDETA (1.0)	85	24	*no polymerization*			
27	CuBr	DMAc	Me_6TREN (1.0)	85	24	2	520	2 100	1.30
28	CuBr	IPA	PMDETA (1.0)	85	24	9	1 900	4 400	1.12
29	CuBr	IPA	Me_6TREN (1.0)	85	24	31	6 400	7 400	1.18
30	CuBr	toluene	Me_6TREN (1.0)	85	22	92	18 600	23 500	1.58
31	CuBr	dioxane	Me_6TREN (1.0)	85	22	86	17 400	20 700	1.69
32	CuCl	dioxane	PMDETA (1.0)	85	23	83	16 800	17 700	1.16

[a] Standard polymerization conditions: M/I = 200:1; monomer/solvent = 1:1 (v/v), catalyst (Cat.): 10 cm of activated copper wire in Cu(0)-RDRP, 1 eq. of Cu(I) salt in ATRP.

[b] Monomer conversion determined gravimetrically.

[c] Theoretical M_n calculated from the M/I ratio and conversion, assuming 100% initiation efficiency.

[d] Determined by SEC with poly(MMA) calibration.

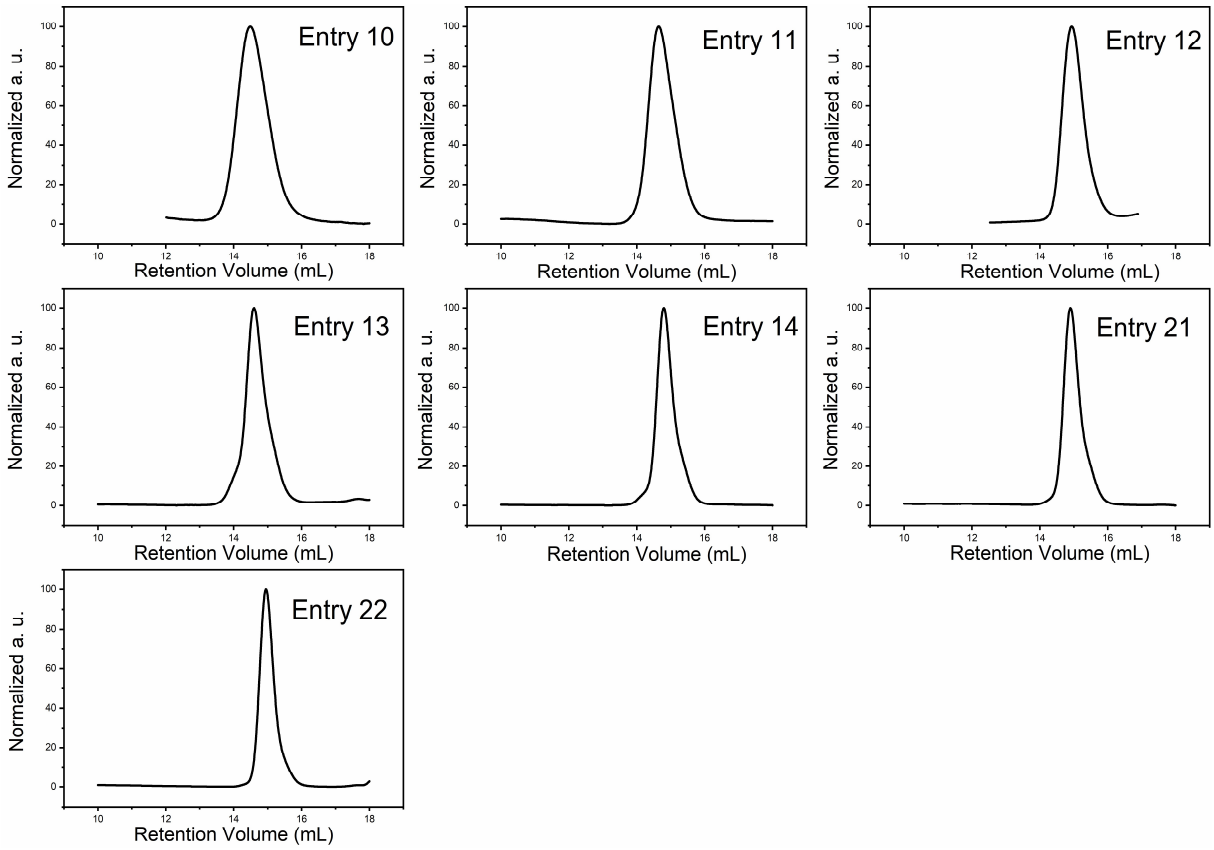

Figure S5. SEC elugrams of poly(MMA) prepared by MTAC-initiated Cu-RDRP at M/I = 200:1 under optimized conditions (description corresponds to Table 1).

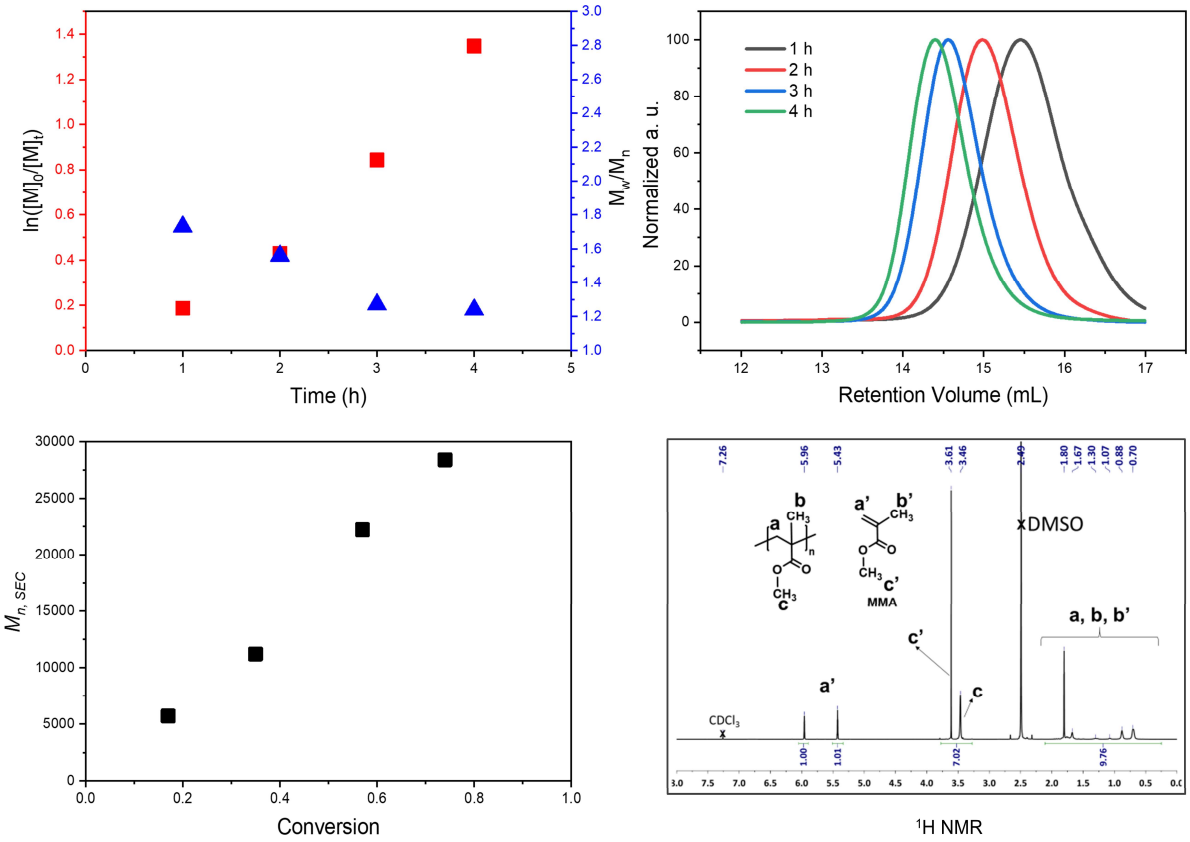

Time (h)	Conv. (%)[a]	M_n (theor.)[b]	M_n (SEC)[c]	$Đ$[c]
1	17	3 600	5 700	1.73
2	35	7 200	11 200	1.56
3	57	11 600	22 200	1.27
4	74	15 000	28 400	1.24

[a] Monomer conversion determined via ^{1}H NMR.

[b] Theoretical M_n calculated from the M/I ratio and conversion, assuming 100% initiation efficiency.

[c] Determined by SEC with poly(MMA) calibration.

Figure S6. Kinetics of MTAC-initiated Cu(0)-RDRP of MMA in DMSO. Experimental conditions: MMA/MTAC/Me_6TREN = 200:1:0.2; MMA/DMSO = 1:1 (v/v), 85 °C, 10 cm of activated Cu wire. Monomer conversion was determined by ^{1}H NMR analysis (in $CDCl_3$) of the reaction mixture (a sample spectrum is shown together with the signal assignment; the conversion calculation was done in a similar way as for MA).

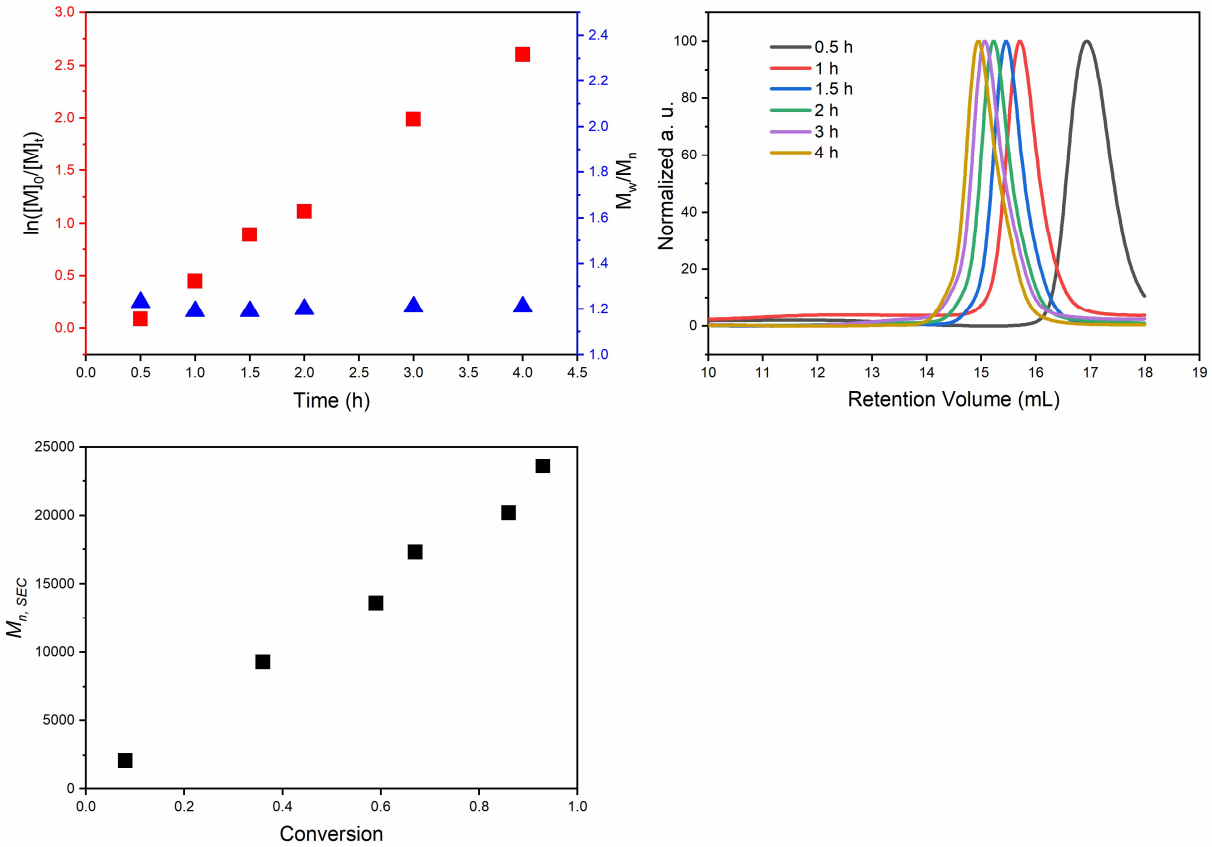

Time (h)	Conv. (%)[a]	M_n (theor.)[b]	M_n (SEC)[c]	$Đ$[c]
0.5	8	1 900	2 100	1.23
1	36	7 500	9 300	1.19
1.5	59	12 000	13 600	1.19
2	67	13 600	17 300	1.20
3	86	17 500	20 200	1.21
4	93	18 700	23 600	1.21

[a] Monomer conversion determined via ^{1}H NMR.

[b] Theoretical M_n calculated from the M/I ratio and conversion, assuming 100% initiation efficiency.

[c] Determined by SEC with poly(MMA) calibration.

Figure S7. Kinetics of MTAC-initiated Cu(0)-RDRP of MMA in dioxane. Experimental conditions: MMA/MTAC/ PMDETA = 200:1:1; MMA/dioxane = 1:1 (v/v), 85 °C, 10 cm of activated Cu wire.

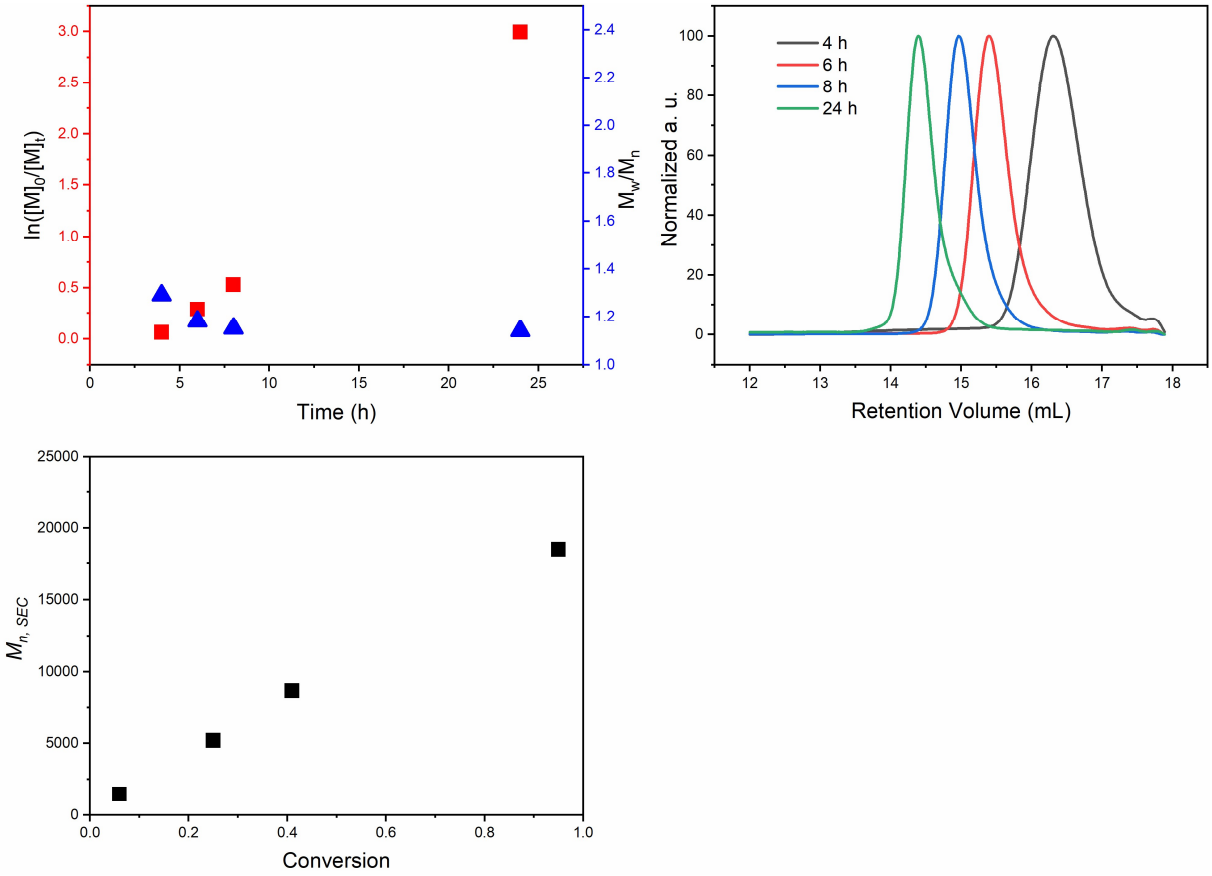

Time (h)	Conv. (%)[a]	M_n (theor.)[b]	M_n (SEC)[c]	$Đ$[c]
4	6	1 400	1 500	1.29
6	25	5 200	5 200	1.18
8	41	8 400	8 700	1.15
24	95	19 200	18 500	1.14

[a] Monomer conversion determined via ^{1}H NMR.

[b] Theoretical M_n calculated from the M/I ratio and conversion, assuming 100% initiation efficiency.

[c] Determined by SEC with poly(MMA) calibration.

Figure S8. Kinetics of MTAC-initiated ATRP of MMA in dioxane. Experimental conditions: MMA/MTAC/CuBr/ PMDETA = 200:1:1:1; MMA/dioxane = 1:1 (v/v), 85 °C.

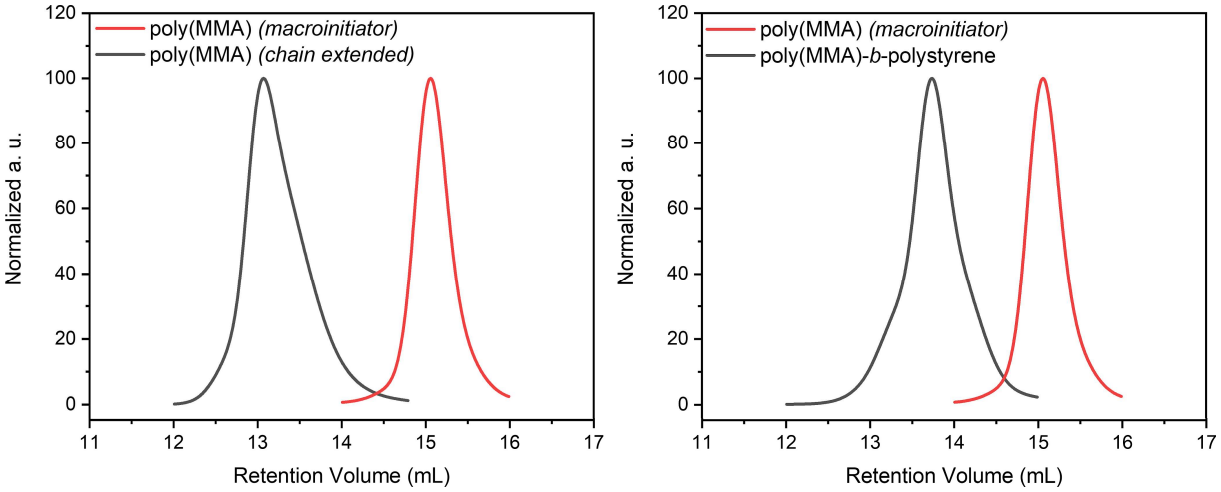

Entry[a]	Monomer	Cat.	Solvent	Ligand (eq.)	M/I	T (°C)	Time (h)	Conv. (%)[b]	M_n (theor.)[c]	M_n (SEC)	$Đ$
1	MMA	CuBr	dioxane	PMDETA (1.0 eq.)	400	85	2	73	38 700	34 400[d]	1.25[d]
2	styrene	CuBr	-	Me_6TREN (1.0 eq.)	800	110	1.5	26	31 000	30 000[e]	1.26[e]

[a] Polymerization conditions: poly(MMA) macroinitiator (M_n = 9 500, Đ = 1.13; entry 24, Table 1), CuBr (1 eq.), solvent/monomer = 1:1 (v/v).

[b] Monomer conversion determined by ^{1}H NMR.

[c] Theoretical M_n calculated from the M/I ratio and conversion, assuming 100% initiation efficiency; the macroinitiator M_n is included in the calculation.

[d] Determined by SEC with poly(MMA) calibration.

[e] Determined by SEC with polystyrene calibration.

Figure S9. Chain-extension study. Top: SEC elugrams of the poly(MMA) macroinitiator (M_n = 9 500, Đ = 1.13) and the chain-extended poly(MMA) (left) or the poly(MMA)-*b*-polystyrene block copolymer (right). Bottom: a table with experimental data.

Table S3. Additional results obtained during the optimization of polymerization conditions for MTAC-initiated Cu-RDRP of styrene[a]

Entry	Cat.	Solvent	Ligand (eq.)	T (°C)	Time (h)	Conv. (%)[b]	M_n (theor.)[c]	M_n (SEC)[d]	$Đ$[d]
1	Cu(0)	DMSO	PMDETA (0.5)	90	24	51	10 800	27 300	2.30
2[e]	Cu(0)	DMSO	Me_6TREN (0.5)	90	24	60	12 800	18 100	1.27
3[e]	Cu(0)	DMSO	Me_6TREN (1.0)	90	24	81	17 100	25 800	1.31
4	Cu(0)	DMAc	PMDETA (0.5)	90	24	36	7 800	12 500	1.65
5[e]	Cu(0)	DMAc	Me_6TREN (0.5)	90	24	56	12 000	17 300	1.28
6[e]	Cu(0)	DMAc	Me_6TREN (1.0)	90	24	54	11 400	20 500	1.45
7	Cu(0)	dioxane	PMDETA (1.0)	90	24	75	15 800	28 000	1.62
8	Cu(0)	dioxane	Me_6TREN (1.0)	90	24	71	15 000	61 600	5.29
9	Cu(0)	toluene	PMDETA (0.5)	90	24	*no polymerization*			
10[e]	Cu(0)	toluene	Me_6TREN (0.5)	90	24	49	10 400	13 000	1.38
11[e]	Cu(0)	toluene	Me_6TREN (1.0)	90	24	65	13 700	19 000	1.44
12	Cu(0)	toluene	Me_6TREN (0.2)	90	48	57	12 000	14 700	1.21
13[e]	Cu(0)	-	PMDETA (0.5)	90	9	15	6 300	9 200	2.01
14[e]	Cu(0)	-	Me_6TREN (0.5)	90	24	67	28 300	31 300	1.25
15[e]	Cu(0)	-	Me_6TREN (1.0)	90	24	89	37 200	42 500	1.36
16[e]	Cu(0)	-	Me_6TREN (0.2)	90	24	37	15 600	16 800	1.24
17	CuBr	DMSO	PMDETA (1.0)	90	24	*no polymerization*			
18	CuBr	DMSO	Me_6TREN (1.0)	90	24	*no polymerization*			
19	CuBr	DMAc	PMDETA (1.0)	90	24	*no polymerization*			
20	CuBr	DMAc	Me_6TREN (1.0)	90	24	*no polymerization*			
21	CuBr	IPA	PMDETA (1.0)	90	24	*no polymerization*			
22	CuBr	IPA	Me_6TREN (1.0)	90	24	*no polymerization*			
23	CuBr	dioxane	PMDETA (1.0)	90	24	*no polymerization*			
24	CuBr	dioxane	Me_6TREN (1.0)	90	24	15	3 300	4 200	1.29
25	CuBr	toluene	PMDETA (1.0)	90	24	*no polymerization*			
26	CuBr	toluene	Me_6TREN (1.0)	90	24	42	8 900	10 000	1.23
27	CuBr	-	PMDETA (1.0)	90	24	12	5 200	5 200	1.38
28	CuBr	-	Me_6TREN (1.0)	90	22	87	36 300	45 000	1.20
29	CuCl	-	Me_6TREN (1.0)	90	24	10	4 200	4 600	1.16
30[f]	CuBr	-	Me_6TREN (1.0)	110	3	91	5 000	5 900	1.61

[a] Standard polymerization conditions: M/I = 200:1 in solvents and 400:1 in bulk; monomer/solvent = 1:1 (v/v), catalyst (Cat.): 10 cm of activated copper wire in Cu(0)-RDRP, 1 eq. of Cu(I) salt in ATRP.

[b] Monomer conversion determined gravimetrically.

[c] Theoretical M_n calculated from the M/I ratio and conversion, assuming 100% initiation efficiency.

[d] Determined by SEC with polystyrene calibration.

[e] Gel formation on Cu wire was observed.

[f] Bulk polymerization at M/I = 50:1

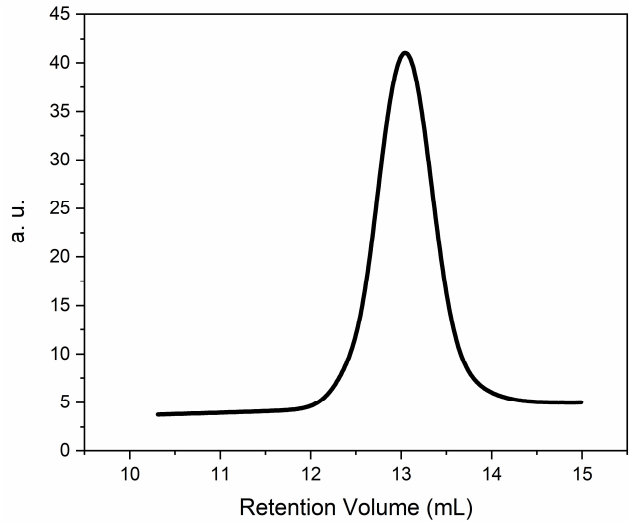

Figure S10. SEC elugram for polystyrene prepared by MTAC-initiated Cu(0)-RDRP in toluene (Entry 26, Table 1).

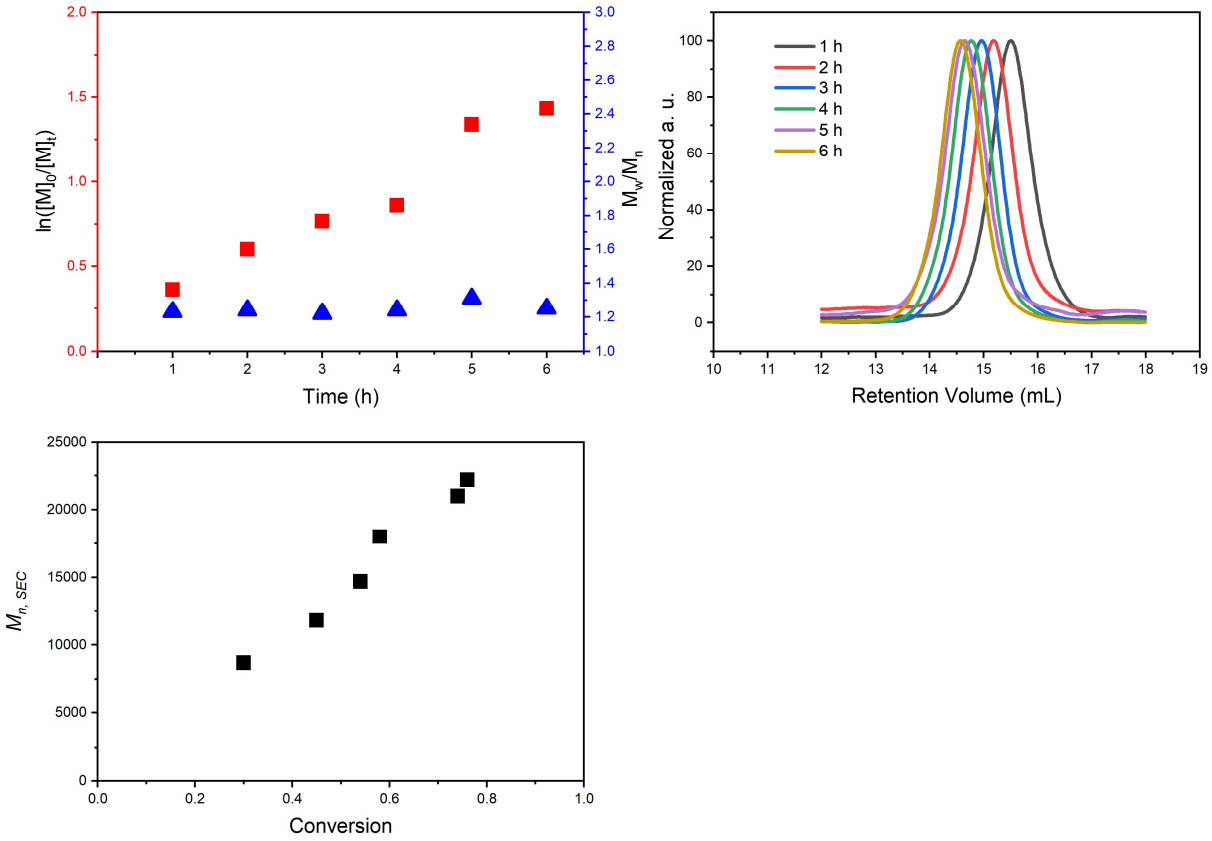

Time (h)	Conv. (%)[a]	M_n (theor.)[b]	M_n (SEC)[c]	Đ[c]
1	30	6 500	8 700	1.23
2	45	9 600	11 800	1.24
3	54	11 400	14 700	1.22
4	58	12 200	18 000	1.24
5	74	15 600	21 000	1.31
6	76	16 100	22 200	1.25

[a] Monomer conversion determined gravimetrically.

[b] Theoretical M_n calculated from the M/I ratio and conversion, assuming 100% initiation efficiency.

[c] Determined by SEC with polystyrene calibration.

Figure S11. Kinetics of MTAC-initiated ATRP of styrene performed in bulk. Experimental conditions: styrene/MTAC/CuBr/ Me_6TREN = 200:1:1:1; 110 °C.

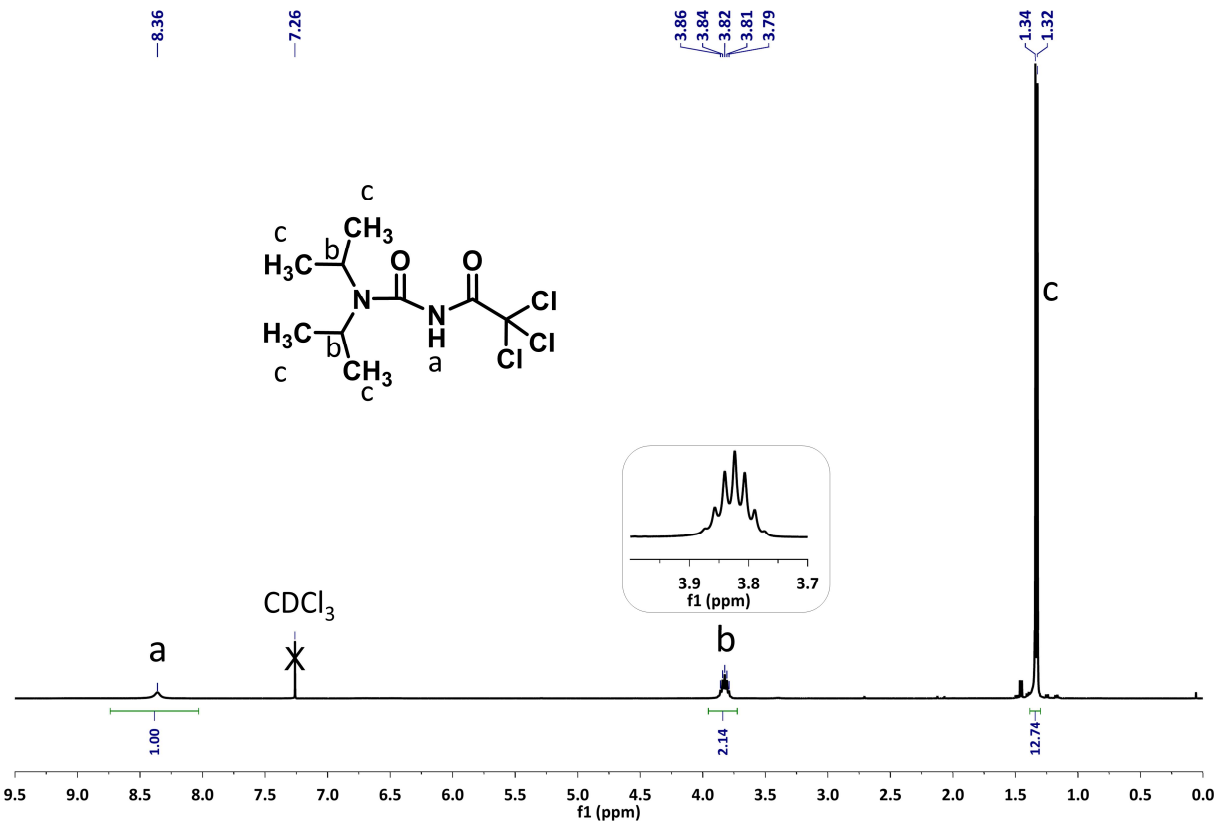

Figure S12. ^{1}H NMR ($CDCl_3$) spectrum of the synthesized 1,1-diisopropyl-3-(2,2,2-trichloroacetyl)-urea (DTAU).

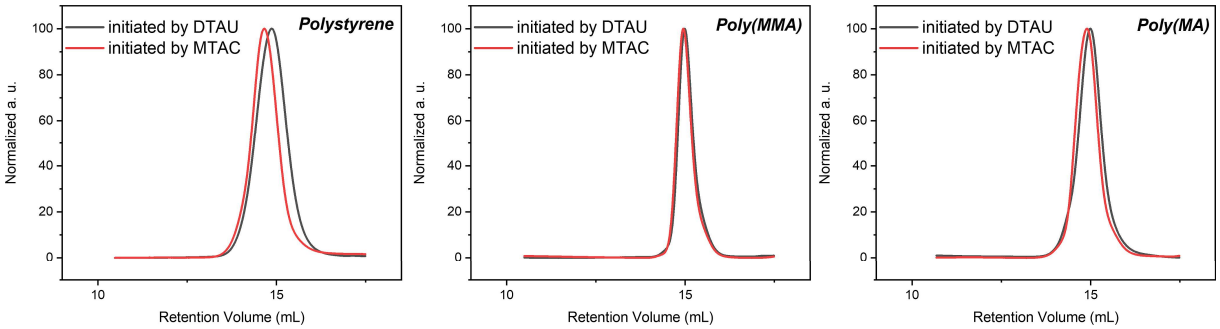

Entry[a]	Monomer	Cat.	Solvent	Ligand (eq.)	T (°C)	Time (h)	Conv. (%)[b]	M_n (theor.)[c]	M_n (SEC)[d]	$Đ$[d]
1	styrene	CuBr	-	Me_6TREN (1.0 eq.)	110	6	74	15 700	18 200	1.30
2	MMA	CuBr	dioxane	PMDETA (1.0 eq.)	85	24	75	15 300	18 900	1.10
3	MA	Cu(0)	DMSO	Me_6TREN (0.5 eq.)	60	5	96	16 600	21 800	1.30

[a] Standard polymerization conditions: M/I = 200:1; catalyst (Cat.): 10 cm of activated copper wire in Cu(0)-RDRP, CuBr (1 eq.) in ATRP; monomer/solvent = 1:1 (v/v).

[b] Monomer conversion determined gravimetrically (styrene, MMA) or by ^{1}H NMR (MA).

[c] Theoretical M_n calculated from the M/I ratio and conversion, assuming 100% initiation efficiency.

[d] Determined by SEC with polystyrene (for polystyrene) or poly(MMA) calibration (for poly(MA) and poly(MMA)).

Figure S13. Comparison of MTAC- and DTAU-initiated Cu-RDRP of styrene, MMA, and MA. Top: SEC elugrams of the polymers synthesized under identical conditions using MTAC and DTAU initiators. Bottom: experimental data for the DTAU-initiated Cu-RDRP of styrene, MMA, and MA.

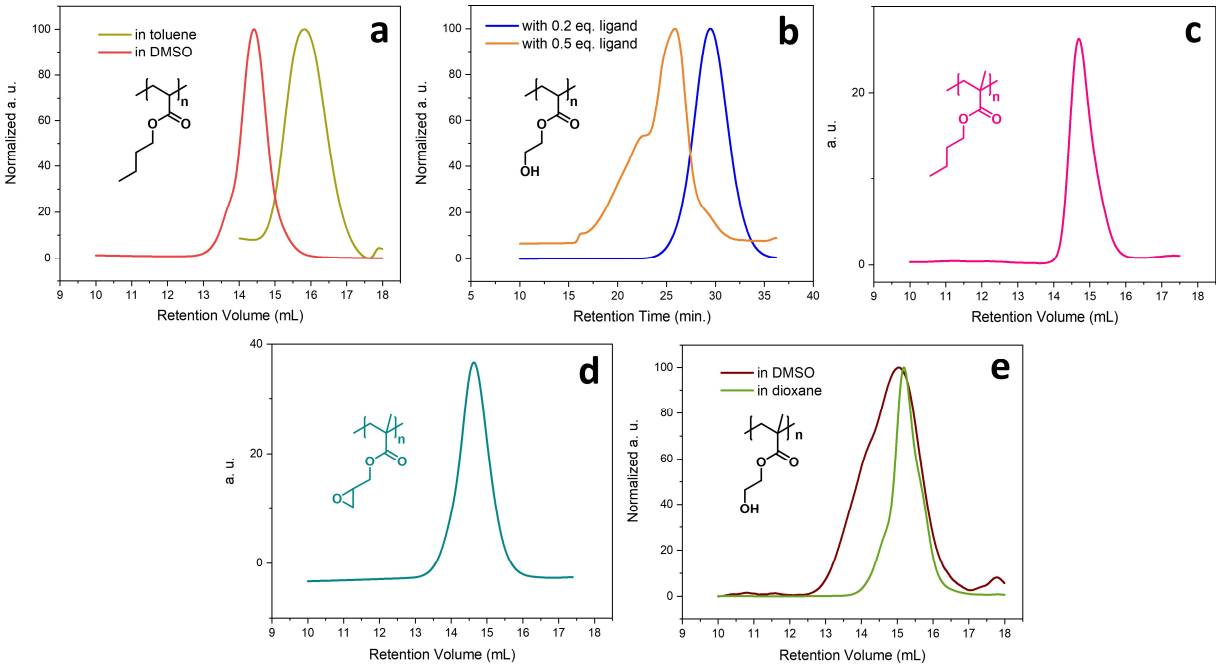

Figure S14. SEC elugrams of a) poly(BA), b) poly(HEA), c) poly(BMA), d) poly(GMA), and e) poly(HEMA) prepared using the previously optimized polymerization conditions (with or without modification). Experimental conditions and product characteristics are provided in Table 2.

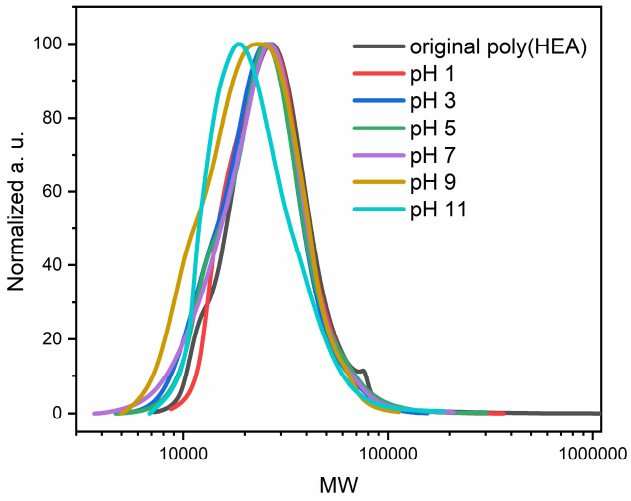

Buffer pH	M_n	M_p	Đ	dn/dc (mL/g)
-	24 300	27 100	1.28	0.072
1	24 700	27 000	1.21	0.073
3	21 300	25 000	1.26	0.075
5	22 200	25 400	1.28	0.075
7	21 000	25 600	1.29	0.074
9	19 000	22 800	1.28	0.070
11	20 500	20 700	1.21	0.060

Figure S15. Study of the hydrolytic stability of the in-chain carbamate linkers in ETAC-initiated poly(HEA). *Left:* MWDs of the ETAC-initiated poly(HEA) before and after exposure to buffers of different pH for 24 h at 37 °C. The data were obtained for isolated samples by TD-SEC.
Right: Table with the experimental results (data for the starting poly(HEA) are provided in the first line). Experimental conditions: polymer concentration 5 mg/mL, 24 h at 37°C; MWs of the isolated polymers were determined by TD-SEC in DMAc/LiBr. The dn/dc values were determined by the OMNISEC software assuming 100% sample recovery.

Additional discussion: In order to gain a preliminary insight into the hydrolytic stability of the TAI-derived carbamate linker employed prevalently in this work, we prepared a model poly(HEA) polymer through Cu(0)-RDRP of HEA initiated with ethane-1,2-diyl bis((2,2,2-trichloroacetyl)carbamate) (ETAC) using the HEA/ETAC/Me_6TREN ratio of 400:1:0.2 in DMSO at 60 °C. ETAC was synthesized by the reaction of ethylene glycol with an excess of TAI and used without further purification; its ^{1}H NMR spectrum is provided in **Figure S16**. Samples of the prepared poly(HEA) of M_n = 24 300, Đ = 1.28, featuring the 6-arm star architecture (based on the assumed TAG trifunctionality), was then dissolved in six different buffers, covering the pH range of 1 to 11, and maintained at 37 °C for 24 h. The polymer MW was evaluated by TD-SEC, expecting that the cleavage of the carbamate linker would result into halving of the polymer MW. As can be seen from the MW distributions (MWDs) displayed in **Figure S15**, the carbamate linker has shown to be considerably resistant to hydrolysis in the whole studied pH range. Only at pH 9 and 11, a noticeable change to MWDs could be observed; however, as is apparent from the M_n and, particularly, M_p (main fraction MW) values reported in **Figure S15**, the actual shift in MWs is rather small, inconsistent with extensive hydrolysis of the carbamate linkers. Instead, we ascribe this small MW shift to partial hydrolysis of poly(HEA) ester side groups at alkaline pH. This assumption is supported by the observed decrease in the determined polymer dn/dc from 0.072 mL/g (original poly(HEA)) to 0.060 mL/g (the pH 11 sample), which indicates a change in polymer composition (**Figure S15**). On the whole, this preliminary investigation points to the considerable hydrolytic stability of the in-chain TAI-derived carbamate linker in a wide pH range as compared to low-MW carbamates,[4] which could be ascribed to the steric crowding resulting from the polymeric chains growing from the nearby multifunctional initiation sites.

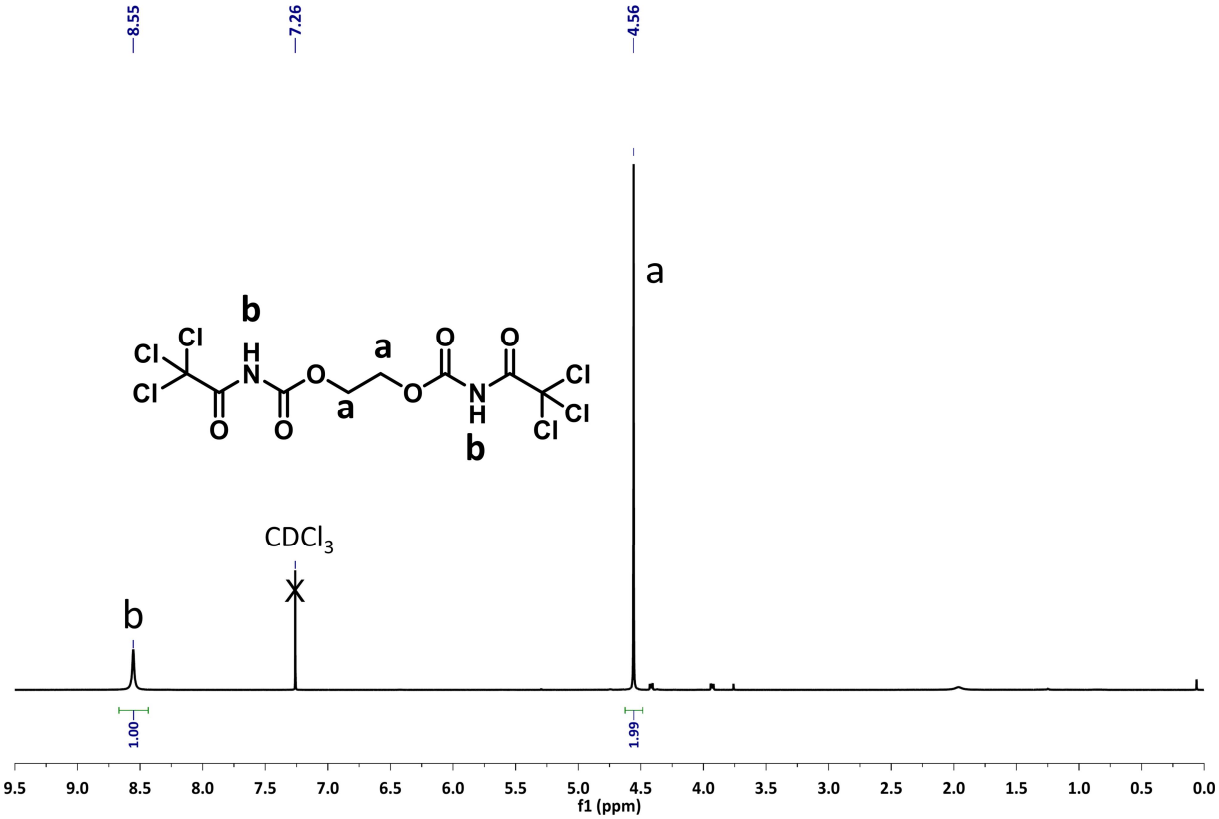

Figure S16. ^{1}H NMR ($CDCl_3$) of ethane-1,2-diyl bis((2,2,2-trichloroacetyl)carbamate) (ETAC).

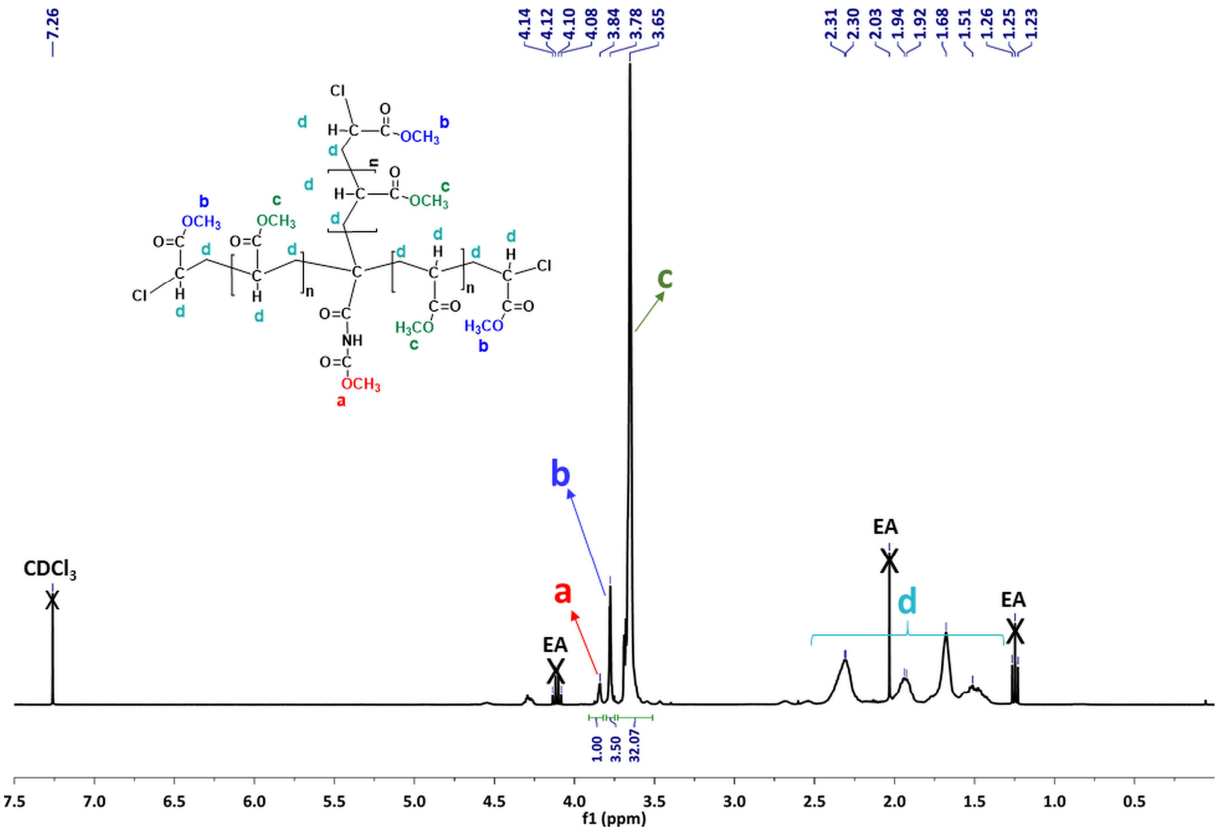

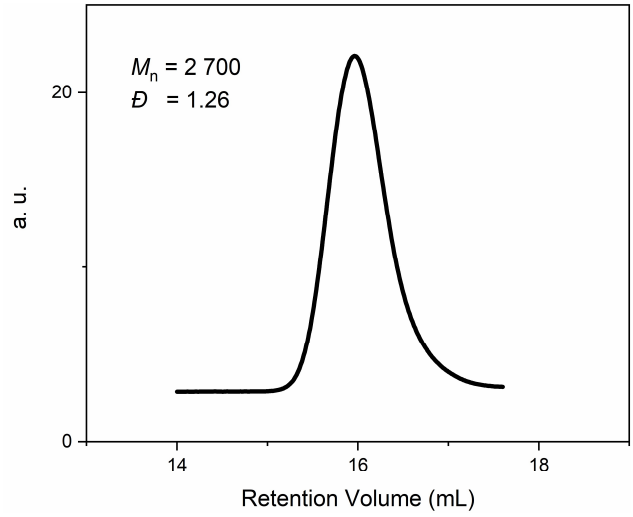

Figure S17. ^{1}H NMR study of the MTAC initiator functionality in Cu-RDRP of MA. Top: ^{1}H NMR ($CDCl_3$) of the isolated model poly(MA). Bottom: SEC elugram of the model poly(MA) (MW determined using poly(MMA) calibration). Polymerization conditions: Cu(0)-RDRP, DMSO, Me_6TREN 0.5 eq., 2.5 h, 60°C, 42 % conversion; polymer isolation: ethyl acetate-diluted polymerization mixture was extracted with water 3x, salted out with brine, dried with $MgSO_4$, and evaporated; the obtained solids were dried in vacuum.

Calculation of initiator functionality (IF) from NMR signal intensity (I):

1st approach: IF = I_b/I_a = 3.5/1 = **3.5**

2nd approach: $M_{n(\text{single chain})} = [(I_c + I_b)/ I_b] \times M_{MA} = [(32.07+3.50)/3.50] \times 86.09 = 875$

IF = $M_{n(SEC)}/M_{n(\text{single chain})}$ = 2700/875 = **3.1**

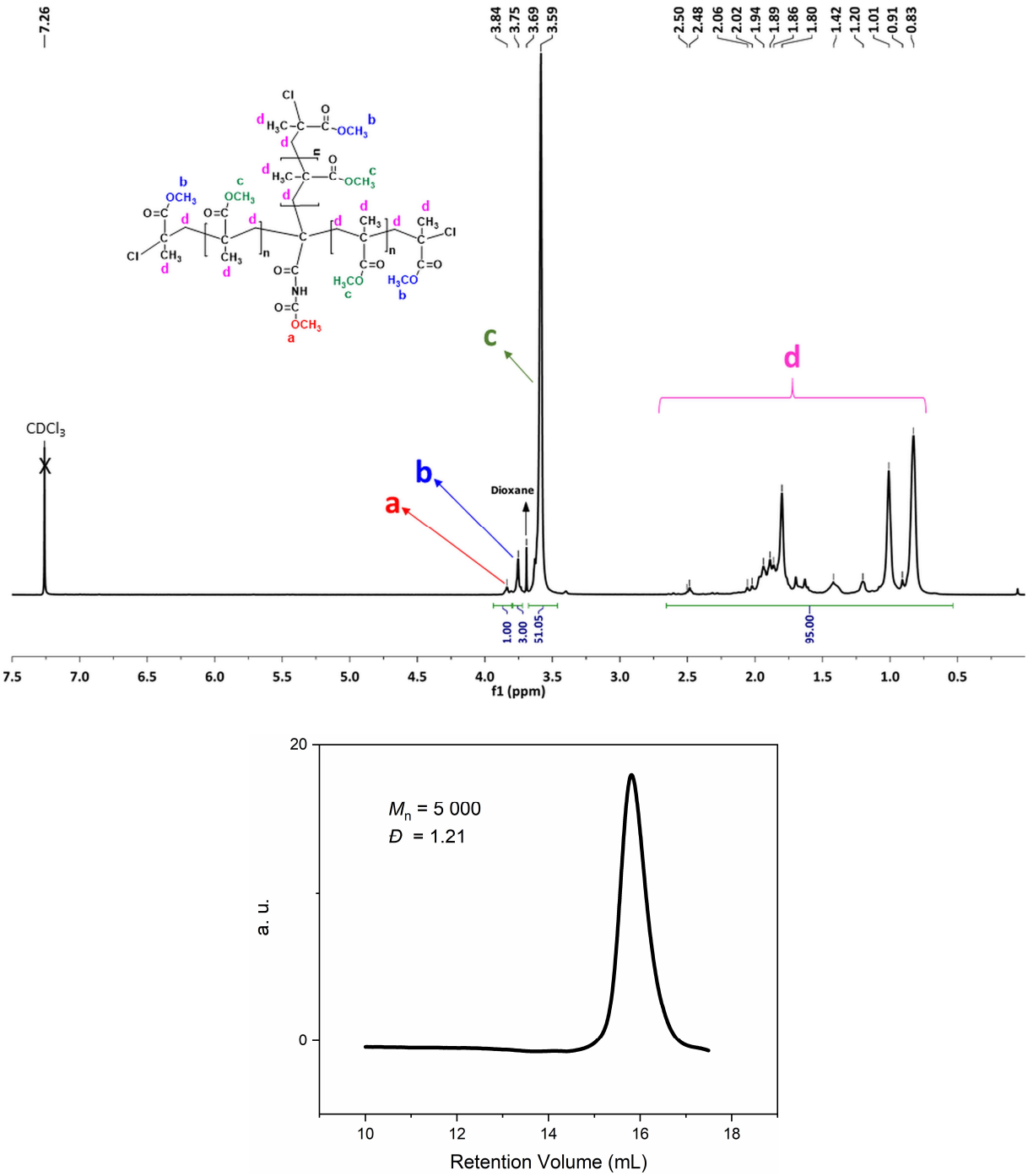

Figure S18. ^{1}H NMR study of the MTAC initiator functionality in Cu-RDRP of MMA. Top: ^{1}H NMR ($CDCl_3$) of the isolated model poly(MMA). Bottom: SEC elugram of the model poly(MMA) (MW determined using poly(MMA) calibration). Polymerization conditions are provided in entry 23, Table 1; the polymer was isolated via precipitation in MeOH/water (1:1 v/v) and dried in vacuum.

Calculation of IF from NMR signal intensity (I):

1st approach: IF = I_b/I_a = 3/1 = **3**

2nd approach: $M_{n(\text{single chain})} = [(I_c+I_b)/I_b] \times M_{MMA} = [(51.05+3.00)/3.00] \times 100.12 = 1804$

IF = $M_{n(SEC)}/M_{n(\text{single chain})}$ = 5000/1804 = **2.8**

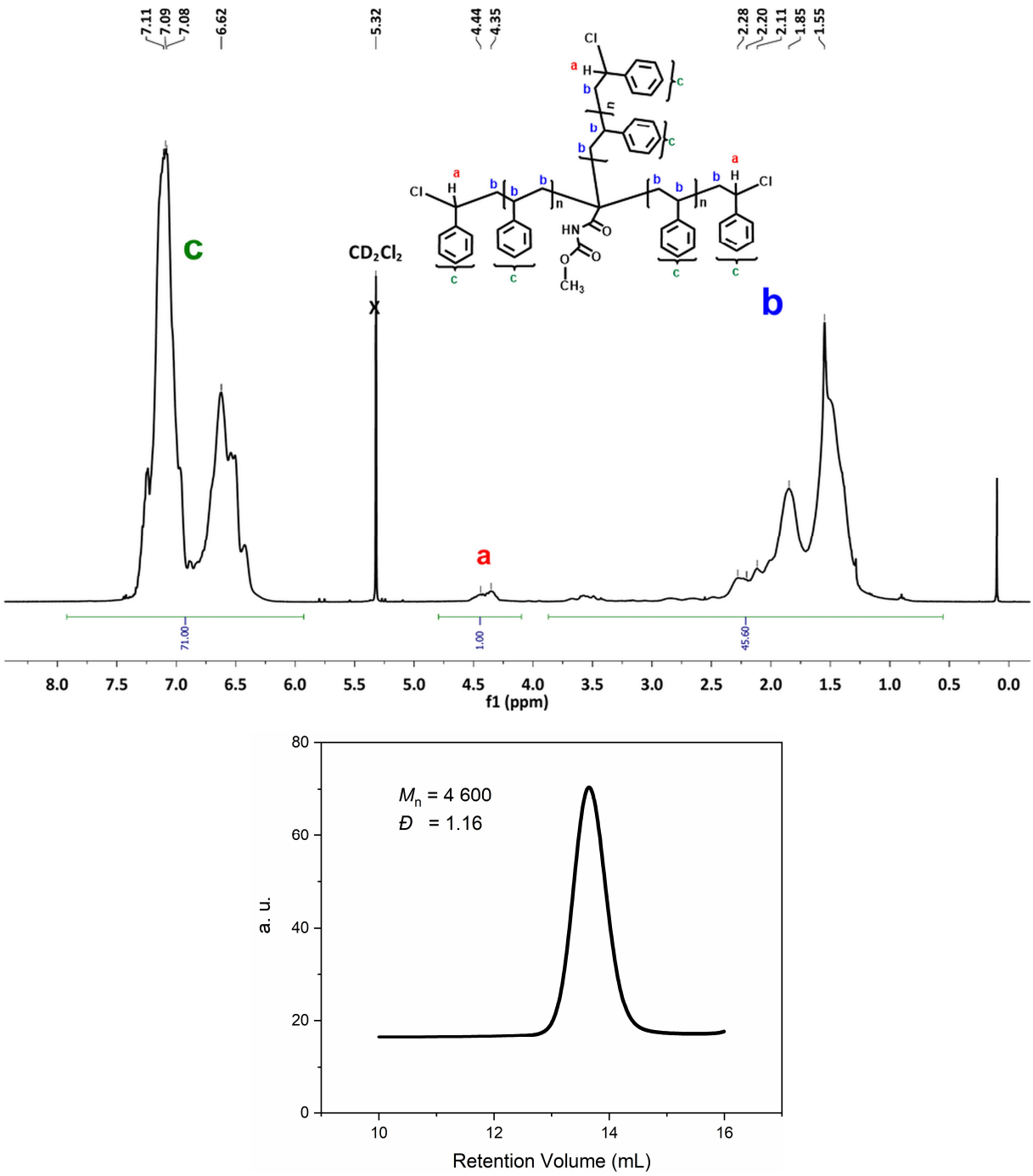

Figure S19. ^{1}H NMR study of the MTAC initiator functionality in Cu-RDRP of styrene. Top: ^{1}H NMR (CD_2Cl_2) of the isolated model polystyrene. Bottom: SEC elugram of the model polystyrene (MW determined using polystyrene calibration). Polymerization conditions are provided in entry 29, Table S3; the polymer was isolated via precipitation in MeOH and dried in vacuum.

Calculation of IF from NMR signal intensity (I):

$M_{n(single\ chain)} = [(I_c/5)/I_a] \times M_{St} = [(71.00/5)/1.00] \times 104.15 = 1479$

IF = $M_{n(SEC)}/M_{n(single\ chain)}$ = 4600/1479 = **3.1**

(Note: This is the calculation by the 2nd approach; for all the studied polymers, the IF value calculated in this way is inherently slightly underestimated due to the underestimation of the M_n value determined by SEC with relative calibration that does not reflect the branching-related decrease in polymer hydrodynamic volume).

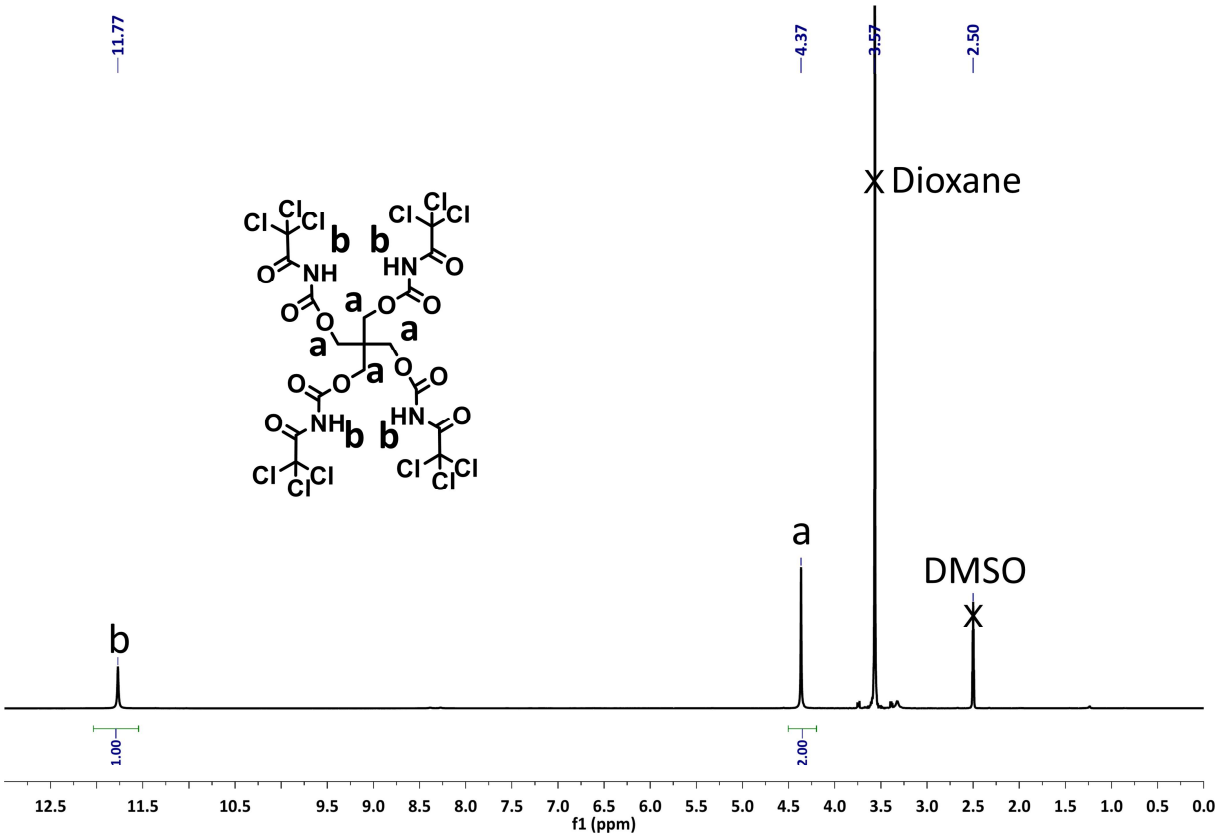

Figure S20. ^{1}H NMR (DMSO-*d6*) of pentaerythritol tetrakis((2,2,2-trichloroacetyl)carbamate) (PTAC)

Table S4. Synthesis of star polymers via PTAC-initiated Cu-RDRP of MMA, styrene, and MA[a]

Monomer	Stage	Time (h)	Conv. (%)[b]	M_n (theor.)[c]	M_n (SEC)[d]	$Đ$[d]
MMA	original star polymer	6	92	37 700	48 600	1.21
	hydrolyzed segments	-	-	9 400	14 900	1.08
styrene	original star polymer	6	50	84 200	74 700	1.69
	hydrolyzed segments	-	-	21 100	29 000	1.14
MA	original star polymer	4	92	32 000	32 600	1.48

[a] Polymerization conditions: MMA polymerization - MMA/PTAC/CuBr/PMDETA = 400:1:1:1, MMA/dioxane = 1:1 (v/v), 85 °C; styrene polymerization - styrene/PTAC/CuBr/Me_6Tren = 1600:1:1:1, in bulk, 110 °C; MA polymerization - MA/PTAC/Me_6TREN = 400:1:0.5, MA/DMSO = 1:1 (v/v), copper wire 10 cm, 60 °C. Alkaline hydrolysis was conducted according to a literature procedure.[2]

[b] Monomer conversion was determined gravimetrically (MMA and styrene) or through a ^{1}H NMR analysis (MA).

[c] Theoretical M_n calculated from the M/I ratio and conversion, assuming 100% initiation efficiency.

[d] Determined by TD-SEC.

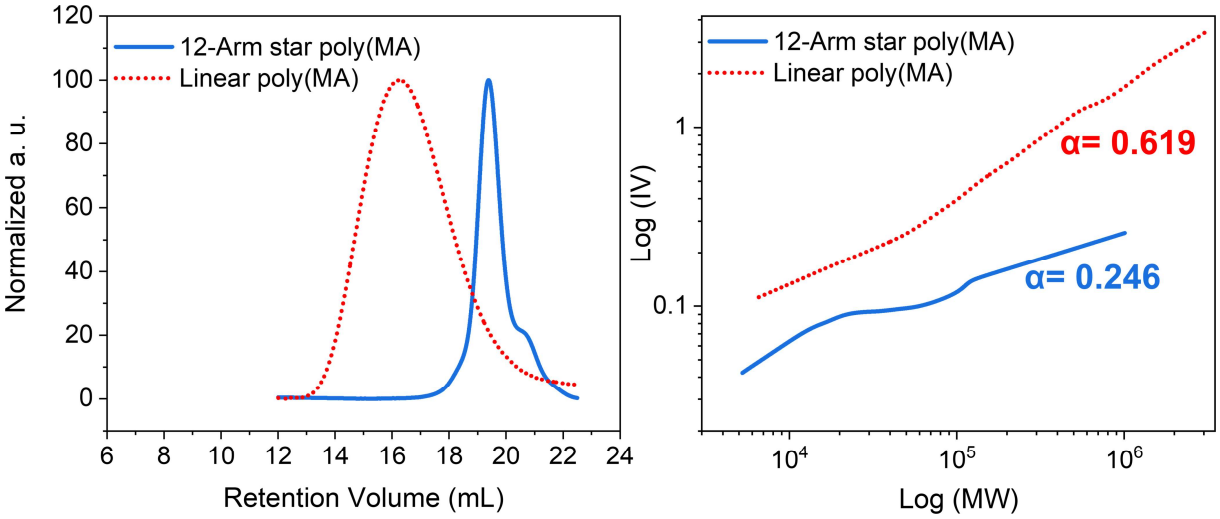

Figure S21. TD-SEC analysis of multi-arm star poly(MA) based on a pentaerythritol core and synthesized via the TAI strategy. Left: SEC elugrams (RI traces), right: corresponding M-H plots. Data for a broad linear poly(MA) synthesized through free-radical polymerization are shown for comparison.

Table S5. Experimental results of the d*e novo* one-pot synthesis of the poly(HEMA-*co*-MMA)-*graft*-poly(MMA) "star-on-star" graft copolymer[a]

Stage	Conv. (%)[b]	M_n (theor.)	M_n (SEC)[e]	$Đ$[e]
poly(HEMA-*co*-MMA)	99	10 800[c]	23 400	1.23
poly(HEMA-*co*-MMA)-*graft*-poly(MMA)	30	288 300[d]	328 000	1.95
removed poly(MMA) grafts	-	12 000[c]	16 200	1.05

[a] Polymerization conditions: MMA/HEMA copolymerization: MMA/HEMA/MTAC/PMDETA = 80/20/1/1, 4 cm of activated copper wire, monomers/solvent = 1:1 (v/v), 85 °C, 3 h; grafting: MMA/TAI/PMDETA = 400:1:1, 4 cm of activated copper wire from the previous step, monomer/solvent = 3:1 (v/v), 85 °C, 2 h.

[b] Monomer conversion as determined by ^{1}H NMR.

[c] Theoretical M_n calculated from the M/I ratio and conversion, assuming 100% initiation efficiency.

[d] Theoretical M_n calculated from the M_n(SEC) and the known composition of the macroinitiator, the average number of initiating sites per one macroinitiator chain, and the determined MW of the macroinitiator and grafts.

[e] Determined by TD-SEC.

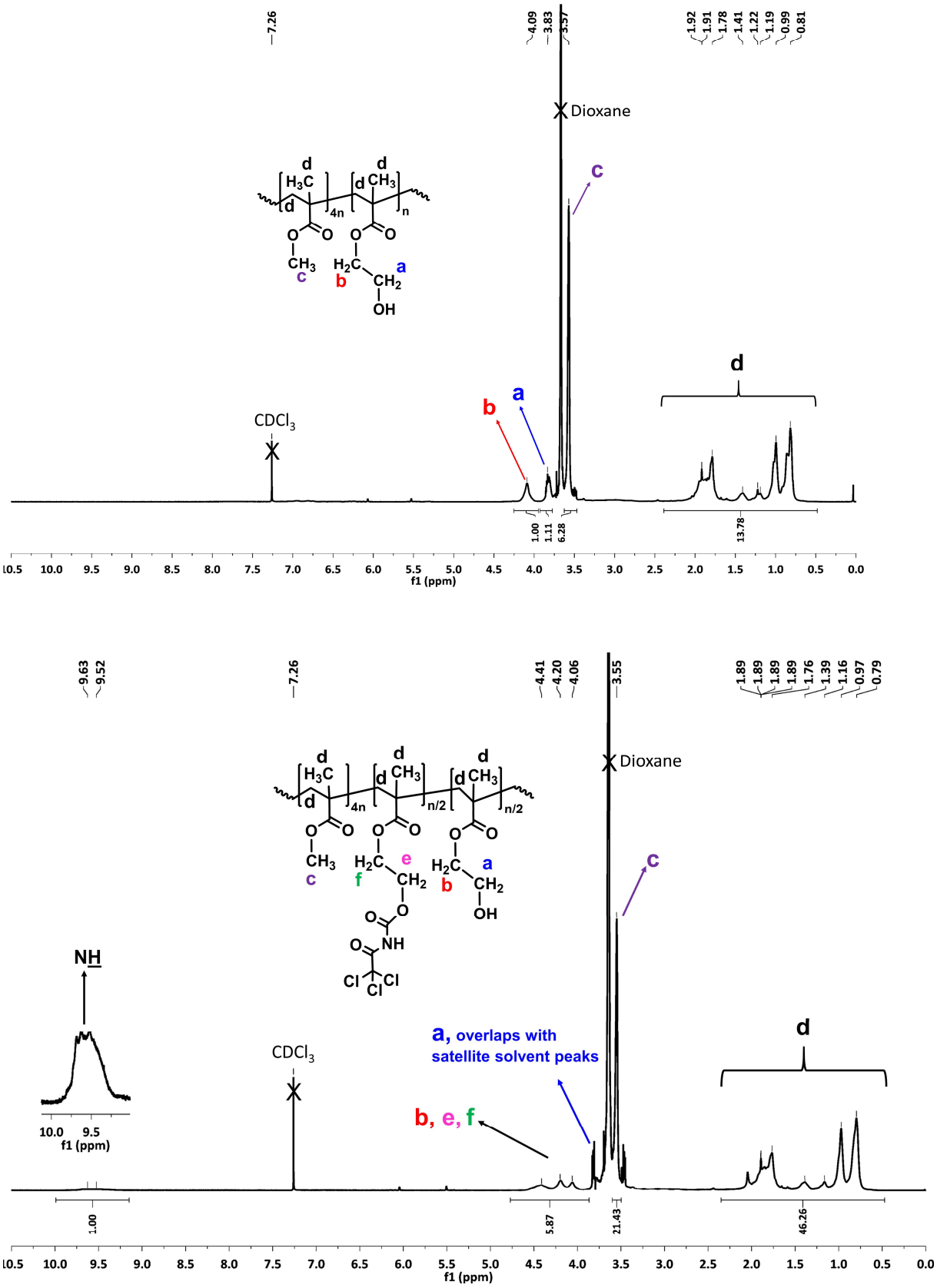

Figure S22. ^{1}H NMR (reaction mixture; $CDCl_3$) of poly(MMA-*co*-HEMA) synthesized by MTAC-initiated Cu(0)-RDRP in dioxane before (top) and after (bottom) modification of a part of the hydroxyl groups by TAI (steps 1 and 2 in the *de novo* one-pot synthesis of a graft copolymer as per Figure 3).

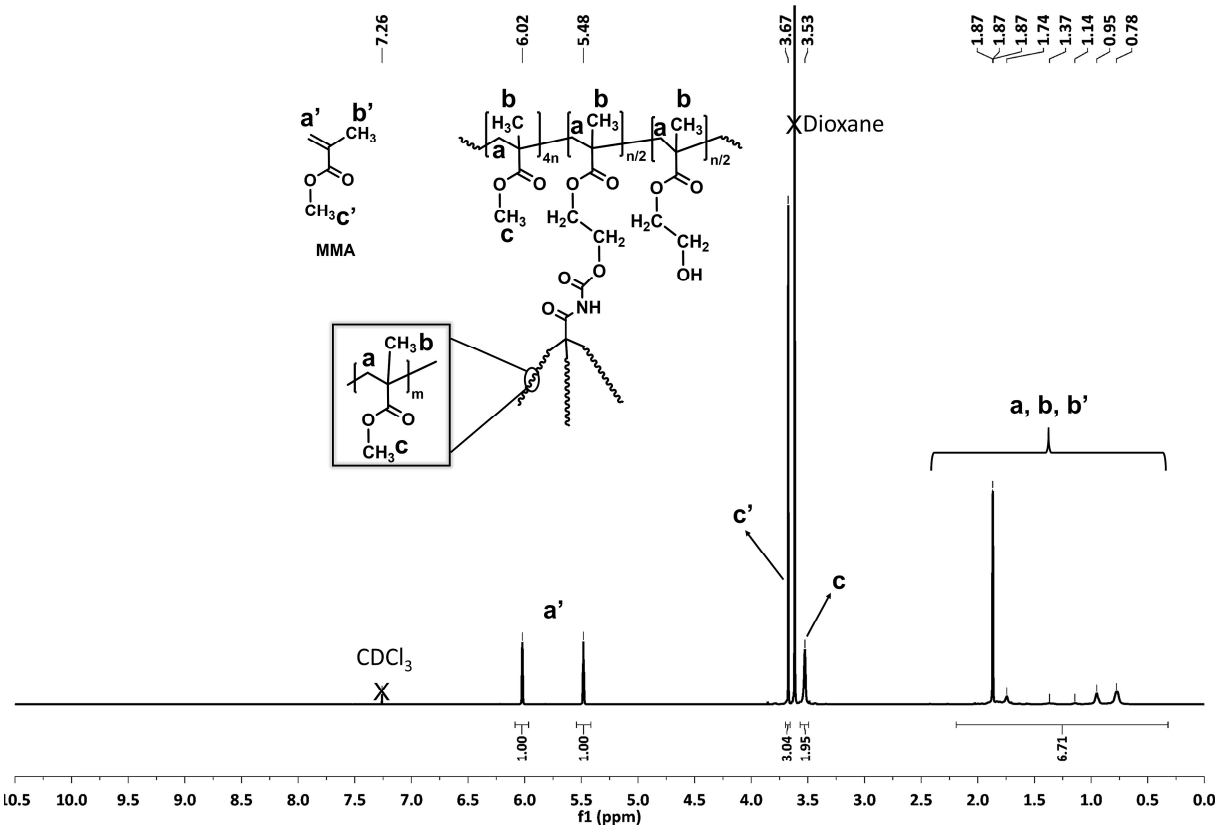

Figure S23. ^{1}H NMR (reaction mixture; $CDCl_3$) of poly(MMA-*co*-HEMA)-*graft*-poly(MMA) synthesized via Cu(0)-RDRP of MMA initiated by the TAI-modified poly(MMA-*co*-HEMA) copolymer (step 3 in the *de novo* one-pot synthesis of a graft copolymer as per Figure 7).

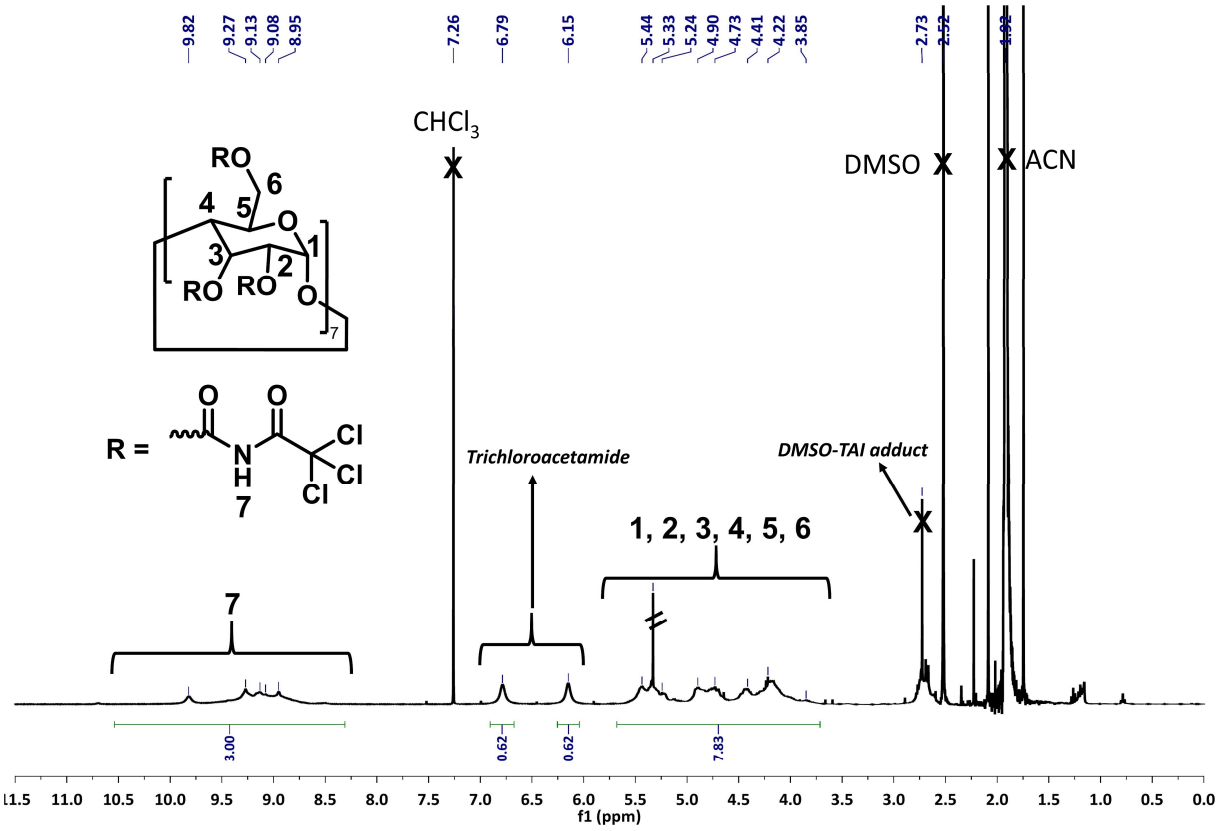

Figure S24. ^{1}H NMR (reaction mixture; $CDCl_3$) of ß-CD modified with TAI in acetonitrile.

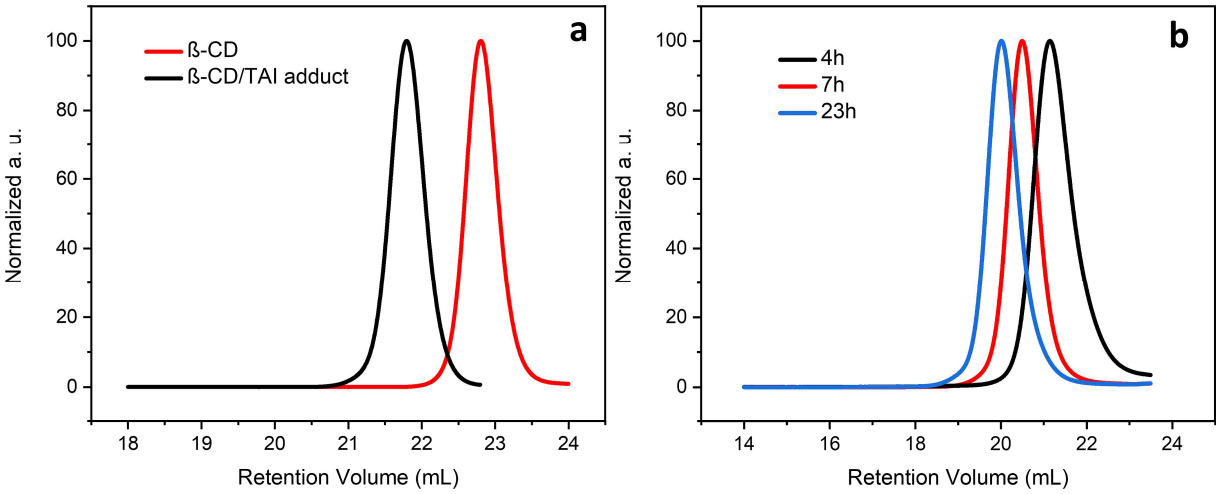

Figure S25. TD-SEC analysis (RI traces) of **(a)** ß-CD and ß-CD/TAI adduct (M_n(theor.) = 5 100, M_n(SEC) = 5 800, $Đ$ = 1.02) and **(b)** the polymers obtained after alkaline hydrolysis of isolated samples of poly(MMA) star polymer synthesized via ATRP initiated by the ß-CD/TAI adduct.

Table S6. Synthesis of multi-arm poly(MMA) stars through ATRP initiated by the ß-CD/TAI adduct[a]

Time (h)	Conv. (%)[b]	Star polymer		Free-growing chains		Hydrolysis product		
		M_n (SEC)[c]	$Đ$[c]	M_n (SEC)[c]	$Đ$[c]	M_n (theor.)[d]	M_n (SEC)[c]	$Đ$[c]
4	46	157 500	1.05	14 400	1.06	6 400	13 000	1.06
7	69	255 100	1.08	18 900	1.06	9 700	18 400	1.05
23	96	399 900	1.15	26 200	1.07	13 500	25 500	1.05

[a] Polymerization conditions: MMA/TAI/CuBr/PMDETA = 140:1:1:1; MMA/dioxane = 1:1 (v/v), 85 °C.

[b] Monomer conversion determined by ^{1}H NMR.

[c] Determined by TD-SEC.

[d] Theoretical M_n calculated from the monomer/TAI ratio and conversion, assuming 100% initiation efficiency.

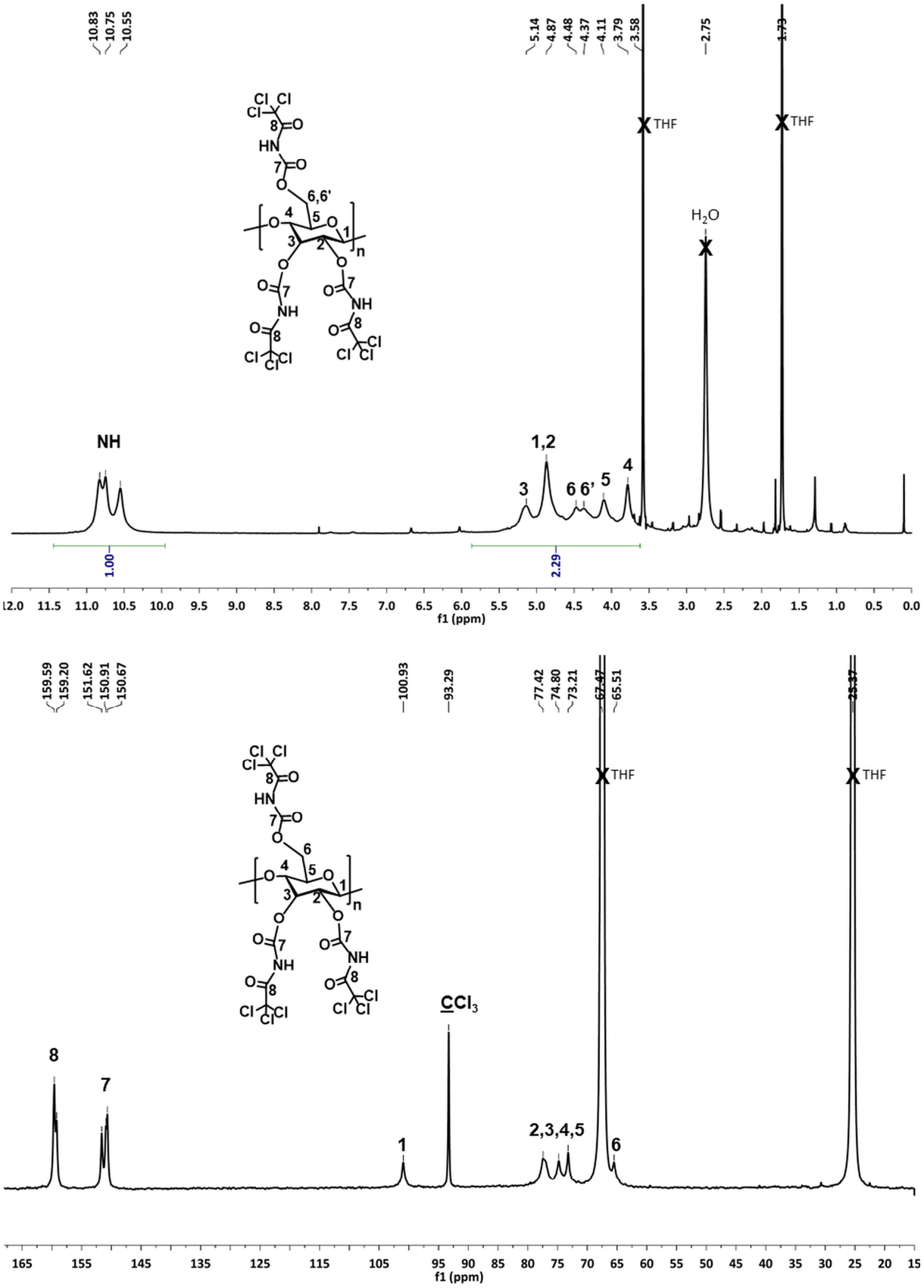

Figure S26. ^{1}H (top) and ^{13}C NMR (bottom) spectra (THF-d_8) of cellulose AVICEL PH-101 fully modified with TAI (modification performed in 7.7 wt.% DMAc/LiCl).

Table S7. Synthesis of ultra-dense bottle-brush cellulose-*graft*-poly(MMA) copolymers via ATRP initiated by the cellulose/TAI adduct.[a]

Time	Conv.	Graft copolymer			Free-growing chains		Hydrolysis product		
(h)	(%)[b]	M_n (theor)[c]	M_n (SEC)[d]	$Đ$ [d]	M_n (SEC)[d]	$Đ$ [d]	M_n (theor)[e]	M_n (SEC) [f]	$Đ$ [f]
5	27	9 644 000	3 174 000	1.93	28 300	1.07	21 600	24 400	1.06
24	72	25 539 000	nd	nd	nd	nd	57 700	62 000	1.11

[a] Polymerization conditions: MMA/TAI/CuBr/PMDETA = 800:1:1:1; MMA/dioxane = 1:1 (v/v), 85 °C; cellulose/TAI adduct macroinitiator: M_n = 106 700, $Đ$ = 2.17

[b] Monomer conversion determined by ^{1}H NMR.

[c] Theoretical M_n calculated from the M/I ratio, monomer conversion, and the number-average degree of polymerization (DP_n) of 147 determined by the TD-SEC of the cellulose/TAI adduct (monomeric unit weight of 727.34), assuming that three TAI-modified hydroxyl groups per one monomeric unit initiate the polymerization.

[d] Determined by TD-SEC using universal calibration.

[e] Theoretical M_n calculated from the monomer/TAI ratio and monomer conversion.

[f] Determined by TD-SEC using a light scattering detector.

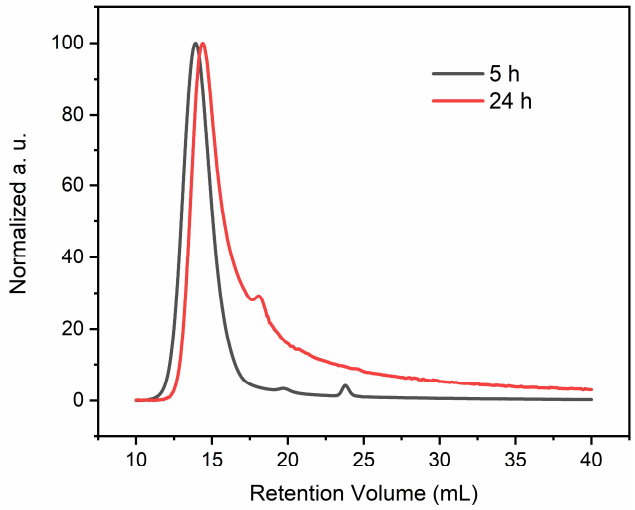

Figure S27. Light scattering signals from the TD-SEC analysis of samples of cellulose-*graft*-poly(MMA) bottle-brush graft copolymers taken at different polymerization time.

Due to an unknown non-SEC elution mechanism,[5] a high-MW fraction of the sample shows delayed elution, co-eluting with lower-MW fractions. This impacts significantly on the light scattering signal traces, resulting in the blending of the peaks of the graft copolymer and free-growing chains (this is particularly pronounced for the 24 h sample). Consequently, the light scattering signal intensity of the graft copolymer is diminished to an unknown extent while the signal intensity of the free-growing chains is markedly inflated. As a result, the calculation of MWs based on light scattering data is highly inaccurate or even impossible (a software limitation). Due to the comparatively lower sensitivity of the viscometric detector to the high-MW species, we were able to obtain relatively reliable MW values for the low-MW peak of the 5 h sample using the universal calibration approach (**Table S7**).

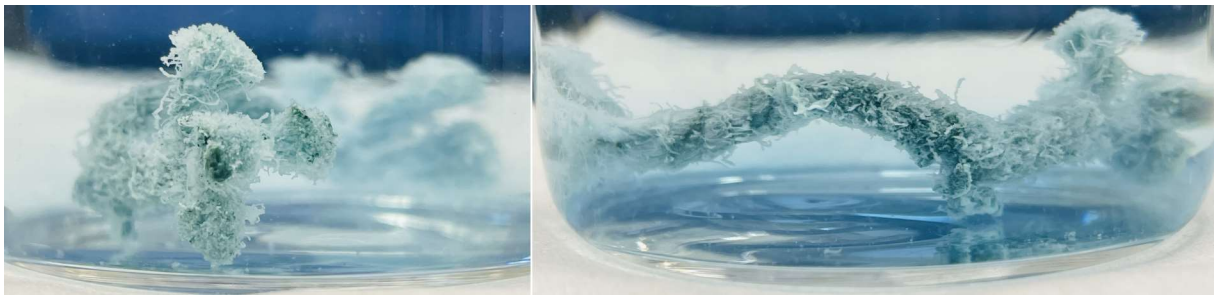

Figure S28. Surface-initiated ATRP grafting of poly(MMA) from a cotton thread modified with TAI. The photographs were taken during the purification of the grafted thread (washing in methanol).

Figure S29. Surface-initiated ATRP grafting of poly(MMA) from the pine tree cone modified with TAI. The photographs were taken during the purification of the grafted cone (left – washing in THF, right - washing in methanol).

REFERENCES

[1] G. J. P. Britovsek, J. England, A. J. P. White, *Inorg. Chem.* **2005**, *44*, 8125-8134.

[2] V. Raus, M. Štěpánek, M. Uchman, M. Šlouf, P. Látalová, E. Čadová, M. Netopilík, J. Kříž, J. Dybal, P. Vlček, *J. Polym. Sci., Part A: Polym. Chem.* **2011**, *49*, 4353-4367.

[3] V. Raus, A. Sturcova, J. Dybal, M. Slouf, T. Vackova, P. Salek, L. Kobera, P. Vlcek, *Cellulose* **2012**, *19*, 1893-1906.

[4] L. W. Dittert, T. Higuchi, *J. Pharm. Sci.* **1963**, *52*, 852-857.

[5] M. Gerle, K. Fischer, S. Roos, A. H. E. Müller, M. Schmidt, S. S. Sheiko, S. Prokhorova, M. Möller, *Macromolecules* **1999**, *32*, 2629-2637.